[Journal of the Faculty of Science, Hokkaidô University, Japan, Ser. VII, Vol. I, No. 6, 1962]

Viscosity and Related Properties of Volcanic Rocks at 800° to 1400°C

Tsutomu MURASE

(Received Sept. 28, 1962)

Contents

Abstract

Viscosity and some related physical properties of volcanic rocks which are of importance in geophysics, especially in volcanology, are investigated in the temperature range from 800° to 1400°C. Main results obtained in this paper are summarized as follows:

In Chapter I, using ordinary bending method in reheating process, the viscoelastic behaviors of volcanic rocks and their artificially prepared glasses were examined in order to investigate the problem of mechanical and chemical effects of crystallization in rocks upon the viscosity of volcanic rocks. Comparison of the two results showed that the effect was considerably large. It

was concluded that the results by reheating experiment exhibited the upper limit at or before the time of extrusion of the rocks. Also some elastic properties were briefly described in this chapter.

In Chapter II, first, the relation between viscosity and chemical composition was examined in order to estimate the viscosity of any hand specimen at high temperature. It was found that such viscosity may be estimated sufficiently well by β-value or bridge density. Next, it was shown that viscosity of molten rock was proportional to the inverse of temperature. Activation energy for viscous flow in molten rocks, logarithm of pre-exponential term and the change of viscosity were examined in connection with chemical composition and ions which were substituted for silica. The activation energy and the logarithm of pre-exponential term were well expressed as a function of silica content or bridge density. The substituted ions reduced the viscosity of molten rocks. These results could be explained by the effect of the break of Si-O bond as attempted in the field of glass technology. In the final section, using the concept of bridge density, the writer made an attempt to explain quantitatively the influence of water content upon viscosity. The attempt was led to successful results, which were extended to some rocks.

In Chapter III, the electrical conductivity of molten rocks over a wide range of silica content was measured. Also logarithm of electrical conductivity was shown to be proportional to the inverse of temperature, so the comparison between electrical conductivity and viscosity of molten rocks was discussed; it was shown that the activation energy for electrical conductivity was smaller than that for viscosity in the range of relatively high silica content and the ratio of both the activation energies was expressed as a linear function of silica content, but the logarithm of pre-exponential term could not be expressed as a simple function of silica content.

In the final chapter, the viscosity-temperature relation of the Showashinzan dome lava at or before the time of extrusion was investigated in view of the kinetics of crystal fusion. The result obtained as an upper limit was extended to the problem of when the dome lava begun suddenly to solidify undergound, and it was concluded the sudden solidification of the dome lava was antecedent to the appearance of the dome in the order of a few decades at most.

General introduction

Even at a glance at various volcanological phenomena, investigators are confronted with a difficult problem of how the viscosity of rocks at high temperatures affects the phenomena (1). It is well established that there are some different characteristics for each volcano in the mode of eruption such as the flow of lava, earthquakes originating from the volcano and crustal deformations around the volcano (2). Without knowledge of viscosity of volcanic rocks at high temperatures, it would be impossible to make clear the characteristics of a volcano which are important for volcanology, especially for predicting volcanic eruptions.

The viscosity of rock is a dominant factor controlling not only the mode of eruption but also phenomena occurring in subterranean magma which may be an even more essential problem of volcanology. The problem of gravitative magmatic differentiation by crystallization is intimately related to the viscosity of magma, because when the phenomenon takes place in heterogeneous melts due to segregation of crystals from the magma (3) (4), the velocity of rising or sinking of cyrstals is, according to Stokes' law, a function of the viscosity of the liquid in which they move. Moreover the viscosity of magma exerts an effect on the crystallization of minerals. The relation between the viscosity and the rate of crystal growth has been discussed as a kinetic phenomenon in the undercooled melt phase (5).

In order to comprehend the problems mentioned above, it is necessary to be able to estimate the value of the viscosity in natural magmas by experiment; there are rather abundant results of viscosity measurements of lavas or silicate mineral melts, but only in the "dry", i.e., anhydrous and gas-free states (6) (7). The complete comprehension of the problems requires, of course, examination of the influence of the water on the viscosity of the magma. A recent experiment on that influence at high water pressure and temperature has shown that the reduction of viscosity is very considerable (8).

Although considerable attention has been paid to the viscosity of volcanic rocks, comparatively little is known of the problem of restoration of rocks to the viscosity possessed at or before the time of extrusion. It is from this aspect that the present writer is interested in the viscosity of volcanic rocks; so in this paper, the viscosity of volcanic rocks, as an important factor in understanding various phenomena in volcanology, is the chief topic. The problems of how the existence of crystals in rock melts changes the viscosity mechanically and chemically are treated in Chapter I. The results of observations are

discussed in the aspect of restoration of rocks to the viscosity possessed at or before the time of extrusion. In Chapter II the effect of the chemical composition on viscosity are examined on the basis of the results for the molten state. Using both the results and the concept of bridge density, the writer attempts to explain the results of experiments on the influence of water on the viscosity. The relation among the viscosity, the electrical conductivity of rocks and related properties, e.g., diffusion coefficient, is treated in Chapter III. In the final chapter, in order to find out the viscosity-temperature relation of the Showa-shinzan dome lava at or before the time of extrusion, the kinetics of the melting of the dome lava is experimentally examined and the problem of when the dome lava began suddenly to cool under ground is discussed.

References

1) RITTMANN, A. Vulkane und ihre Tätigkeit, Ferdinand Enke Verlag. Stuttgart, (1960).
2) MINAKAMI, T. Fundamental research for predicting volcanic eruptions. (Part 1) Earthquakes and crustal deformations originating from volcanic activities, Bull. Earthq. Res. Inst., **38** (1960), 497–544.
3) BOWEN, N.L. Crystallization-differentiation in silicate liquids, Amer. J. Sci., **39** (1915), 175–191.
4) DALY, R.A. Igneous rocks and the depths of the earth, McGraw-Hill Book Co., New York, (1933), 278.
5) FRENKEL, J. Kinetic theory of liquids, Clarendon Press, Oxford, (1956).
6) KANI, K. and HOSOKAWA, K. On the viscosities of silicate rock-forming minerals and igneous rocks, (in Japanese, with abstract in English), Res. Electrotech. Laboratory, No. 391 (1936), 1–105.
7) VOLAROVIČ, M.P. and KORČEMKIN, L.I. Der Zusammenhang zwischen der Viskosität geschmolzener Gesteine und dem Aziditätskoeffizienten nach F.J. Loewinson-Lessing, Compt. Rend. (Doklady) Acad. Sci. USSR, **17** (1937), 417–425.
8) SABATIER, G. Influence de la teneur en eau sur la viscosité d'une rétinite, verre ayant la composition chimique d'un granite, Compt. Rend. Acad. Sci. (Paris), **242** (1956), 1340–1342.

Chapter I. Viscoelastic behavior

§ 1. Introduction

Some investigators (1) (2) (3) have measured the viscosity of molten rocks and have mentioned that the low viscosity of rocks gradually increases, when kept at a constant temperature. KANI (1) ascribed the rapid increase of the viscosity within the narrow temperature range from 1250° to 1200°C in basalt glasses to the commencement of crystallization of magnetite and plagioclase. Also PRESTON (4) studied the similar effect of crystallization on viscosity of two kinds of glasses below the liquidus temperature; he showed, if the glasses were held for only a short time at temperatures lower than the liquidus temperature, then the viscosity-temperature curves obtained are merely continuations of those obtained when the glasses are in the true liquid condition. When longer times are allowed, crystallization commences, in the case of these two glasses, with separation of silica, and the viscosity of the resulting liquid-crystal mixture rises with the lapse of time in which the glass is left at the test temperature, and moreover on reheating the reverse phenomenon takes place.

The crystallization of mineral matters in a molten rock may cause some change of the chemical composition of the resulting molten rock in which segregated crystals are suspended. Both these effects increase chemically and mechanically the viscosity of rocks below liquidus temperature. Accordingly one can not neglect the effect of the crystallization in attempting to deduce the viscosity-temperature relation of lava at the time of extrusion or of the magma in the magma reservoir.

The principal purpose of the present chapter is to determine the viscosity of some volcanic rocks by reheating samples of the original rock and to find how much the existence of crystals affects the viscosity. Moreover, the writer will discuss the significance, if any, of the results, in order to gain a better understanding of some matters related to the restoration of rocks to the viscosity possesed at or before the time of extrusion.

§ 2. Apparatus and method

For the determination of the elasticity and slow viscous flow, measurements were made of the ordinary bending or sagging of a centrally loaded rock strip of a rectangular cross-section (5) (6). The apparatus employed is essentially the same as that used by SAKUMA (6). In stead of measuring the actual deflection of the mid-point of the loaded strip, the change in curvature

of the strip caused by the applied load was observed by double reflections through the two rectangular prisms which were set face to face on the both ends of the strip. The prisms (*P*) were fixed on a small fused silica platform. The method of mounting and loading of the specimen is shown diagrammatically in Fig. I–1. The specimen (*S*) was supported on two knife-edges.

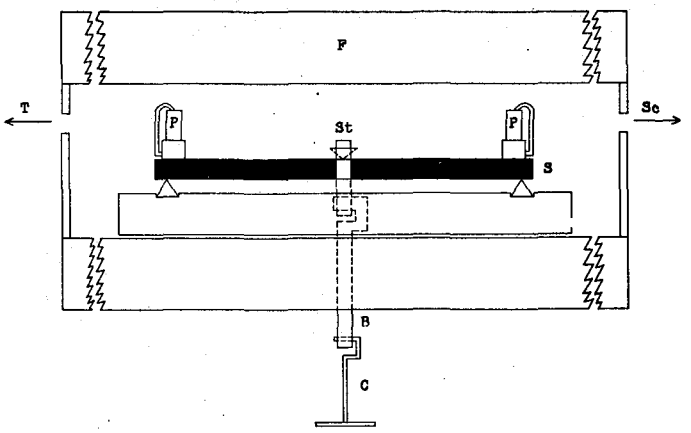

Fig. I-1. Diagram of the apparatus used for measuring the bending of rock specimens.
S: specimen, P: prism, St: stirrup, B&C: hook-shaped suspenders, F: furnace, T: telescope, Sc: scale.

The load was applied vertically downwards at the mid-point of the specimen by a loose stirrup (*St*) (3 g weight) carrying a horizontal knife-edge which in turn was loaded by the hook-shaped suspender (*B*) (5g weight) which passed through a tiny hole in the bottom parts of furnace. Then suspender (*B*) was loaded by another one (*C*) (8g weight). The whole system was fixed on a solid platform. All parts of the apparatus were made of fused silica or porcelain.

The whole contrivance was inserted horizontally into a doubly wound nichrome electric furnace below ca. 1200°C, and "EREMA" furnace above ca. 1200°C. The incident and reflected light was allowed to enter and go out through the small holes in the lids at both sides of the furnace. Though such holes disturbed the uniformity of temperature in both radial and axial directions in the furnace, the actual difference in temperature was found to be less than ± 5°C within the space which was to be occupied by the specimen itself. The temperature of the specimen was measured with a Pt-PtRh thermocouple which was inserted in the furnace close to the specimen. The specimen

was heated up to the required temperature step by step during the measurement.

Experimental procedure is as follows:

In Fig. I–2 is represented diagrammatically the behavior of a rock sample when a constant load W_0 is applied at time zero, and removed at a

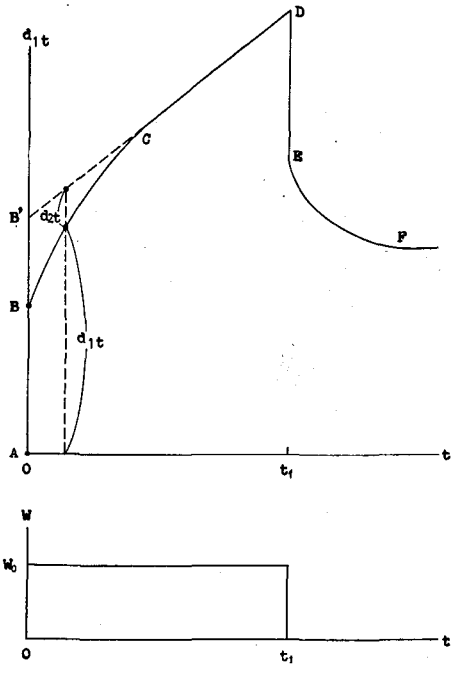

Fig. I–2. Diagrammatical representation of the deflection-time curve.

subsequent time t_1, which may be of the order of minutes to hours. Application of the load caused an instantaneous elastic deflection represented by AB, and then an elastico-viscous deflection BC, followed by a uniform rate of viscous flow, CD. When the load was removed an instantaneous recovery DE occurred, followed by a slow elastic recovery EF.

The results obtained as to the deflection-time curves were analyzed by rheological method. For such results as shown in Fig. I–2, it is useful to consider the behavior of the well-known mechanical model as shown in Fig. I–3. This figure shows the "Burgers model" (four element model), which is a combination of the Maxwell model and the Kelvin (or Voigt model) in series.

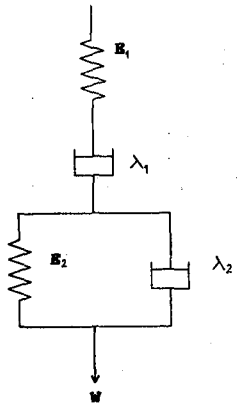

Fig. I-3. Rheological model for explaining the mechanical behavior of rock at high temperature.

The Maxwell model and the Kelvin model are made of a spring and a dash-pot in series or parallel respectively. The springs represent the elastic behavior, i.e., they are Hookean, while the dash-pots exhibit Newtonian flow behavior, the rate of deflection being proportional to the force.

In a simple bending, the relation between the stress, strain and time in the Burgers model for a constant load is given by following equation (7) (8) (9),

$$x=\left(\frac{Wl^3g}{4ab^3}+\frac{5wl^4g}{32ab^3}\right)\left[\frac{1}{E_1}\left(1+\frac{t}{\tau_M}\right)+\frac{1}{E_2}\left\{1-\exp\left(-t/\tau_K\right)\right\}\right] \qquad \text{(Eq. I-1)}$$

where x: the amount of deflection,

a and b: the breadth and thickness of specimen,

l: the distance between the supporting knife-edges,

$W=W_0+W_1$: the applied load,

W_0: the load applied instantaneously,

W_1: the weight of a loose stirrup and two hook-shaped suspenders,

w: the weight of the specimen per unit length,

E_1 and E_2: the Young's modulus,

$\tau_M=\lambda_1/E_1$: the relaxation time,

$\tau_K=\lambda_2/E_2$: the retardation time,

λ_1 and λ_2: the normal viscosity coefficients,

t: the time.

x is related to the observed scale reading (d_{1t}) by the following equation

(10):

$$x = \frac{l\, d_{1t}}{6\,(2D + B + 4\,\delta/\mu)}$$

where D: the distance between the scale and the hypotenuse face of the further prism,

B: the distance between the hypotenuse faces of the two prisms,

δ: the height of the prism measured from the hypotenuse face,

μ: the refractive index of the prism.

The stress (P_n) and the strain (e_n) at the mid-point of the lower surface are calculated by the following equation:

$$P_n = \frac{3\,(W_0 + W_1)\,l\,g}{2\,a\,b^2} + \frac{3\,w\,l^2\,g}{4\,a\,b^2} \quad (\mathrm{dyne/cm^2}),$$

$$e_n = \frac{6\,b\,d}{l^2} + \frac{24\,b\,d}{5\,l^2}.$$

In this experiment the stress is of the order of 10^8 to 10^5 dyne/cm^2.

From Eq. (I–1), thus, each value can be calculated according to the following ways,

i) Putting $t=0$ in Eq. (I–1), i.e., $d_{1t\to 0}=d_1=AB$ in Fig. I–2, one gets E_1.

ii) Putting $t=\infty$ in Eq. (I–1) and then differentiating it, i.e., $\mathrm{d}(d_{1t\to\infty})/\mathrm{dt}$ in Fig. I–2, one gets λ_1.

iii) Putting $t=\infty$ in Eq. (I–1) and extrapolating it to $t=0$, i.e., $(d_{1t\to\infty})_{t\to 0}$ $=d_2=AB'$ in Fig. I–2, and then combining E_1 in (i), one gets E_2.

iv) From Eq. (I–1) and Fig. I–2 one gets

$$ln\left(-x + \frac{1}{E_1} + \frac{1}{E_2} + \frac{t}{\lambda_2}\right) = ln\, d_{2t} \propto ln\, \frac{1}{E_2} - \frac{t}{\tau_K}$$

and then τ_K is got from this equation.

v) From $\tau_K=\lambda_2/E_2$, one gets λ_2.

vi) From $\tau_M=\lambda_1/E_1$ one gets τ_M.

Shear viscosity η_1 can be found from $\lambda_1=3\eta_1$ which is based on the assumption of imcompressible viscous liquid (11) (12).

The original apparatus mentioned above was unsuitable for the extension of these measurements to the extremely fast rates of sag at temperatures above ca. 1100–1200°C, i.e., to the measurement of temperatures for viscosities

lower than ca. 10^{10} poises.

In order to extend measurements of viscosity down to the neighbourhood of 10^5 poises, the deflection at the mid-point of a short specimen unloaded was measured directly without the optical system described above, i.e., the actual deflection was measured by means of a calibrated eyepiece reticule of the telescope.

This calibration method may produce errors due to the measurements of somewhat large deflections, hence the method was checked by comparison with the viscosity of a glass (Asahi glass) which was known by other methods.*

The chemical composition of the glass is shown in Table I–1.

Table I–1. Chemical composition of Asahi glass.*

SiO_2	71.5
Al_2O_3	1.6
Fe_2O_3	0,1
TiO_2	0.3
CaO	8.0
MgO	3.9
SO_3	0.3
Na_2O, K_2O	14.3
Total	100.0

* The data on viscosity and chemical composition of the glass were kindly supplied from Dr. H. UKIHASHI, Research Laboratory of the Asahi Glass Co.

The viscosity of the glass was determined by the restrained sphere method above ca. 950°C, below which it was determined from the softening point as $10^{7.65}$ poises, the incipient softening point as 10^{11}–10^{12} poises and the transformation point as 10^{13}–10^{14} poises as used in the field of glass technology. The results obtained by the writer are in fair agreement with those of the glass as shown in Fig. I–4.

The percentage error in the results due to all factors contained in Eq. (I–1) was less than ±5% below ca. 1150°C and ±10% above ca. 1150°C owing to the non-uniformity of thermal expansion of specimens. These errors, however, leave no objections in discussions which follow in this paper because the logarithmic scale is used.

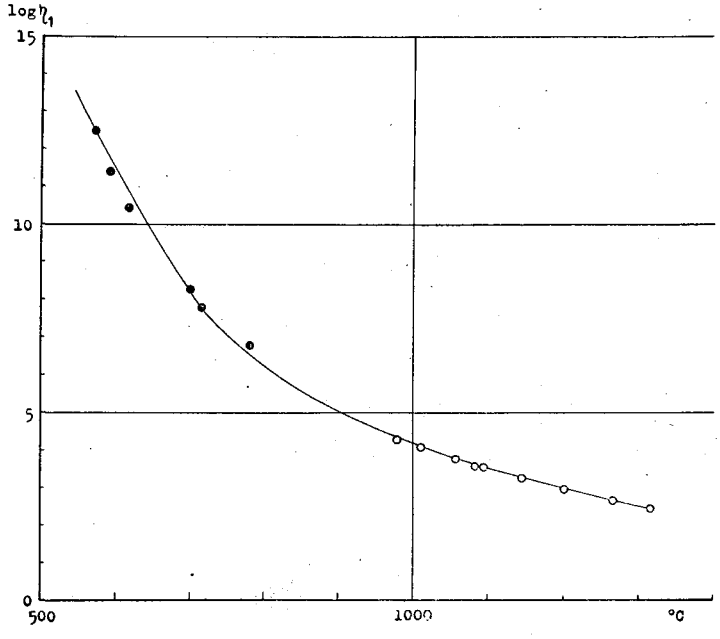

Fig. I-4. Change in log viscosity (in poises) with temperature in Asahi glass.
●: data by the present method.
○ & solid line: known data supplied by Asahi Glass Co. Research Laboratory.

§ 3. Specimens

The rock specimens were cut out of a piece of rock from the respective lava flows and were ground smoothly to the size of ca. $8.0\times1.0\times0.3$ cm^3. Artificial glasses of original rocks were prepared by melting the fine powders of original rocks at 1550°C for 3 hours; they were then quenched in the air.

The chemical compositions of the specimens used in this experiment are given in Table I–2 (A) together with those of some rocks discussed in connection with the value of viscosity in another chapter. One can find petrographical descriptions referring to literatures. Also the chemical compositions as free from water which were recalculated from Table I–2 (A) are given in Table I–2 (B) together with the values discussed in another chapter. The locality of each rock is as follows:

1) Nagahama, Shimane Pref. (Nepheline basalt) (2).
2) Karatsu Oshima, Nagasaki Pref. (Olivine dolerite) (2).

3) Konoura, Kagawa Pref. (Olivine basalt) (2).
4) Genbudo, Hyogo Pref. (Olivine basalt) (2) (21).
5) Motomachi, Izu-Oshima, Seven Izu islands (Andesitic basalt) (2).
6) Oshima volcano, Izu Oshima, Seven Izu islands (1950–lava) (13).
7) Usu volcano, Hokkaido (Somma lava) (14).
8) Miyakejima, Seven Izu islands (1874–lapilli) (19) (22).
9) Tarumai volcano, Hokkaido (1909–dome lava) (2) (17).
10) Asama volcano, Nagano and Gunma Pref. (Onioshidashi, 1783–lava) (2) (25).
11) Sakurajima, Kagoshima Pref. (1914–lava) (2).
12) Sakurajima, Kagoshima Pref. (1946–lava) (15).
13) Komagadake, Hokkaido (1929–pumice) (18) (23) (24).
14) Kasugayama, Nijo-san, Osaka Pref. (Sanukite) (20).

Table I-2. (A) and (B). Chemical compositions

		1	2	3	4	5	6	7	8	9	10	11
A	SiO_2	35.66	47.56	49.24	49.29	51.80	52.02	53.46	53.27	57.40	59.90	60.80
	Al_2O_3	11.97	15.84	16.81	18.49	15.00	15.83	18.99	14.38	16.84	15.99	16.04
	Fe_2O_3	5.19	6.99	6.16	2.38	3.68	2.28	2.75	5.41	3.68	2.86	2.89
	FeO	9.69	4.73	3.60	6.77	10.14	10.80	6.74	8.65	5.96	4.77	4.63
	MgO	8.35	9.85	8.02	6.09	5.36	4.47	3.82	1.61	3.28	4.68	3.50
	CaO	14.39	9.19	9.49	8.14	9.77	9.48	9.79	10.97	6.60	6.08	4.74
	Na_2O	3.65	2.32	2.67	3.93	1.76	1.58	2.47	1.93	2.88	3.39	3.74
	K_2O	1.89	0.81	1.09	1.79	0.32	0.29	0.48	0.90	1.21	1.28	1.75
	H_2O+	4.04	1.04	1.50	0.88	0.62	0.99	0.33	0.16	0.36	0.58	0.74
	H_2O-						0.24	0.24				
	TiO_2	3.74	1.55	1.33	2.22	0.60	1.52	1.06	1.87	0.65	0.05	0.87
	P_2O_5	1.37	0.31	0.43	Tr.	0.31	n.d.	0.32	0.12	Tr.	n.d.	Tr.
	MnO	0.30	0.17	0.17	0.22	0.20	0.09	0.22	0.35	1.08	0.89	0.33
	S								n.d.	0.02	Tr.	0.01
	ZrO_2											
	Total	100.24	100.36	100.51	100.20	99.56	99.59	100.63	99.62	99.96	100.47	100.04
B	SiO_2	37.07	47.88	49.73	49.63	52.35	52.90	53.43	53.56	57.63	59.97	61.21
	Al_2O_3	12.44	15.95	16.98	18.62	15.16	16.10	18.98	14.46	16.91	16.01	16.15
	Fe_2O_3	5.40	7.04	6.22	2.40	3.72	2.32	2.75	5.44	3.69	2.86	2.91
	FeO	10.07	4.76	3.64	6.82	10.25	10.98	6.74	8.70	5.98	4.78	4.66
	MgO	8.68	9.92	8.10	6.13	5.42	4.55	3.82	1.62	3.29	4.69	3.52
	CaO	14.96	9.25	9.58	8.20	9.87	9.64	9.78	11.03	6.63	6.09	4.77
	Na_2O	3.79	2.34	2.70	3.96	1.78	1.61	2.47	1.94	2.89	3.39	3.76
	K_2O	1.96	0.82	1.10	1.80	0.32	0.29	0.48	0.90	1.21	1.28	1.76
	TiO_2	3.89	1.56	1.40	2.24	0.61	1.55	1.06	1.88	0.65	0.05	0.88
	P_2O_5	1.42	0.31	0.43	Tr.	0.31	—	0.32	0.12	Tr.	n.d.	Tr.
	MnO	0.31	0.17	0.17	0.22	0.20	0.09	0.22	0.35	1.08	0.89	0.33
	S								n.d.	0.02	Tr.	0.01
	ZrO_2											
	β	0.94	0.55	0.48	0.43	0.47	0.46	0.37	0.45	0.32	0.29	0.26
	b/Si	−0.14	0.53	0.62	0.64	0.83	0.92	0.81	0.90	1.02	1.10	1.14

15) Unzendake, Nagasaki Pref. (1792–lava) (2).
16) Saigo, Aichi Pref. (Grano-diorite) (2).
17) Showa-shinzan, Hokkaido (Dome lava) (14).
18) Usu volcano, Hokkaido (Glassy lava) (14).
19) Arita, Nagasaki Pref. (Pitchstone) (2).
20) Oki, Shimane Pref. (Obsidian) (2).
21) Shirataki, Hokkaido (Obsidian) (16).
22) Sumiyoshi, Hyogo Pref. (Hornblende granite) (2).
23) Niijima, Seven Izu islands (Liparite, pumice) (2).
24) Wadatoge, Nagano Pref. (Obsidian) (16).

The above specimens used by the present writer were kindly presented by Drs. T. ISHIKAWA, Y. KAWANO, Y. KATSUI, J. OSSAKA, M. IWANAGA, and Y. KONDO

and other constants of rocks.

12	13	14	15	16	17	18	19	20	21	22	23	24
61.26	61.41	61.72	65.15	61.06	69.74	70.60	70.26	71.37	74.41	75.23	75.90	76.24
16.14	15.42	19.18	14.25	17.47	15.59	15.00	12.25	14.72	13.33	13.69	15.41	12.56
2.88	2.64	0.53	3.27	1.34	1.52	1.37	0.27	1.08	0.08	0.50	0.36	0.68
4.71	4.93	4.11	2.50	4.70	2.59	2.49	0.86	1.38	0.86	1.03	0.22	0.58
2.77	2.34	2.12	2.36	2.65	0.85	0.77	0.32	0.35	0.43	0.49	0.21	0.23
6.80	6.70	5.59	4.60	6.08	3.63	3.30	0.97	1.36	1.90	1.32	0.84	0.96
2.65	4.72	2.65	3.80	3.06	3.43	4.42	4.24	3.74	2.99	3.25	4.41	2.84
1.46	1.10	1.99	2.52	1.57	1.36	0.98	3.60	5.69	4.30	3.19	2.88	4.20
0.21	0.52	0.45	0.90	1.34	0.67	0.69	5.44	0.33	0.23	0.96	0.08	0.69
0.09	0.02	0.23			0.23	0.12	1.10	0.10	0.29			0.17
0.74	0.46	0.62	0.05	0.77	0.45	0.36	Tr.	0.04	0.05	0.15		0.38
0.18	n.d.	0.10	Tr.	0.10	0.22	0.21	0.17	0.12	0.23	0.21		0.05
0.14	Tr.	0.18	0.56	0.17	0.08	0.09	0.03	0.06	0.05	0.09		0.25
	n.d.		n.d.									
				0.02						0.03		
100.03	100.26	99.47	99.96	100.33	100.36	100.40	99.51	100.34	99.15	100.14	100.31	99.83
61.43	61.58	62.47	65.77	61.67	70.09	70.89	75.57	71.44	75.41	75.85	75.73	77.00
16.18	15.46	19.41	14.39	17.64	15.67	15.06	13.18	14.73	13.52	13.80	15.37	12.69
2.89	2.65	0.54	3.30	1.35	1.53	1.38	0.29	1.08	0.08	0.50	0.36	0.69
4.72	4.94	4.16	2.52	4.75	2.60	2.50	0.93	1.38	0.87	1.04	0.22	0.59
2.78	2.35	2.15	2.38	2.68	0.85	0.77	0.35	0.35	0.44	0.50	0.21	0.23
6.82	6.72	5.66	4.64	6.14	3.65	3.31	1.04	1.36	1.93	1.33	0.84	0.97
2.66	4.73	2.68	3.84	3.09	3.45	4.44	4.56	3.74	3.03	3.28	4.40	2.87
1.46	1.10	2.01	2.54	1.59	1.37	0.98	3.87	5.70	4.36	3.22	2.87	4.24
0.74	0.46	0.63	0.05	0.78	0.45	0.36	Tr.	0.04	0.05	0.15		0.38
0.18	n.d.	0.10	Tr.	0.10	0.22	0.21	0.18	0.12	0.23	0.21		0.05
0.14	Tr.	0.18	0.57	0.17	0.08	0.09	0.03	0.06	0.05	0.09		0.25
	n.d.		n.d.	—						—		
				0.02						0.03		
0.26	0.29	0.19	0.21	0.24	0.15	0.15	0.08	0.09	0.07	0.08	0.06	0.06
1.15	1.17	1.16	1.30	1.15	1.40	1.42	1.55	1.46	1.55	1.55	1.53	1.59

§ 4. Results and discussion

i) Deflection-time curves.

The procedure during an actual experimental run may be understood by examination of Figs. I–5–13, in which deflection-time curves of three lava specimens are given for some runs at different temperatures. The scale reading of deflections (d_{1t}) are plotted in the ordinate. In these figures three lavas, for example, were selected for examination of remarkable effects,

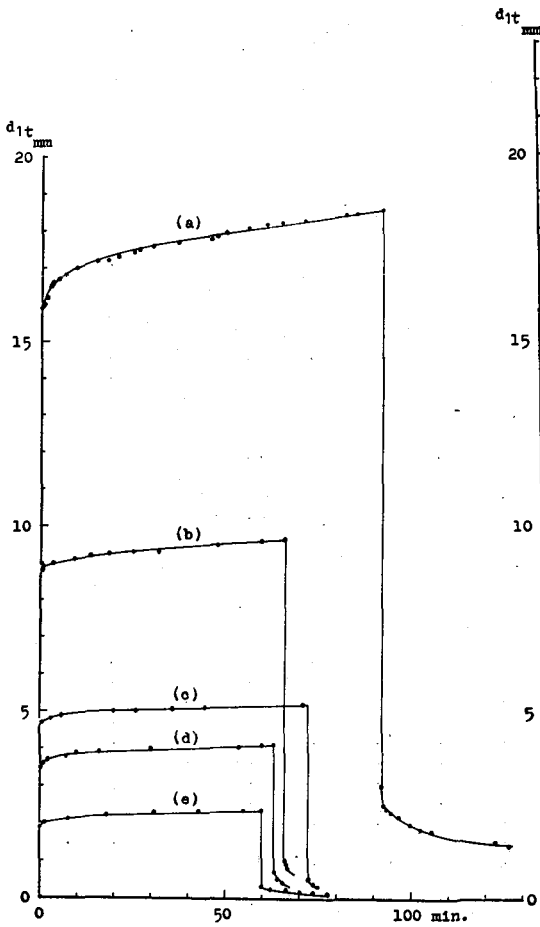

Fig. I-5. Showa-shinzan dome lava. (at 815°C lst heating run. W_0=337 g(a), 187 g(b), 100 g(c), 75 g(d) and 38 g(e)).

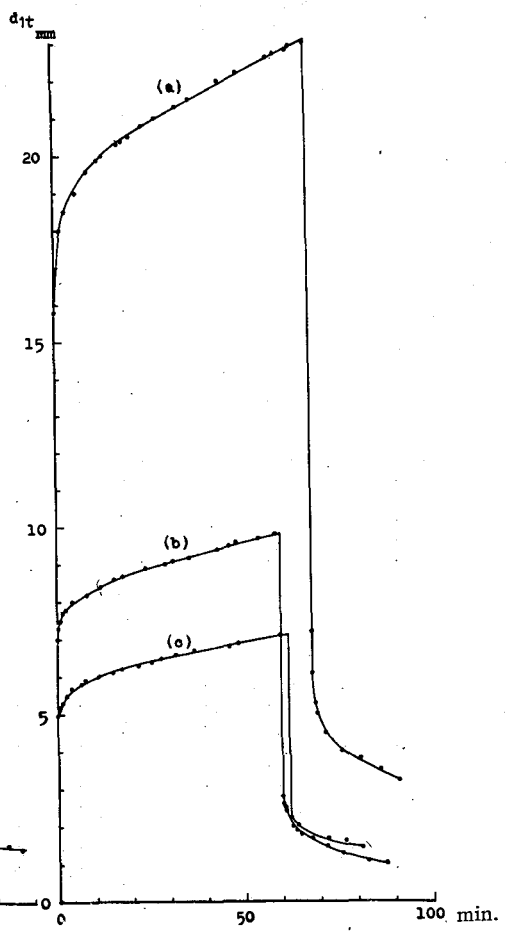

Fig. I-6. Showa-shinzan dome lava. (at 905°C 1st heating run. W_0= 337 g(a), 150 g(b) and 100 g(c)).

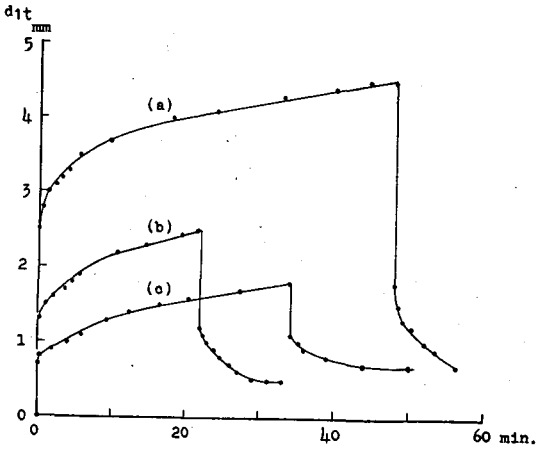

Fig. I-7. Showa-shinzan dome lava. (at 1005°C, lst heating run, W_0=150 g(b), 75 g(c) and at 915°C, 2nd heating run, W_0=337 g(a)).

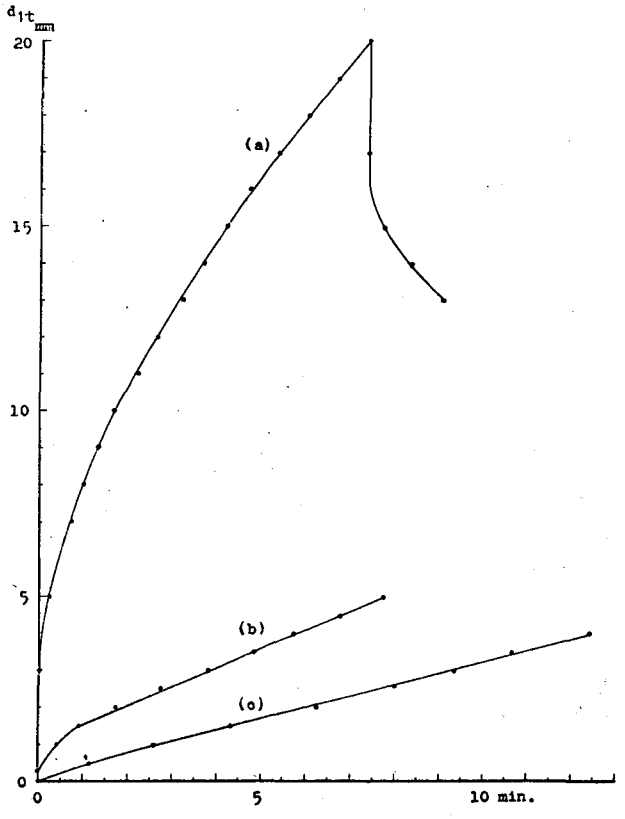

Fig. I-8. Showa-shinzan dome lava. (at 1100°, 3rd heating run; W_0=38 g(a), 0 g (W_1=16 g) (b) and 0 g(W_1 =8 g) (c)).

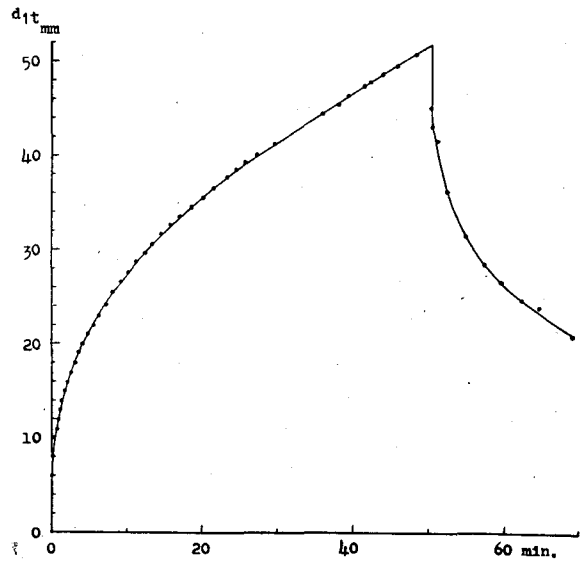

Fig. I-9. Showa-shinzan dome lava. (at 1000°C, 3rd cooling run, W_0=187 g.)

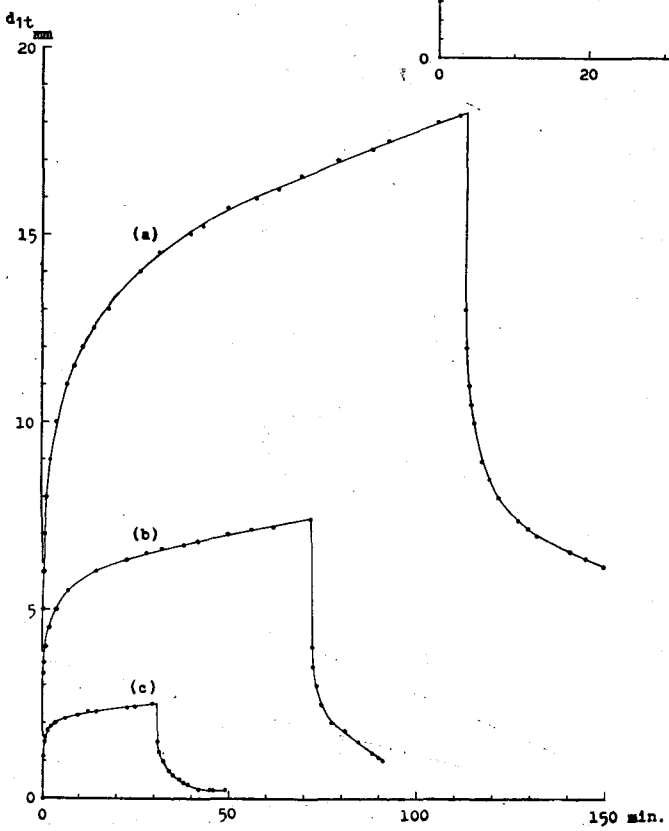

Fig. I-10.
Asama Onioshidashi lava. (at 825°C, W_0=600 g(a), 375 g(b) and 150 g(c)).

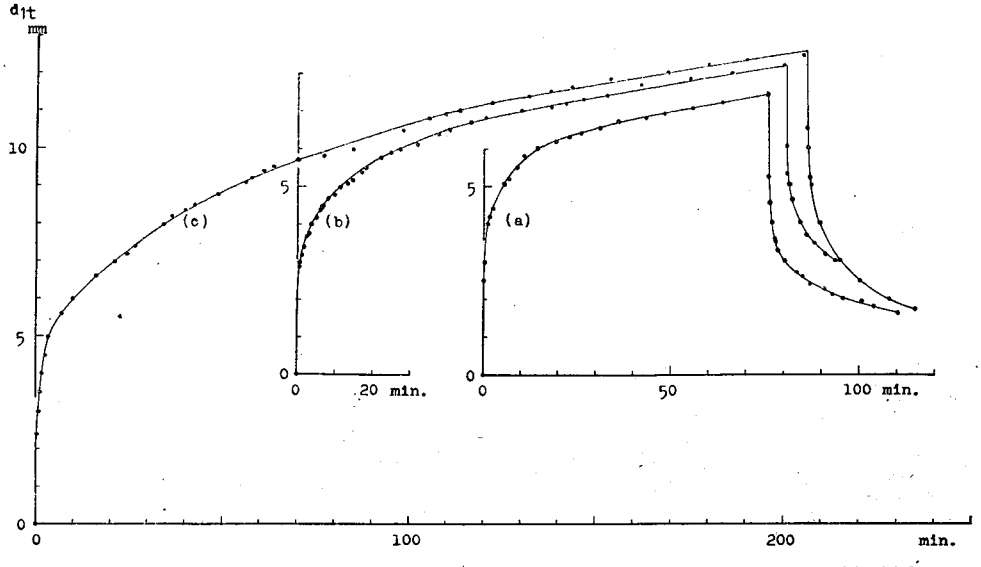

↑ Fig. I-11. Asama Onioshidashi lava. (heating process is R.T. → 815 (a) →950 → 810(b) → R.T. → 1000 → 805°C(c), W_0=337 g).

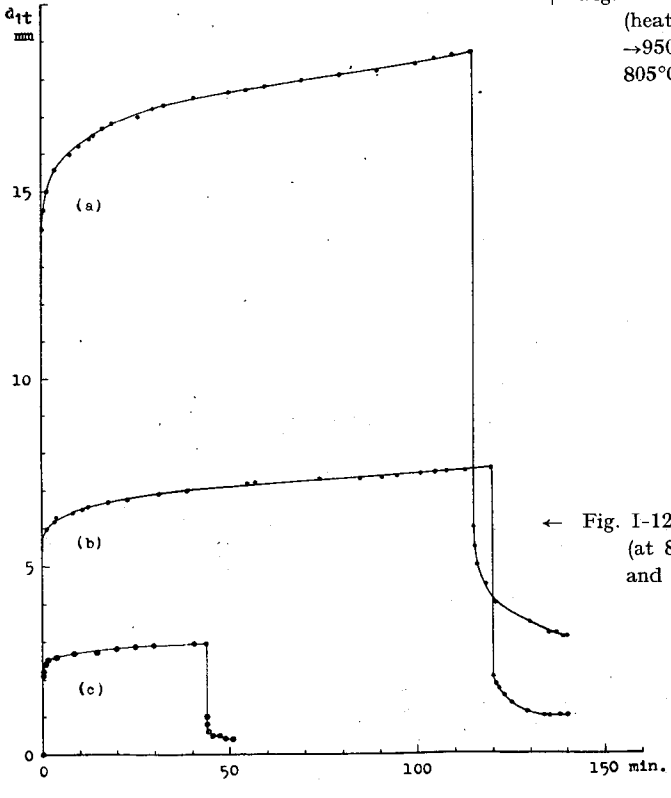

← Fig. I-12. Oshima 1950-lava. (at 815°C, W_0=600 g(a), 250 g(b) and 100 g(c)).

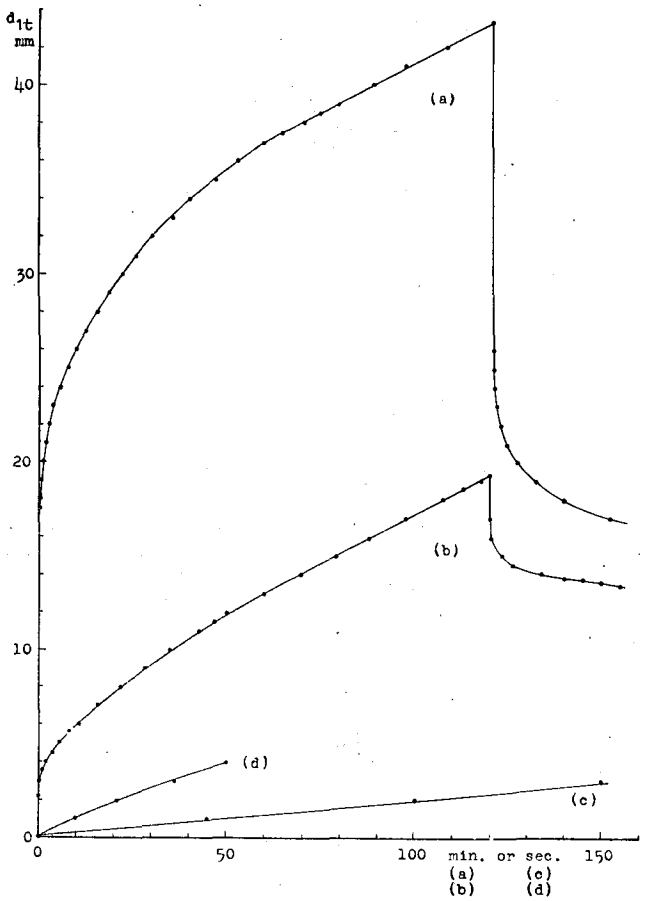

Fig. I-13. Oshima 1950-lava.
(at 910°C, W_0=600 g(a), at 995°C, W_0=75g(b), at 1095°C, W_0=0 g(W_1=8 g)(c), at 1105°C, W_0=0g (W_1=16 g)(d)).

if any, of the difference of chemical compositions on the deflection-time curves. The three lavas, viz., the Showa-shinzan dome lava, the Asama Onioshidashi lava and the Oshima 1950–lava have ca. 70, 60 and 50% of silica content respectively.

(A) The Showa-shinzan dome lava.

The (a), (b), (c), (d) and (e) curves in Fig. I–5 show the deflection-time relation for a specimen at 815°C, loaded W_0=337g, 187g, 100g, 75g and 38g,

w=0.34g and W_1=16g. The size of the specimen was 4.0×1.18×0.112 cm³ and the magnification of deflection by optical lever (M)=141. After the above noted procedure, the (a), (b) and (c) curves in Fig. I–6 were next obtained at 905°C, by loading W_0=337 g, 150g and 100g for (a), (b) and (c) respectively. After this procedure, the specimen was heated up to 1000°C and subsequently cooled down to the room temperature at the cooling rate of ca. 500°C/hour.

In order to examine existence of any hysteresis phenomena due to a previous heat treatment, a new specimen was heated up to high temperatures and cooled down to the room temperature again and again, i.e., room temperature ($R.T.$)→1005→$R.T.$→915→$R.T.$→1100→1000°C→$R.T.$ The (b) and (c) curves in Fig. I–7 show the results obtained with the specimen at 1005°C in the first heating run. The size of the specimen was 8×1.032×0.3645 cm³. M=76, w=0.91g, W_1=16g and W_0=150g and 75g respectively. The (a) curve in Fig. I–7 shows the result obtained for the specimen at 915°C in the second heating run. W_0=337g.

The (a), (b) and (c) curves in Fig. I–8 show the results obtained for the specimen at 1100°C in the third heating run, W_0=38g, 0g (W_1=16g only) and 0g (W_1=8g only) respectively. Fig. I–9 shows the results obtained for the specimen at 1000°C after the heating procedure at 1100°C. W_0=187g.

(B) The Asama Onioshidashi lava.

The (a), (b) and (c) curves in Fig. I–10 show the results obtained for a specimen at 825°C. W_0=600g, 375g and 150g, w=0.69g and W_1=16g respectively. The size of the specimen was 5.5×0.191×0.3115 cm³. M=101.

Fig. I–11 shows an example of the hysteresis phenomena due to a previous heat treatment. The heating-cooling procedure for a new specimen was $R.T.$→815 (Fig. (a))→950→810 (Fig. (b))→$R.T.$→1000→805°C (Fig. (c)). W_0=337g, w=0.69g and W_1=16g. The size of the specimen was 5.0×1.096×0.2639 cm³. M=102.

(C) The Oshima 1950–lava.

The (a), (b) and (c) curves in Fig. I–12 show the results obtained for a specimen at 815°C. W_0=600g, 250g, w=0.45g and W_1=16g respectively.

The (a), (b), (c) and (d) curves in Fig. I–13 show the results obtained for the same specimen at 910°, 995°, 1095° and 1105°C. W_0=600g, 75g, 0g (W_1=8g only) and 0 g (W_1=16g only). The size of the specimen was 8×0.193×0.9922 cm³. M=81. Thus, both the temperature and the stress are seen to affect the shape of the deflection-time curve for a constant-temperature.

From Figs. I–5, 6, 7 (c,b), 8, 10 and 12 of deflection-time curves at a single

temperature it can be seen that an instantaneous elastic strain and a uniform time rate of viscous flow (final slope) increase with the increase in stress. The time taken for the commencement of the final slope varies according to the applied stress.

The effect of temperature on the behavior of rocks can also be seen. Comparison of the deflection-time curves at different temperatures under the same applied stress, i.e., Figs. I–5 (a), 6 (a), Figs. I–5 (c), 6 (c) and Figs. I–12 (a), 13 (a) show that the deflection is more rapid when the temperature is higher. At lower temperatures, are seen substantially instantaneous deformations, which disappear immediately after removal of load, while at higher temperatures, as represented in Fig. I–8 (c) and Figs. I–13 (c) and (d), a uniform rate of viscous flow is immediately observed so large that it is not possible to observe any retarded elastic deformation.

A typical example of the hysteresis phenomenon due to a previous heat treatment is represented in Fig. I–11. From this figure one can see changes of the instantaneous elastic strain which are not systematic, and changes of the time taken for the commencement of final slope, which are the result of heat treatments. At the same time one can see that the heat treatment does not exert any effect upon the final slope, i.e., viscosity (see also Figs. I–28–31).

ii) Suitability of Burgers model in estimating deflection-time curves.

It will next be examined whether such Burgers model as shown in Fig. I–3 is suitable for estimating the deflection-time curves just described.

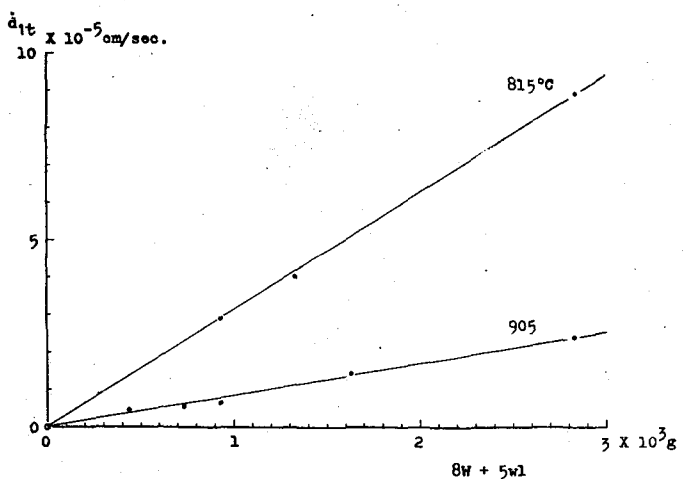

Fig. I-14. Showa-shinzan dome lava.

(A) Irreversible viscosity (η_1 or λ_1).

Figs. I–14–17 exhibit Newton's law of the proportionality of the shear-rate to the shearing stress at a constant temperature; therefore, η_1 can be regarded as a true Newtonian viscosity. In these figures the shear-rate ($\dot{d}_{1t}$) taken from scale readings and the total weight ($8W+5wl$) were taken as convenient measures of the shear-rate and shearing stress respectively, because the same specimen was used in the whole experimental procedure.

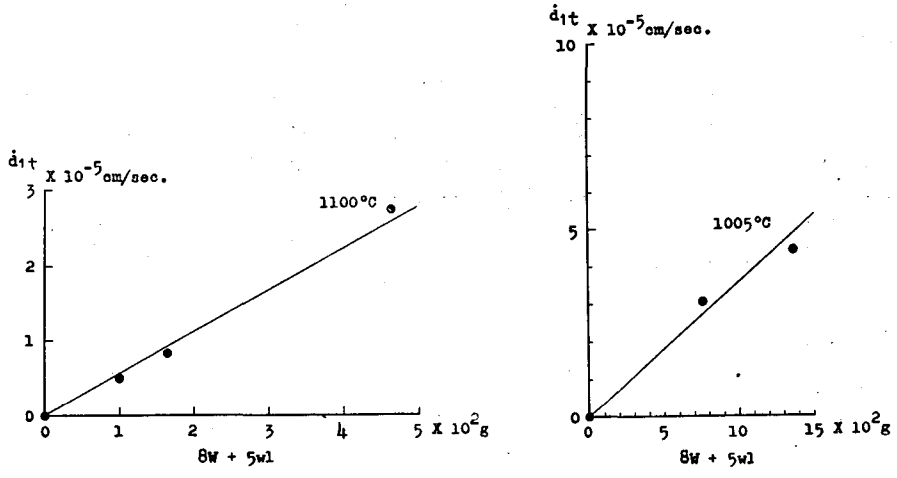

Fig. I-15. Showa-shinzan dome lava.

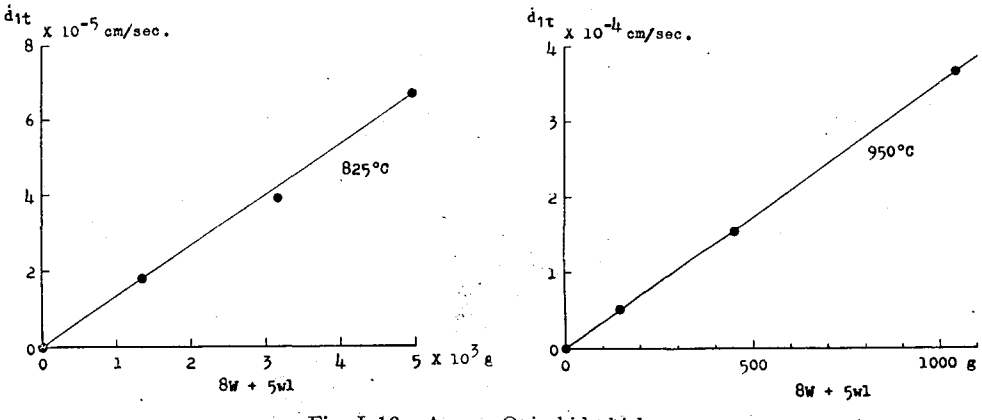

Fig. I-16. Asama Onioshidashi lava.

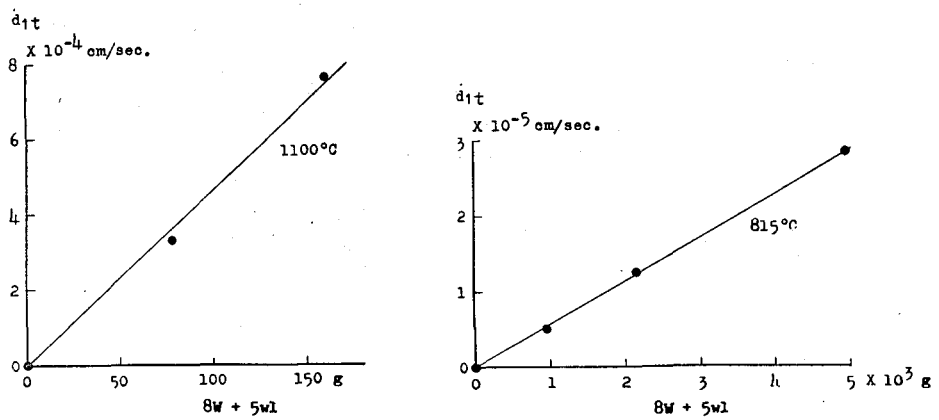

Fig. I-17. Oshima 1950-lava.

(B) Instantaneous Young's modulus (E_1).

Figs. I–18–20 exhibit Hooke's law of the proportionality of stress and strain for E_1 between the room temperature and ca. 1000°C. In these figures load applied instantaneously (W_0) and scale reading (d_1) were taken as the measure of stress and strain respectively.

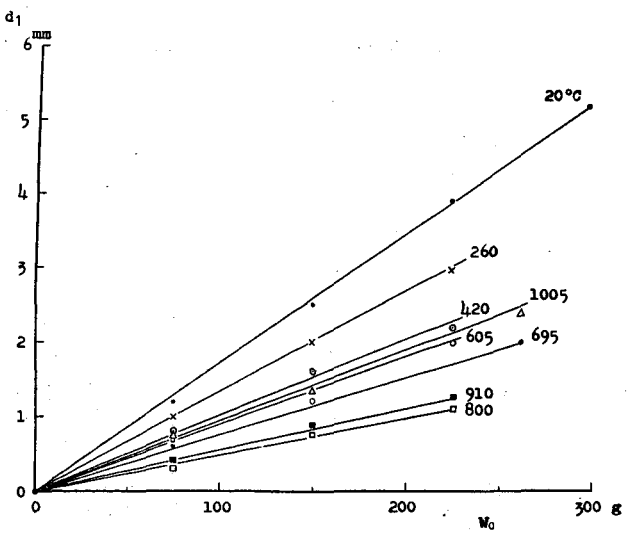

Fig. I-18. Showa-shinzan dome lava. lst heating run.

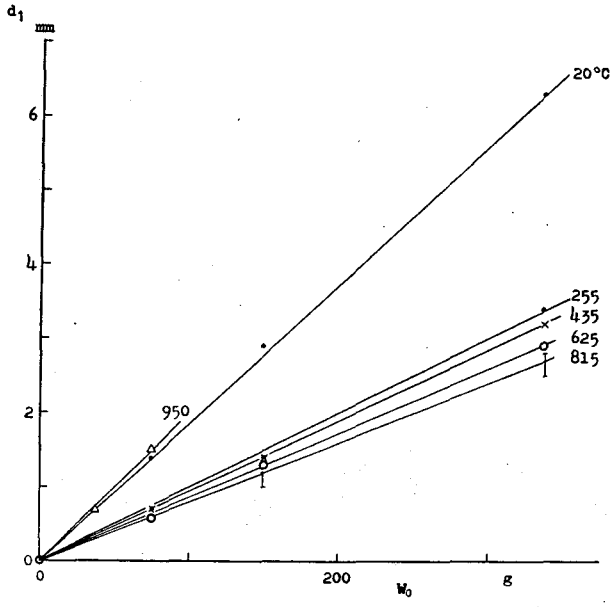

Fig. I-19. Asama Onioshidashi lava. lst heating run.

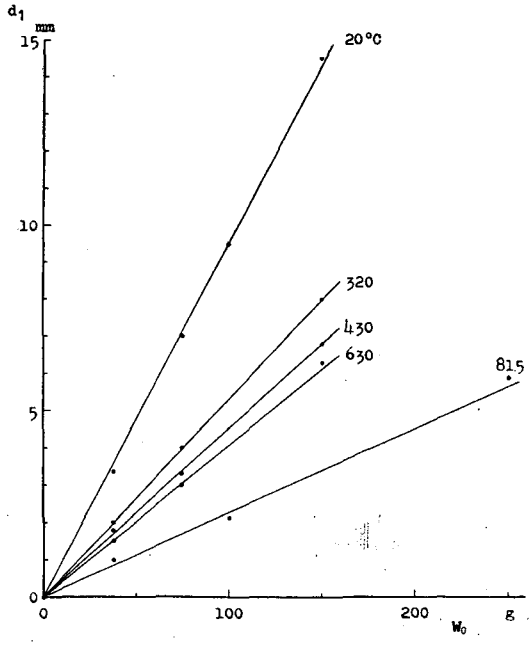

Fig. I-20. Oshima 1950-lava. lst heating run.

(C) Delayed elastic constants (E_2 and λ_2 or η_2).

In a similar way Figs. I–21–23 represent Hooke's law for E_2 at ca. 800° to 1000°C though the data were few at high temperatures. Therefore, E_2 is determined uniquely. η_2 is determined from E_2 and τ_K, τ_K is calculated from the slope of ln $(d_2/2.3)$-time relation as shown in Figs. I–24–27. The slopes obtained at a fixed temperature under different stresses are parallel to each

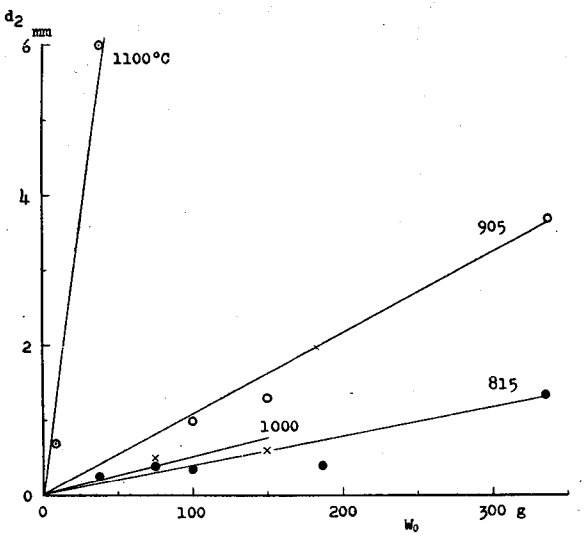

Fig. I-21. Showa-shinzan dome lava.

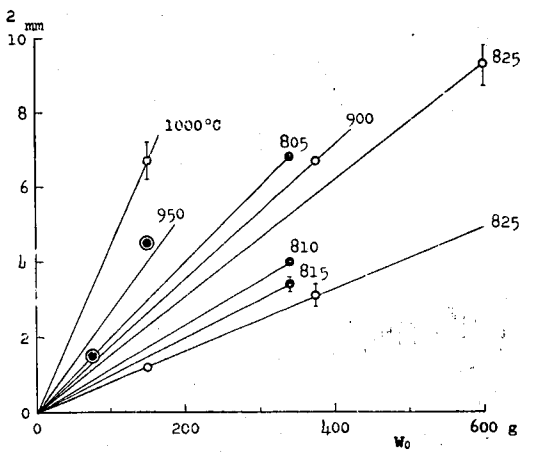

Fig. I-22. Asama Onioshidashi lava.

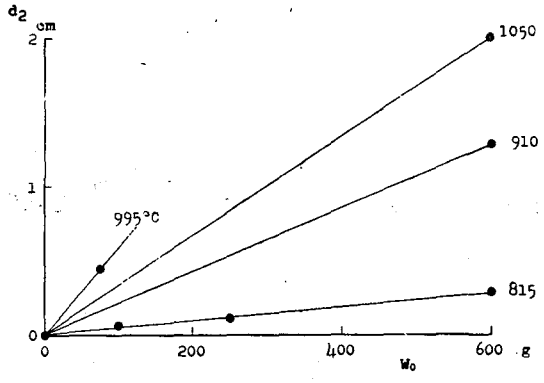

Fig. I-23. Oshima 1950-lava.

other, except for $t \approx 0$. Therefore, η_2 is determined uniquely. τ_M is determined by E_1 and η_1.

Thus the deflection-time curve of volcanic rocks at high temperatures

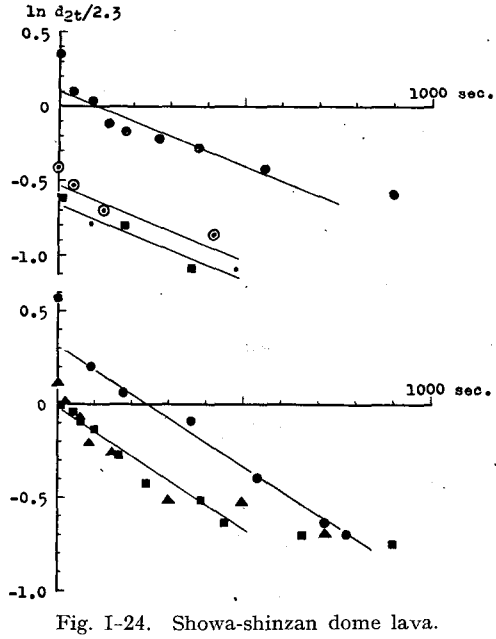

Fig. I-24. Showa-shinzan dome lava.
upper part: 815°C, lower part: 905°C.
●: 337 g, ▲: 150 g, ■: 100 g,
⊙: 75g, •: 38g.

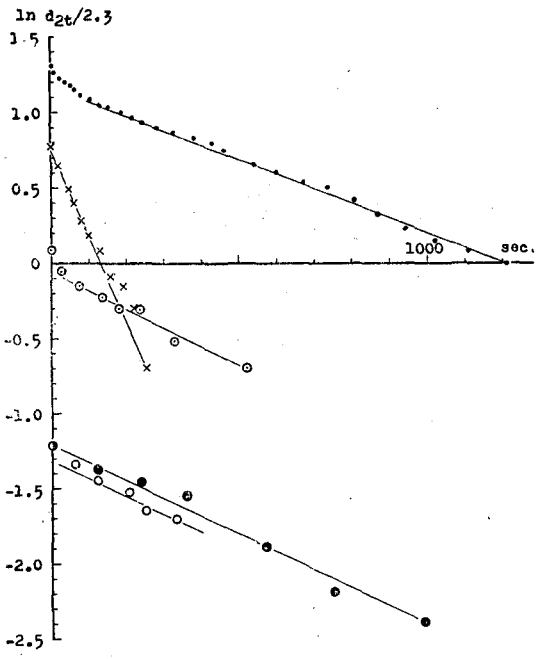

Fig. I-25. Showa-shinzan dome lava.
×: 1100°C, W_0= 38 g, 3rd heating run,
⊙: 915 〃 337 2nd 〃
•: 1000 〃 187 3rd cooling run,
●, ○: 1005 〃 75, 150 1st heating run.

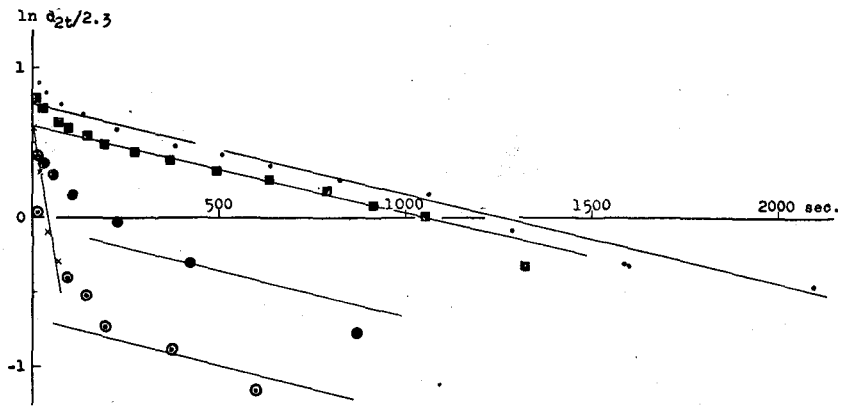

Fig. I-26. Asama Onioshidashi lava.
•: W_0=600 g, ●: 375, ⊙: 100 } 825°C, ■: W_0=375 g, 900°C, ×: W_0=150 g, 1000°C.

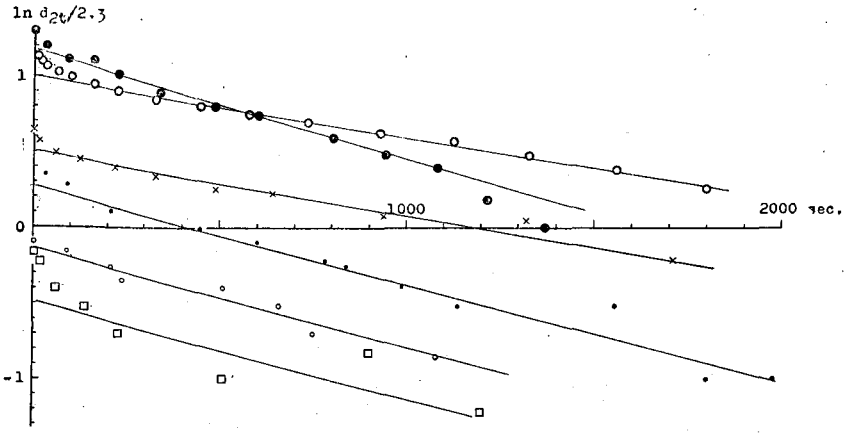

Fig. I-27. Oshima 1950-lava.
•: W_0=600 g
o: 250
□: 16
} 815°C, ×: W_0=75g, 995°C, ○: W_0=600 g, 910°C,
●: W_0=600 g, 1050°C.

may be briefly explained by one single Burgers model, so that all the requirements of Eq. (I–1) are fulfilled, though for the explanation of relation ln (d_{2t}/2.3)-time at $t\approx 0$ it is necessary to combine with it another Kelvin model which should act only at $t\approx 0$.

iii) Experimental values.

Values η_1, E_1, η_2 and E_2 of the three lavas mentioned above and some other lavas are obtained:

(A) η_1.

The change of logarithm of viscosity (in poises) with temperature of some lavas is illustrated graphically in Figs. I–28–38. In these figures are found the results for remolten states obtained by KANI and HOSOKAWA (2) and field observations. Figs. I–39 and 40 are overall diagrams for crystalline lavas and glassy lavas respectively.

Comparison between the first heating run and the third cooling run at ca. 1000°C in Fig. I–28 shows that the deflection-time curves were reversible within 0.1 of logarithm of viscosity. Results of similar examinations are illustrated in Figs. I–30 and 31. Therefore, it may be considered that the previous heat treatment in temperature ranges as in the present experiment does not produce any remarkable effects upon the viscosity.

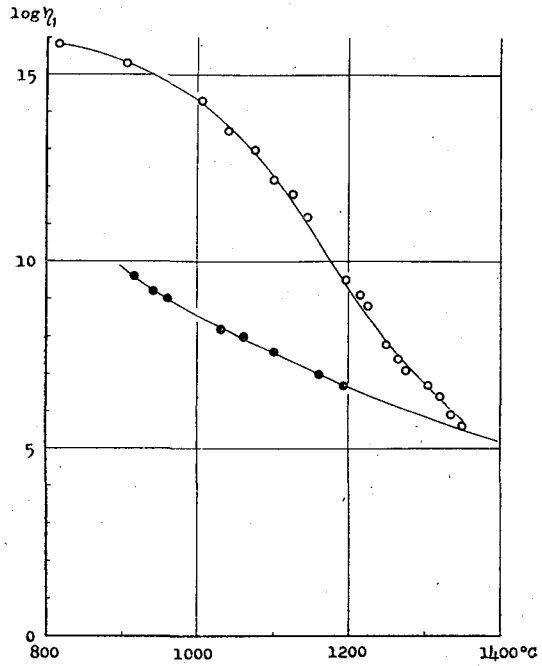

Fig. I-29. Showa-shinzan dome lava.
○: reheating process,
●: artificial glass.

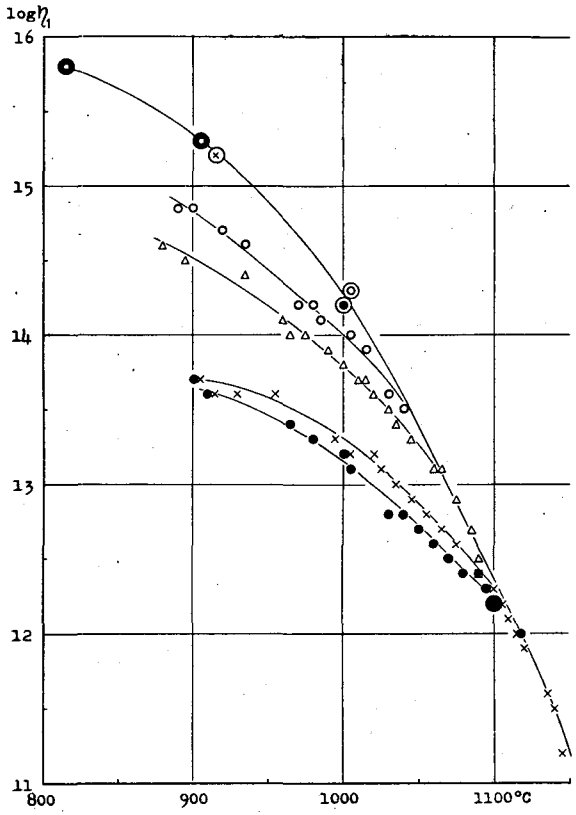

Fig . I-28. Showa-shinzan dome lava.
⊙: 1st heating run (S-1), ⊗: 2nd heating run (S-1),
○: 3rd heating run (S-1), ◉: 3rd cooling run (S-1),
◘: 1st heating run (S-2), •: 1000°C/hour,
×: 600°C/h., △: 100°C/h., ∘: 30°C/h..

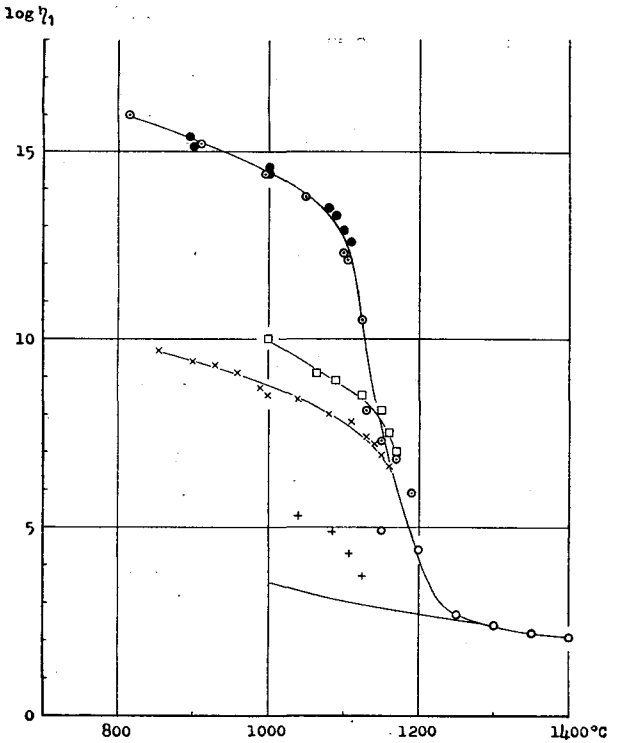

Fig. I-31. Oshima 1950-lava.

⊙: the present writer's data.
●: Sakuma's data,
□: lava having porosity ca. 40%, } reheating process,
×: artificial glass,
○: molten state, +: Minakami's field data,
Solid line: expected value of molten state.

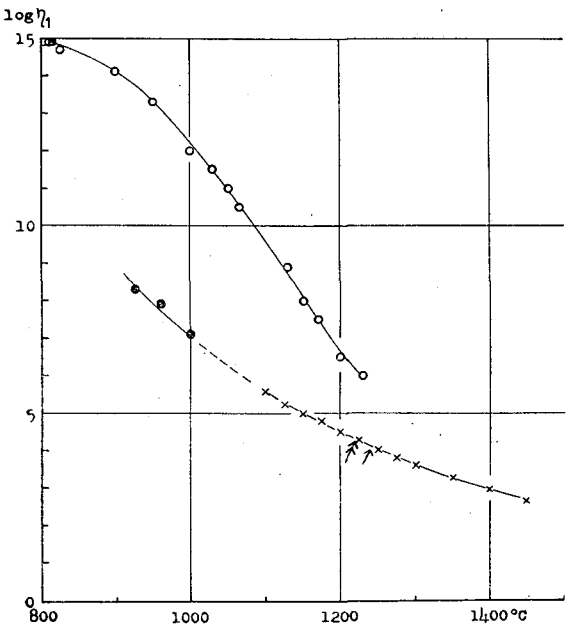

Fig. I-30. Asama Oniosidashi lava.

○: reheating process, ■: 1st heating run at 815°C,
□: 2nd cooling run at 805:C, ●: artificial glass,
×: molten state, ↑: magnetite crystallizes,
↟: magnetite and plagioclase crystallize.

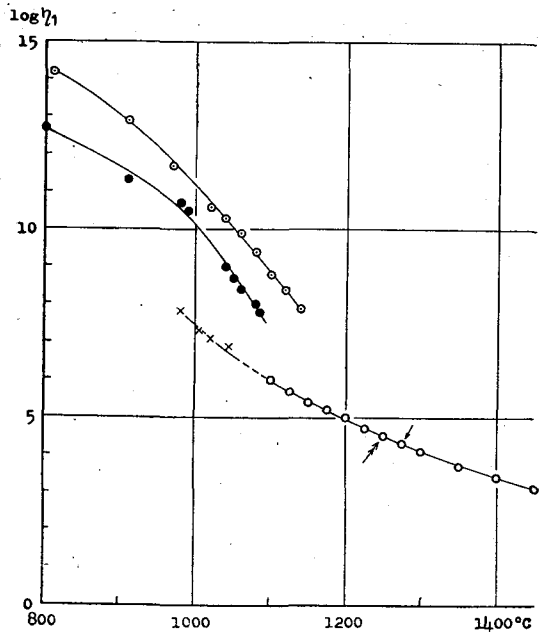

Fig. I-33. Sakurajima lava.

●: 1946-lava,
⊙: 1914-lava,
×: artificial glass,
} reheating process,
○: molten state, ↑: magnetite crystallizes,
↟: magnetite and plagioclase crystallize.

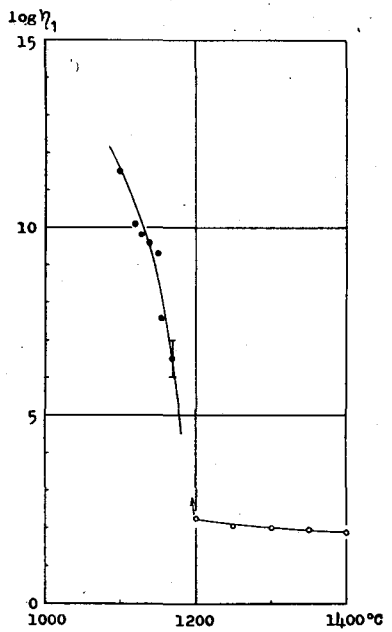

Fig. I-32. Nagahama nepheline basalt.

●: reheating process,
○: molten state.

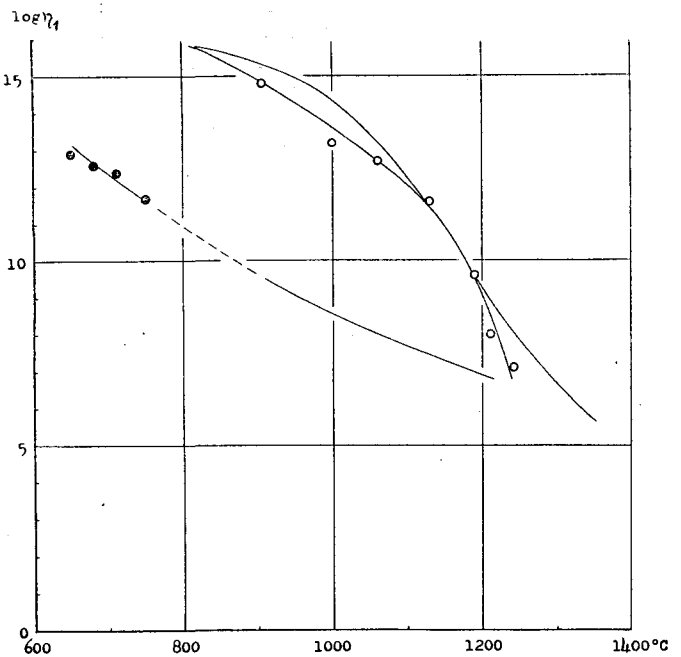

Fig. I-35. Usu lava.

○: somma lava,
●: glassy lava,
Solid lines: Showa-shinzan dome lava for comparison.

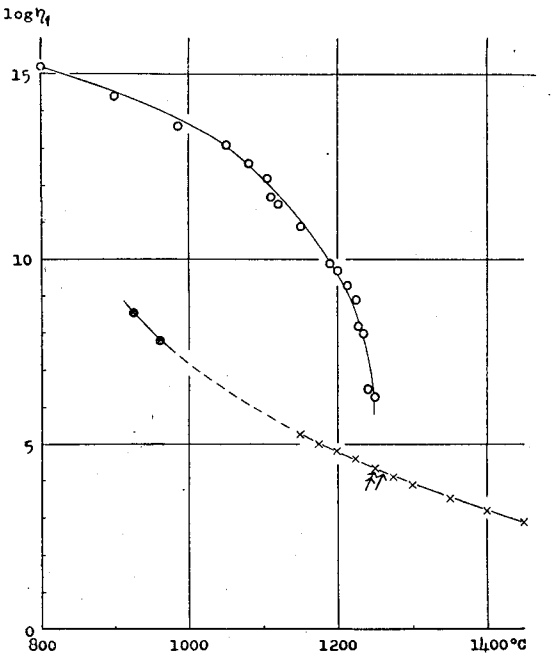

Fig. I-34. Tarumai dome lava.

○: reheating process, ●: artificial glass,
×: molten state, ↑: magnetite crystallizes,
↟: magnetite and plagioclase crystallize.

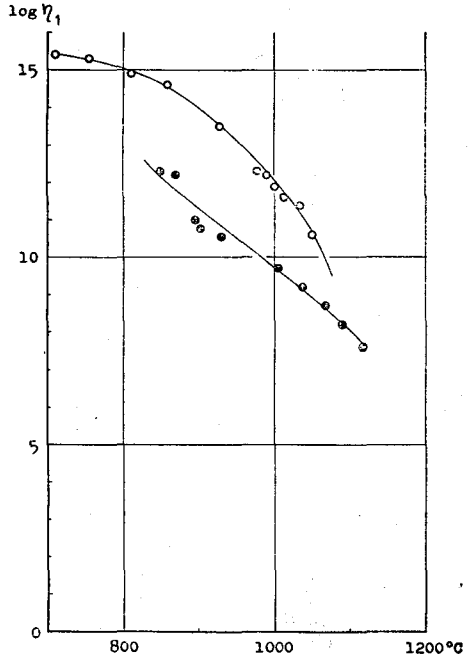

Fig. I-37. Sanukite.
○: step by step process,
●: heated up to the desired temperature.

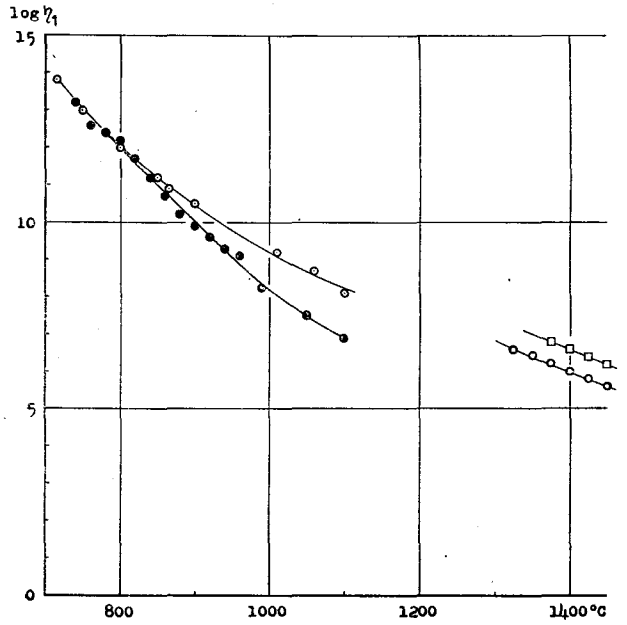

Fig. I-36. Some glassy lavas.
⊙: Shirataki, ●: Wadatoge,
○: Oki, □: Arita.

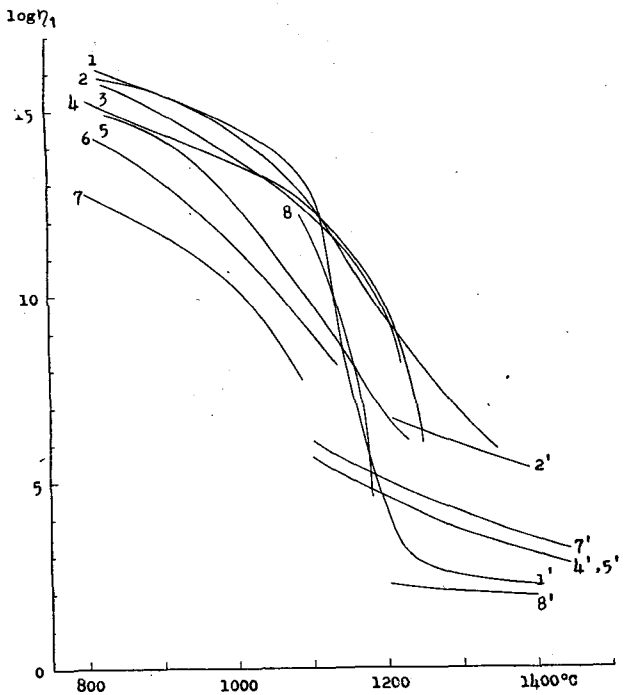

Fig. I-39. Overall diagrams for crystalline lavas.
1 & 1′: Oshima lava, 2 & 2′: Showa-shinzan dome lava, 3: Usu somma lava, 4 & 4′:Tarumai dome lava, 5 & 5′: Asama Onioshidashi lava, 6: Sakurajima 1946-lava, 7 & 7′: Sakurajima 1914-lava, 8 & 8′: Nagahama lava.

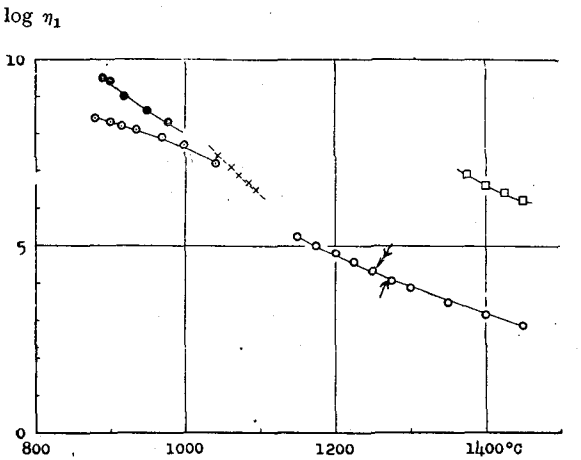

Fig. I-38. Komagadake 1929 pumice.
○: pumice having porosity 72%,
⊙: pumice having porosity 77%, } reheating process,
×: artificial glass,
○: molten state, □: Niijima pumice, ↑: magnetite crystallizes, ↟: magnetite and plagioclase crystallize.

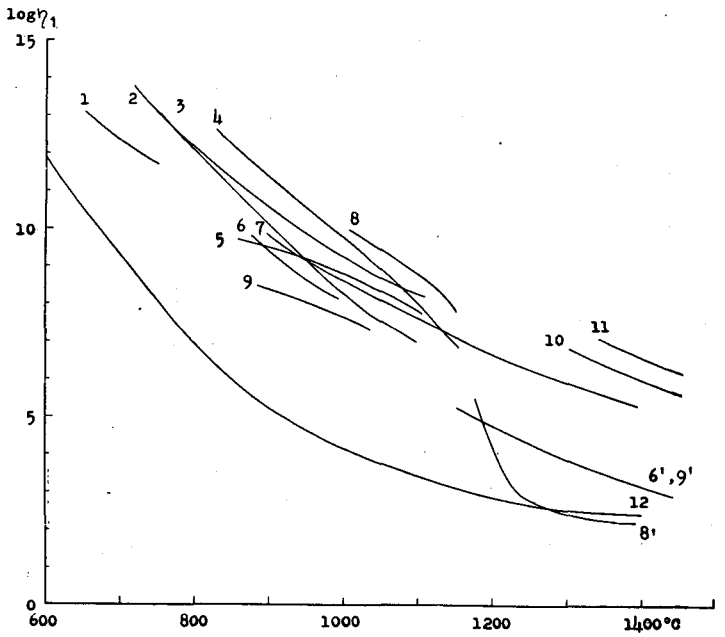

Fig. I-40. Overall diagram for glassy lava and artificial glass.
1: Usu glassy lava, 2: Wadatoge obsidian, 3: Shirataki obsidian, 4: Sanukite, 5: Oshima having porosity, 6: Komagadake pumice's glass, 7: Showa-shinzan dome lava's artificial glass, 8: Oshima 1950-lava's artificial glass, 9: Komagadake pumice, 10: Oki obsidian, 11: Arita pitchstone, 12: Industrial glass.

Viscosities lower than ca. 10^{13} poises were obtained by the measurement of the high deflection rate of the specimen, for which the temperature is raised not step but at a constant and definite rate, viz., 600° or 1000°C/hour. Accordingly a lag of deformation due to the elastic after effect may be observed when this process is used. Fig. I-28, furthermore, shows the apparent viscosity obtained at various heating rates, viz., 1000°, 600°, 100° and 30°C/hour. The apparent viscosity was observed to depend on dT/dt and the more rapidly the specimens were heated, the more fluidal they became, i.e., $\eta_1^{1000} < \eta_1^{600} < \eta_1^{100} < \eta_1^{30}$. The apparent viscosities η_1^{1000}, η_1^{600}, η_1^{100} and η_1^{30} tend to true viscosities, at $10^{12.3}$, $10^{12.3}$, $10^{13.0}$ and $10^{13.5}$ poises respectively. Then, it may be concluded that this method is suitable for measurements of viscosity lower than 10^{12} poises.

Results obtained in the temperature range from ca. 800° to 1400°C are

summarized as follows:

a) The main feature of observations on the crystalline stage, showing the change of viscosity with temperature, is that the curves between 800° and 1400° C are markedly concave or convex towards the origin at low or high temperatures respectively, and the points of inflection of the curves occur at a viscosity of ca. 10^{12}–10^{8} poises. At the same time, the main feature of the results of tests on the glassy state is that the curves behave such as the curve of an ordinary industrial glass, as represented in Fig. I–40.

b) The sharp decrease of viscosity of the crystalline lava at comparatively high temperatures may result from the remelting of minerals contained in the rocks. Fig. I–41 shows the variation of the X-ray diffraction patterns taken by

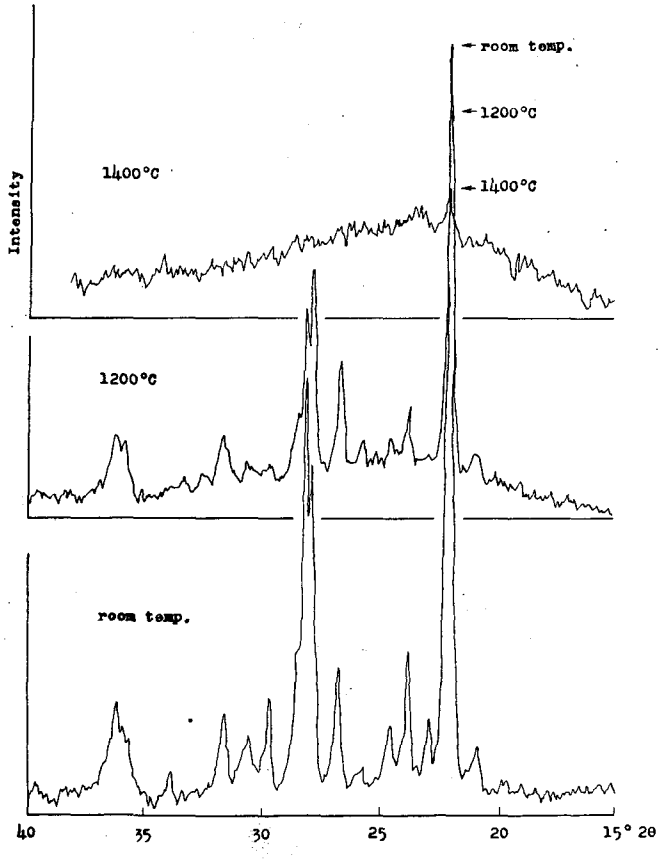

Fig. I-41. X-ray diffraction patterns for the Showa-shinzan dome lava heated up to various temperatures.

a "Norelco" X-ray spectrometer during heat treatments of the Showa-shinzan dome lava samples, which were heated up to the desired temperature under the same heating rate as the principal specimen used in measuring viscosity, and then quenched in the air. In Fig. I–42 the ratio of the maximum spectral

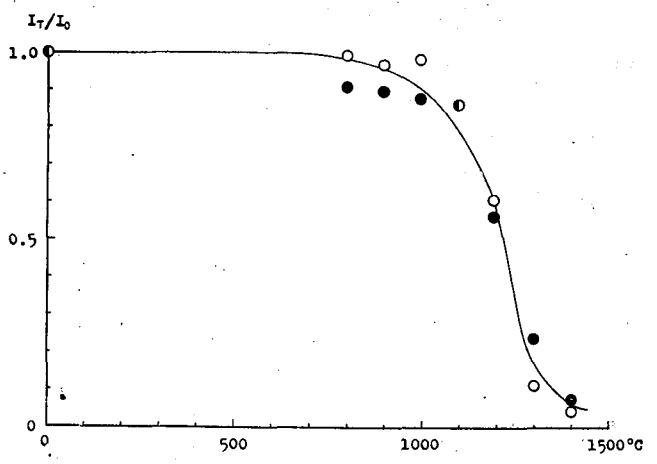

Fig. I-42. Ratio of intensity vs. temperature.
○: plagioclase, ●: cristobalite.

intensity (I_T) of the plagioclase and cristobalite in the specimen heated up to various temperatures to that (I_0) of non-heated specimen is plotted as a function of temperature.

The back grounds of the patterns in Fig. I–41 appear like that of glass, as the temperature is raised, then the intensity decreases abruptly above 1000°C as shown in Fig. I–42. These facts make it reasonable to conclude that

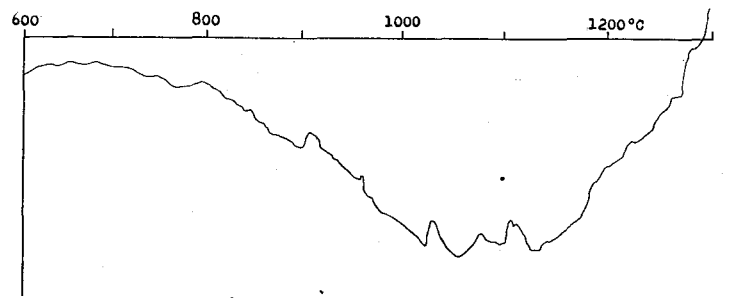

Fig. I-43. Differential thermal analysis pattern for the Showa-shinzan dome lava.

such minerals as plagioclase and cristobalite seem to melt away at a certain high temperature.

Also the differential thermal analysis for the lava at high temperatures, using Pt crucible holder and at a heating rate of 12°C/min. shows the pattern of the endothermic reaction which seems to be caused by the melting of minerals (Fig. I–43).

c) Comparison of viscosities obtained from original lavas with those of glasses prepared by the remelting of the rock exhibited in Figs. I–29, 30, 33 and 34 shows evidently that the former have much higher values than the latter in the temperature range, 900–1300°C. What does the difference mean? Obviously, a special regard should be paid to the effect of chemical composition on the viscosity of molten rock, the composition of which is changed by crystallization as will be discussed below in Chapter II. In addition to this, it should also be noticed that the effective viscosity of a liquid is mechanically increased by suspended materials (26) (27). The viscosity of molten rock increases during measurements at a constant temperature, because of such two effects due to the crystallization of minerals below the liquidus temperature.

In the present experiment the effects occur in the glass prepared by the remelting of the Oshima 1950-lava, i.e., its viscosity is higher than the value expected from the extrapolation of the viscosity of molten state, using Eq. (II–1) in the next chapter (Fig. I–31). After the viscosity measurement the examination of thin section of the glass under the polarization microscope indicated the existence of many fine plagioclases and other minerals which crystallized during one of the reheating process. Furthermore, it may be considered that the difference of viscosity obtained under different heat treatments for the sanukite, as represented in Fig. I–37, is due to a similar effect. Such effect, i.e., the one caused by the existence of crystals in molten rock is so remarkable that equal viscosities of rocks are obtained at low temperatures by reheating experiment in spite of their different chemical composition.

d) The writer would rather believe that the difference of viscosity at low temperatures depends on the porosity of the rock. MacKenzie (28) discussed the effective viscosity of a liquid containing small spherical air bubbles without assuming equal size; he formulated the equation which gives the fractional decrease in the viscosity due to the presence of bubbles:

$$\frac{\eta_0 - \eta_1}{\eta_0} = \frac{5}{3}\alpha$$

where α is the fraction of the volume which is occupied by bubbles, η_1 the effective viscosity and η_0 the true viscosity of the real material. The above relation is compared with experimental data for rock samples at 1000°C in Fig. I–44, where the standards of comparison of porosity and viscosity are the

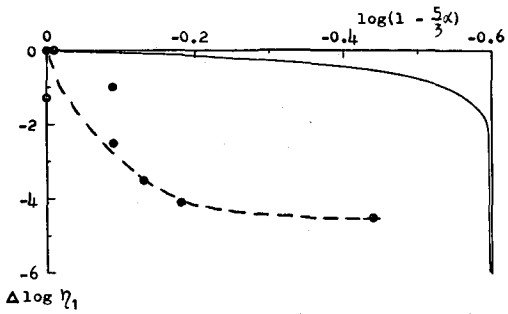

Fig. I-44. Reduction of viscosity at 1000°C vs. pore fraction.
Solid line: MacKenzie's theoretical curve.

values of the Oshima 1950–lava. The discrepancy between them suggests that the shape of bubbles and the way of their connections in rocks are very complicated. Indeed, the above equation was derived on the assumption of closed pores, while the actual rocks have also open pores.

The effect of porosity on viscosity must play a significant role, when viscosity decreases abruptly at a high temperature, where the density decreases

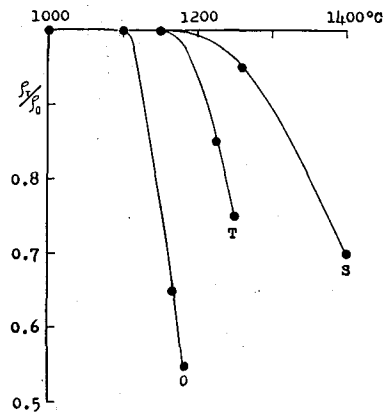

Fig. I-45. Density variation caused by heat treatment.
O: Oshima 1950-lava. T: Tarumai dome lava, S: Showa-shinzan dome lava.

abruptly as exhibited in Fig. I–45. This fact shows the density variation due to bubbling caused by heat treatments. The density variations were measured after quenching other specimens which were heated up to a desired temperature (T) at the same heating rate as the principal specimen used in measuring viscosity.

Accordingly attention must be paid to the fact that the viscosity at temperatures higher than a certain value is not the viscosity of the substantial part of the specimens, because the volatile materials are vesicated. The specimen assumes a foamy state containing many bubbles which considerably decrease the viscosity of the specimens.

From these view points, then, it seems reasonable to conclude that the effect of chemical composition on the viscosity in reheating experiments is non-essential at a relatively low temperature, whilst such effects as porosity and the melting of minerals, consequently the chemical composition, gradually become important at high temperatures.

We are now in a position to discuss the results obtained by the present reheating experiment with respect to the restoration of rocks to the viscosity possessed at or before the time of extrusion.

It has been demonstrated that the presence of crystals in a molten rock may mechanically and chemically exert effects on the viscous behavior of the melt and that, as the temperature is raised, the crystals melt away. Then neglecting the fact that the presence of water affects the viscosity of the melt, the temperature-viscosity curve obtained by the present reheating experiment, i.e., the melting process inverse to the natural cooling process, i.e., the process of the crystallization of crystals, at the time of extrusion. However, each of the experimental values of the viscosity was obtained within several hours at the given temperature, so rocks of such high silica content as the Showa-shinzan dome lava can not attain perfect thermodynamical equilibrium at the given temperature, i.e., if longer times are allowed, the melting of more crystals proceeds, and consequently the viscosity of the sample may gradually decrease at the given temperature (see also Chapter IV below).

On the other hand, in the case of rocks with low silica content and low crystalinity, such as the Oshima 1950–lava, the rocks could not trace the process of thermodynamical equilibrium in the natural cooling process; it follows that the rock minerals crystallize in reheating as indicated in the results of the artificially prepared glass of the Oshima 1950–lava (Fig. I–31).

In any case it may be concluded that the viscosities registered in reheating

experiment are the upper limit for each rock; then the temperature-viscosity relation at or before the time of extrusion of the rock must have been somewhere between the values obtained by reheating experiment and those obtained when the rock is in the ture liquid state, if the presence of water affecting the viscosity of the rock is out of question. The effect of water on viscosity will be treated in Chapter II.

The problem of restoration to the accurate temperature viscosity relation, therefore, requires sufficient knowledge of the crystal growth of minerals in rocks and the cooling rate of the rock. More detailed information on the melting and the crystallization of minerals for the Showa-shinzan dome lava will be discussed in Chapter IV.

For the observed values of the lava extruded in the 1951 Oshima eruption (Fig. I–31) (29) (30), the writer considered the effect of water on the viscosity obtained by reheating experiment in a previous paper (31). However, it is reasonable to consider that the crystallization of some minerals in the process of natural cooling caused higher viscosity than that of the lava in the true liquid condition. Since the effect of water on viscosity seems to be small in case of the Oshima lava, as will be discussed in Chapter II, even if the lava contained water, the crystallization of minerals seems to have been superior to the water in the effect on viscosity, and then the observed values were higher than those in the liquid condition.

Next, attempts will be made to describe briefly some elastic properties obtained by the reheating experiment.

(B) E_1.

The temperature variations of Young's modulus, for the instantaneous part of the elasticity, are shown graphically in Figs. I–46–53. Results obtained are summarized as follows:

a) Young's modulus of crystalline rocks increases with temperature up to a certain point at the first heating, and it decreases abruptly at a high temperature.

b) The modulus of crystalline rocks is greatly affected by the heat treatment, i.e., the modulus in the cooling stage is different from that in heating one.

c) The modulus of glassy rock is almost constant up to a certain temperature, and it decreases abruptly at a high temperature, while the modulus of an ordinary industrial glass decreases slowly with increasing temperature (Figs. I–52 and 53). In this case the heat treatment does not produce any effect

on the modulus.

SHIMOZURU (32) measured the velocity of dilatational waves in a specimen of the Showa-shinzan dome lava in his laboratory. The velocity increased, contrary to the case of ordinary crystalline substances, with temperature. SHIMOZURU ascribed the result to the diminution of the void be-

Figs. I-46-53. Young's modulus vs. temperature for some volcanic rocks.

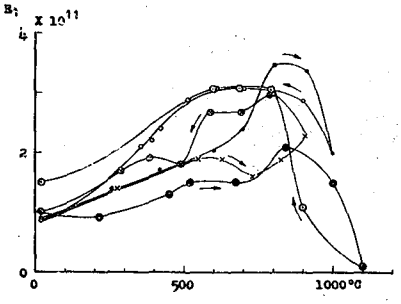

Fig. I-46. Showa-shinzan dome lava.
• : 1st heating run, ○: 1st cooling run,
× : 2nd " ⊗: 2nd "
● : 3rd " ⊙: 3rd "

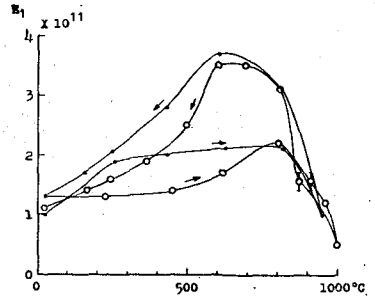

Fig. I-47. Asama Onioshidashi lava.
• : 1st run, ○: 2nd run.

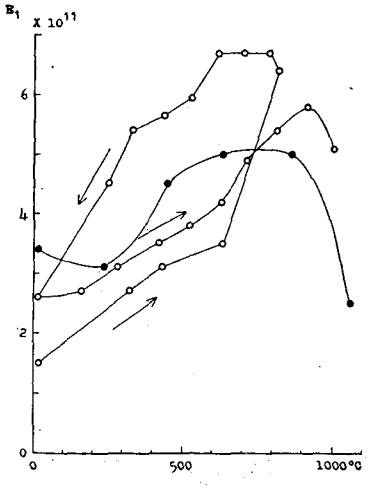

Fig. I-48. Oshima 1950-lava.
○: specimen 0-1,
●: specimen 0-2.

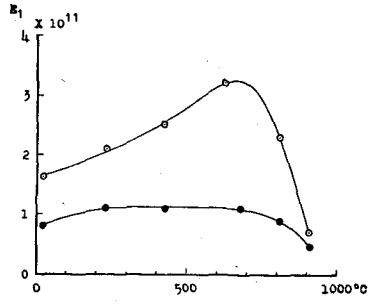

Fig. I-49. Sakurajima lava.
○: 1914-lava,
⊙: 1940-lava.

tween the grain boundaries in consequence of thermal expansion of grains with rising temperatures. Also IIDA and KUMAZAWA (33) obtained the temperature variation of porosity on the basis of the difference between the measured and calculated thermal expansion curves and concluded that an

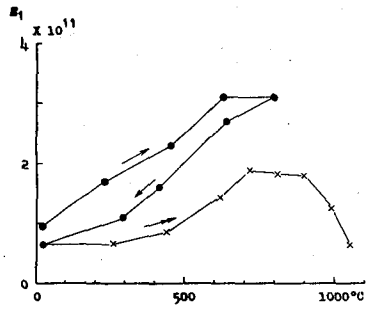

Fig. I-50. Tarumai dome lava.
●: 1st run, ×: 2nd run.

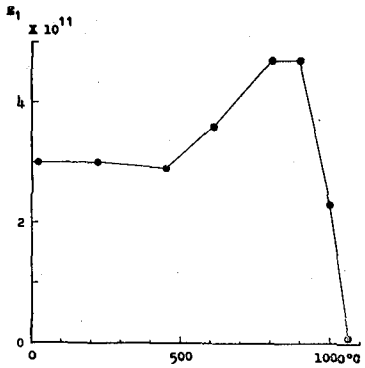

Fig. I-51. Usu somma lava.

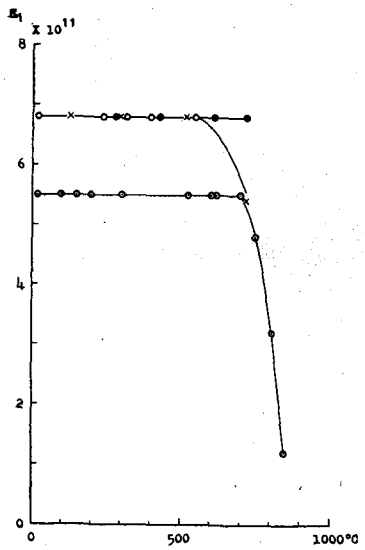

Fig. I-52. Shirataki obsidian.
●: 1st heating run
○: 1st cooling run
×: 2nd heating run
} specimen S-7,
⊙: 1st heating, S-4.

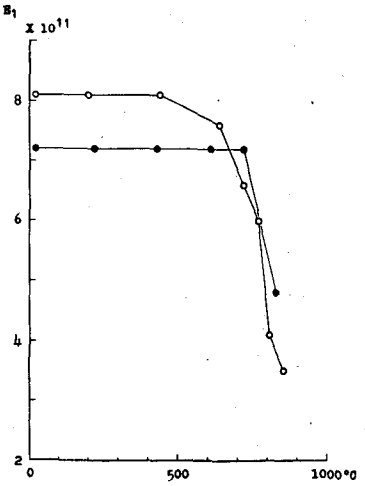

Fig. I-53. Sanukite.
○: specimen Sa-3,
●: Sa-4.

increase in elastic wave velocity is generally correlated to the decrease in porosity and the inversion of an alpha to beta cristobalite is related to the stepwise increase in the wave velocity in the Showa-shinzan dome lava.

A possible explanation of hysteresis phenomena of the Young's modulus obtained in the present experiment also is the change of porosity of rocks due to heat treatment. The elasticity at various porosities up to about 50% has been derived by MACKENZIE (28). Neglecting powers higher than the second of porosity terms, for a typical Poisson's ratio (σ_0=0.3) the changes in Young's modulus may be represented for closed pores in a continuous matrix as

$$E = E_0 (1 - 1.9\alpha)$$

where E and E_0 refer to the actual material and the real material without pores respectively, and α is the fraction of the volume which is occupied by the pores. Taking value E at 800°C as E_0, the above expression gives that the maximum porosity difference (at 1000°C) is evaluated ca. 40%, for the Showa-shinzan dome lava's first run, for example. The porosity difference increasing up to 40% is an extraordinary amount. IIDA and KUMAZAWA, in fact, showed that the decrease in porosity is less than 1%, so further studies to explain the hysteresis phenomena of Young's modulus are necessary in the aspect of the shape of pores as stated already in the discussion of viscosity.

(C) E_2, η_2, τ_K and τ_M.

The temperature variations of delayed elastic constants are shown in Figs. I–54–60. These values diminish with the rise of temperature. Also the temperature variations of τ_K and τ_M which were obtained from η_1/E_1 and η_2/E_2 respectively are shown in Figs. I–54–60. Fig. I–61 is a diagram including all the present results of estimations of τ_K and τ_M. These values are of the order of 10^2–10^4 at temperatures between 800° and 1000°C.

Figs. I-54-60. Delayed elastic constants, retardation and relaxation time vs. temperature for some volcanic rocks.

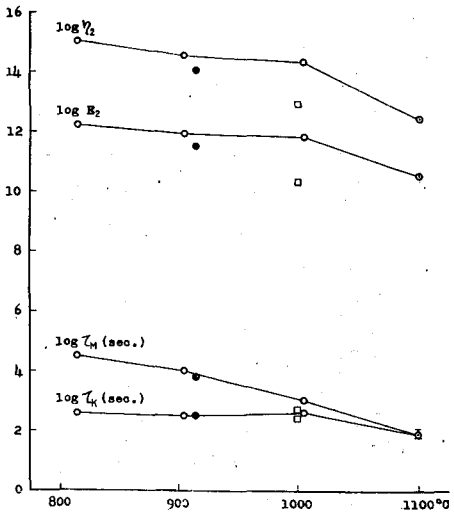

Fig. I-54. Showa-shinzan dome lava.
○: 1st heating run, ●: 2nd heating run, ⊙: 3rd heating run, □: 3rd cooling run.

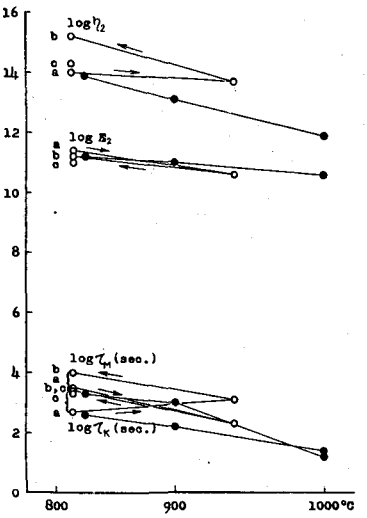

Fig. I55. Asama Onioshidashi lava.
●: specimen A-1, ○: A-2.
(a), (b) and (c) have same meanings as in Fig. I-11.

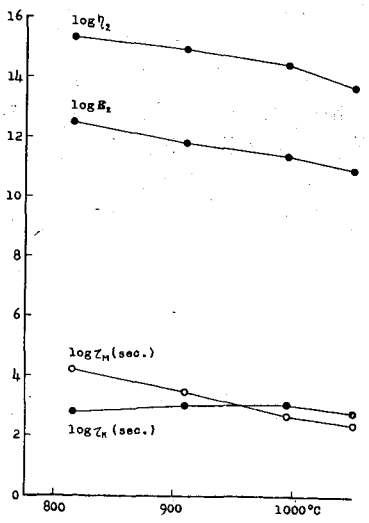

Fig. I-56. Oshima 1959-lava.

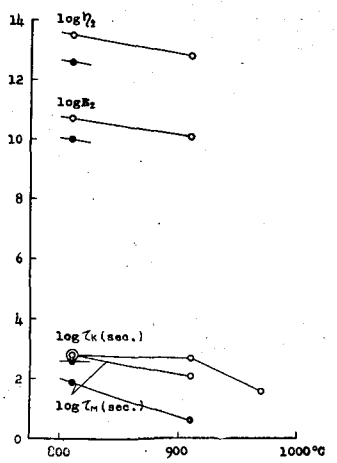

Fig. I-57. Sakurajima lava.
○: 1946-lava, ●: 1914-lava.

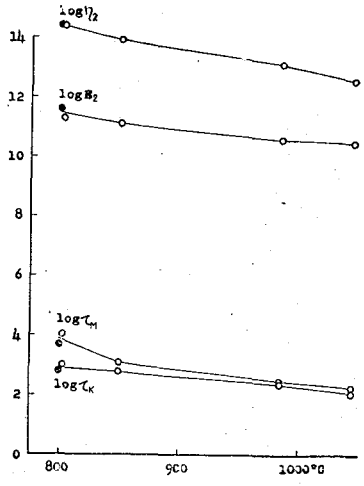

Fig. I-58. Tarumai dome lava.
●: lst run, ○: 2nd run.

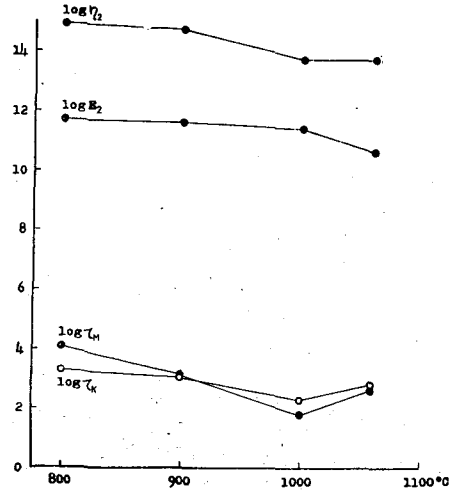

Fig. I-59. Usu somma lava.

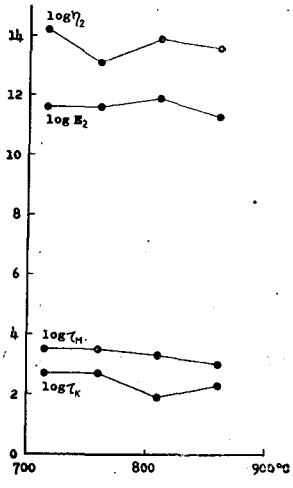

Fig. I-60. Sanukite.

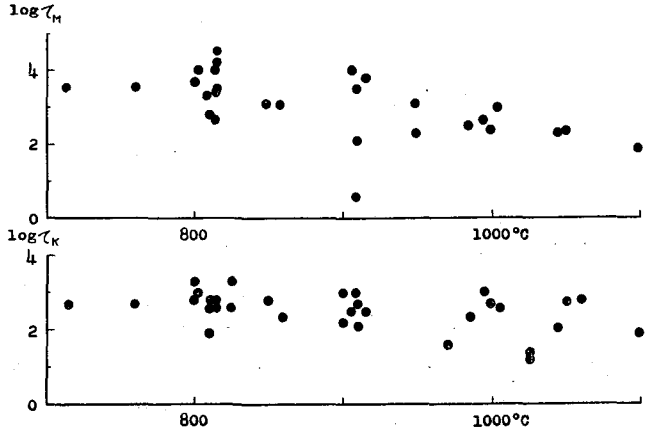

Fig. I-61. Overall diagrams of relaxation and retardation time vs. temperature.

References

1) KANI, K. The measurement of the viscosity of basalt glass at high temperatures, II, Proc. Imp. Acad. Japan, **10** (1934), 79–82.
2) KANI, K. and Hosokawa, K. On the viscosities of silicate rock-forming minerals and igneous rocks, (in Japanese, with abstract in English), Res. Electrotech. Laboratory, No. 391 (1936), 1–105.
3) VOLAROVIČ, M. P., TOLSTOJ, D.M. and KORČEMKIN, L. I. A study of the viscosity of molten lavas from Mount Alaghez, Compt. Rend. (Doklady), Acad. Sci. URSS, **1** (1936), 333–336.
4) PRESTON, E. The viscosity of the soda-silica glasses at high temperatures and its bearing on their constitution, J. Soc. Glass Tech., **22** (1938), 45–81.
5) JONES, G.O. The determination of the elastic and viscous properties of glass at temperatures below the annealing range, J. Soc. Glass Tech., **28** (1944), 432–462.
6) SAKUMA, S. Effect of thermal history on viscosity of Oosima-lava, Bull. Earthq. Res. Inst., **32** (1954), 215–230.
7) REINER, M. Deformation and flow, an elementary to theoretical rheology, Lewis, London, (1949), 279.
8) NAKAGAWA, T. and KANBE, H. Rheology, (in Japanese), Misuzu Book Co. Tokyo, (1959), 526.
9) SAKUMA, S. Op. cit. (6).
10) WATSON, W. A text-book of practical physics, 3rd ed. Longmans, Green and Co., (1926), 98–101.
11) REINER, M. Op. cit. (7), 175.
12) NAKAGAWA, T. and KANBE, H. Op. cit. (8), 528.
13) TSUYA, H. and MORIMOTO, R. Petrography of the 1950–lavas of Oshima volcano, Seven Izu islands, Japan, Bull. Earthq. Res. Inst., **29** (1951), 563–570.
14) YAGI, K. Recent activity of Usu volcano, Japan, with special reference to the formation of Syowa Sinzan, Trans. Amer. Geophys. Union, **34** (1953), 449–456.
15) MORIMOTO, R. Geological and petrological notes on the eruption of Sakura-jima in 1946, Part II, Petrography of 1946–lava, Bull. Earthq. Res. Inst., **26** (1948), 37–40.
16) KAWANO, Y. Natural glasses in Japan, (in Japanese, with abstract in English), Geol. Surv. Japan, Report No. 134 (1950), 1–29.
17) ISHIKAWA, T. The chemical characteristics of the lava from volcano Tarumai, Hokkaido, Japan, J. Fac. Sci. Hokkaido Univ., Ser. 4, **8** (1952), 107–135.
18) TSUYA, H. The volcano Komagatake, Hokkaido, its geology, activity and petrography, Bull. Earthq. Res. Inst., **8** (1930), 238–270.
19) ISSHIKI, N. Miyake-jima, Hachijô-jima, No. 3. Explanatory text of the geological map of Japan. Scale 1:50,000, (in Japanese, with abstract in English), Geol. Surv. Japan, (1960), 1–85.
20) MORIMOTO, R. Unpublished data, oral communications to Prof. SAKUMA, see "Elastic and viscous properties of volcanic rocks at elevated temperatures, Part 2, Bull. Earthq. Res. Inst., **31** (1953), 63–70.
21) KOZU, S., WATANABE, M. and AKAOKA, J. Studies on melting phenomena of volcanic rocks, (in Japanese), J. Geol. Soc. Tokyo, **26** (1919), 57–83.
22) KOZU, S. Studies on the ejectaments of the volcano of Miyakejima, (in Japanese),

Chikyu (the Globe), **9** (1928), 247–264.

23) KOZU, S. and SETO, K. Chemico-petrographic studies of pumice, poured out from Komagatake in 1929 (1), (in Japanese), Gan-Ko (J. Japanese Assoc. Min. Petro. Eco. Geol.), **5** (1931), 255–264.

24) KOZU, S. and SETO, K. Chemico-petrographic studies of pumice, poured out from Komagatake in 1929 (2), (in Japanese), Gan-Ko (J. Japanese Assoc. Min. Petro. Eco. Geol.), **7** (1932), 1–10.

25) ARAMAKI, S. The 1783 activity of Asama volcano, Part 1, Japanese J. Geol. Geogr, **27** (1956), 189–229.
Part II, **28** (1957), 11–33.

26) HAPPEL, J. Viscosity of suspensions of uniform spheres, J. Appl. Phys. **28** (1957), 1288–1292.

27) BECHER, P. Emulsions: theory and practice, Reinhold Pub. Corp. New York, (1957), 54–75.

28) MACKENZIE, J.K. The elastic constants of a solid containing spherical holes, Proc. Phys. Soc. B. **63** (1950), 2–11.

29) MINAKAMI, T. On the temperature and viscosity of the fresh lava extruded in the 1951 Oo-sima eruption, Bull. Earthq. Res. Inst., **29** (1951), 60–69.

30) YOKOYAMA I. The flow and upwelling of lava (Parts I and II), (in Japanese, with abstract in English), Bull. Volc. Soc. Japan, 2nd Ser., **6** (1961), 51–59.

31) MURASE, T. The viscous behavior of Tarumai dome lava and Oshima lava, J, Fac. Hokkaido Univ. Japan, Ser. VII, **I** (1959), 181–194.

32) SHIMOZURU, D. Elasticity of rocks and some related geophysical problems, Japanese J. Geophys. **2** (1960), 1–85.

33) IIDA, K. and KUMAZAWA, M. Elastic wave velocity and thermal expansion of volcanic rocks at high temperatures, (in Japanese, with abstract in English), Bull. Volc. Soc. Japan, 2nd Ser., **6** (1961), 60–69.

Chapter II. Effect of Composition on Viscosity

§ 1. Introduction

In Chapter I. § 4, it was concluded that chemical compositions of rocks may be unessential for the viscosity obtained by reheating experiments at a relatively low temperatures. However, some investigators have carried out experiments on the viscosity of molten rocks of various compositions and found a relation between the viscosity and silica content only (1) or viscosity and Loewinson-Lessing's acidity coefficient (2). Many investigators in the field of glass technology have carried out experiments on the effect of the composition of various sorts of glass on viscosity. The results obtained have been fully dealt with by MOREY in his book (3).

The effect of the water content on the viscosity of a magma is of the greatest importance in connection with volcanological phenomena. From the properties and reactions of industrial glasses with water-vapor, DIETZEL (4) concluded that hydroxyl (or even hydrogen ions) greatly reduce the viscosity of the silicate melts. Also BUERGER (5) came to a similar conclusion on the basis of the concept of bridge density. Neither investigator, however, formulated a quantitative relation. SABATIER (6) investigated experimentally the influence of the water content on the viscosity of rétinite which is a glass having the composition of granite and showed the considerable reduction of viscosity of the rock containing water. The decrease in viscosity due to the change of compositions of molten rocks at relatively high temperatures corresponds directly to weakening of the network structure.

The purpose of this chapter is to describe the effect of the composition of molten rocks on viscosity and to discuss quantitatively the effect of water content on viscosity using the concept of bridge density.

§ 2. Concept of bridge density

The concept of bridge density, as developed by BUERGER (5), may be summarized as follows:

In a molten rock each silicon atom is surrounded by four oxygen atoms. A silicon atom extends every bond of strength 1 to each oxygen (7). If the silicon: oxygen ratio in the melt is high, many oxygen atoms may satisfy their charge of –2 by receiving bonds of strength 1 one by one from each of two silicon atoms. Whenever this sharing of oxygen atoms occurs, it causes the silicon and oxygen atoms to become sets of an irregular but extended space networks in the melt.

Now, the viscosity of a melt pervaded by these sets of networks is directly related to the average number of these Si-O-Si bridges per silicon atom as will be mentioned below in § 3. For example, in the pure molten SiO_2 there are on the average 2 bridges per silicon atom, in the molten $MgSiO_2$ there is on the average 1 bridge per silicon atom; while in the molten Mg_2SiO_4 there are no bridge per silicon atom. It is for this reason that the more siliceous "dry" magmas are the more viscous they are.

This bridge relation can easily be generalized and put into a quantitative form. The total number of oxygen atoms per silicon atom is equal to 4 (the maximum) minus the number of half-oxygens belonging to other silicon atoms due to sharing, or

$$\frac{O}{Si} = 4 - \frac{\frac{1}{2}S}{Si}, \qquad \text{Eq. (II-1)}$$

where O: the total number of oxygen atoms in the molten rock,
Si: the total number of silicon atoms in the molten rock,
S: the total number of shared oxygen atoms in the molten rock,
b: the total number of bridges in the molten rock.

If 100 parts of molten rock is taken, the total number of each kind of atoms equals to the percentage of atoms in the molten rock.

From Eq. (II-1),

$$\frac{\frac{1}{2}S}{Si} = 4 - \frac{O}{Si}, \qquad \text{Eq. (II-2)}$$

Now, where a brdgie occurs, it is shared between two silicon atoms, so the bridge-per-silicon value, i.e., the bridge density is

$$\frac{b}{Si} = \frac{S}{2Si}. \qquad \text{Eq. (II-3)}$$

Comparing this with Eq. (II-2), it is evident that

$$\frac{b}{Si} = 4 - \frac{O}{Si}. \qquad \text{Eq. (II-4)}$$

In case that an OH^- ion is substituted for an oxygen atom at the corner of a silicon tetrahedron, the substitution removes a possible network bridge. Each oxygen bridge must be replaced by two OH^- ions in order to satisfy the

two silicons on opposite ends of the substituted bridge. The effect of hydroxyl can be incorporated into Eq. (II-4). Let OH be the total number of OH^- ions in the molten rocks. Then, since each one of these ions reduces the number of sharable oxygen atoms, the quantity $(4 - OH/Si)$ must be substituted for 4, and $(O+OH)$ must be substituted for O in the preceding three equations II-1, 2 and 4. Thus,

$$\frac{b}{Si} = \left(4 - \frac{O}{Si} - \frac{2OH}{Si}\right). \qquad \text{Eq. (II-5)}$$

The bridge density is connected with the total atoms of metallic ion in rocks. MIYAKE (8) expressed the chemical composition of surface rocks in terms of the ratio of constituent ions, and obtained the following general

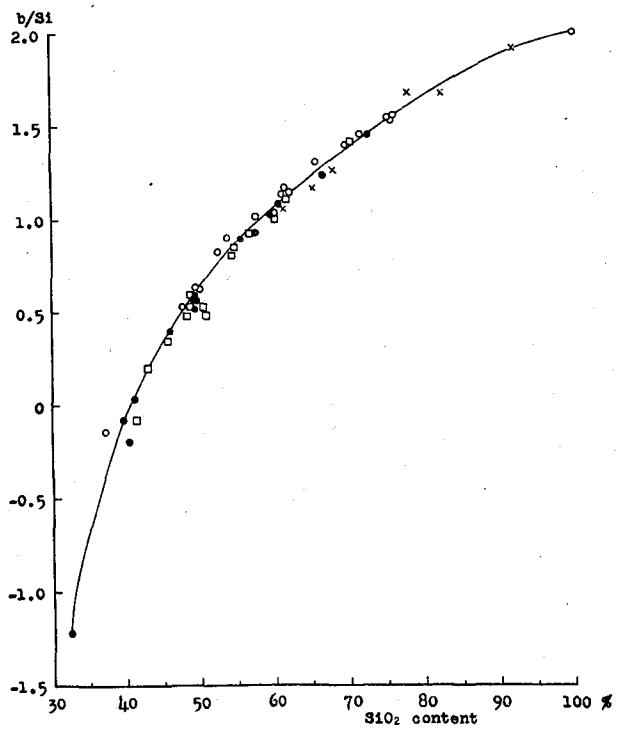

Fig. II-1. Silica content vs. bridge density.
●: igneous rocks, □: plutonic rocks, } Daly's average analysis data,
×: sedimentary rocks,
○: rocks used in Fig. II-3.

relation, using Daly's average analysis data. Let the ratio of silicon and oxygen ions in rocks be Si and O, and let the ratio of total metallic ions (cation and H^+) be R. The one gets

$$O = 1/2 + (1/2)\,Si\,. \qquad \text{Eq. (II-6)}$$

$$O = 2/3 - (1/3)\,R\,. \qquad \text{Eq. (II-7)}$$

Table II-1.

Igneous rocks	Silica content	atomic ratio of Si	atomic ratio of O	O/Si	b/Si
Liparite	72.80	24.27	61.82	2.55	1.45
Dacite	65.68	22.07	61.07	2.77	1.23
Andesite	59.59	20.44	60.82	2.98	1.02
Quartz basalt	55.46	19.50	60.75	3.12	0.88
Basalt	49.06	17.23	59.23	3.44	0.56
Trachyte	60.68	20.80	60.37	2.90	1.10
Phonolite	57.45	19.09	58.67	3.07	0.93
Nephelinite	41.17	14.42	57.10	3.96	0.04
Trachydolerite	49.20	17.37	59.11	3.40	0.60
Tephrite	49.14	17.16	58.91	3.43	0.57
Nephelin-basalt	39.87	14.03	57.08	4.07	−0.07
Leucite-basalt	46.18	15.99	57.52	3.60	0.40
Dunite	40.49	13.17	55.30	4.20	−0.20
Minette	49.45	16.61	57.75	3.48	0.52
Alnoite	32.31	10.06	52.47	5.22	−1.22
Plutonic rocks					
Granite	70.18	23.90	62.14	2.60	1.40
Quartzdiorite	61.59	21.07	60.96	2.89	1.11
Diorite	56.77	19.59	60.28	3.08	0.92
Quartzgabbro	54.39	18.70	59.66	3.19	0.81
Gabbro	48.24	16.87	59.34	3.52	0.48
Syenite	60.19	20.24	60.54	2.99	1.01
Nephelinsyenite	54.63	18.73	59.03	3.15	0.85
Urtite	45.61	15.75	57.52	3.65	0.35
Essexite	48.64	17.13	59.33	3.46	0.54
Theralite	45.61	15.70	57.39	3.66	0.34
Ijolite	42.81	15.92	60.40	3.79	0.21
Shonkinite	48.66	17.24	58.63	3.40	0.60
Anorthosite	50.40	17.46	60.65	3.47	0.53
Picrite	41.30	13.64	55.59	4.08	0.08
Kersantite	50.79	15.89	55.90	3.52	0.48
Sedimentary rocks					
Orthoquartzite	92.3	31.9	66.0	2.07	1.93
Gray-wacke	68.1	22.3	61.3	2.75	1.25
Chert	82.69	25.87	60.41	2.34	1.66
Shale	58.10	18.93	58.07	3.07	0.93
Sandstone	78.33	27.25	63.10	2.32	1.68
Paleozoic Clay-slate (Europe)	58.35	19.25	58.66	3.05	0.95
Paleozoic Clay-slate (Japan)	61.42	20.20	59.65	2.95	1.05
Mesozoic Clay-slate (Japan)	65.66	21.20	60.21	3.84	0.16

From Eqs. (II–6,7) one gets

$$Si = 1/3 - 2R/3 .$$

If one takes $Si+O+R=100$, then,

$$O/Si = (100 - R)/Si - 1 . \qquad \text{Eq. (II–8)}$$

From Eqs. (II–4, 8),

$$b/Si = 5 - (100 - R)/Si . \qquad \text{Eq. (II–9)}$$

Thus, the relation between R/Si and SiO_2 in rocks can be converted into that between b/Si and SiO_2. The relation is shown in Fig. II–1 and Table II–1. This figure is available for the discussion in this chapter.

§ 3. Relation between viscosity and bridge density

Some investigators (1) (2) have attempted to represent the viscosity of molten rocks by a simple relation. These early attempts, however, do not consider the effect of the change of chemical composition on viscosity. The present writer considers that effect and represents a simple relation as follows:

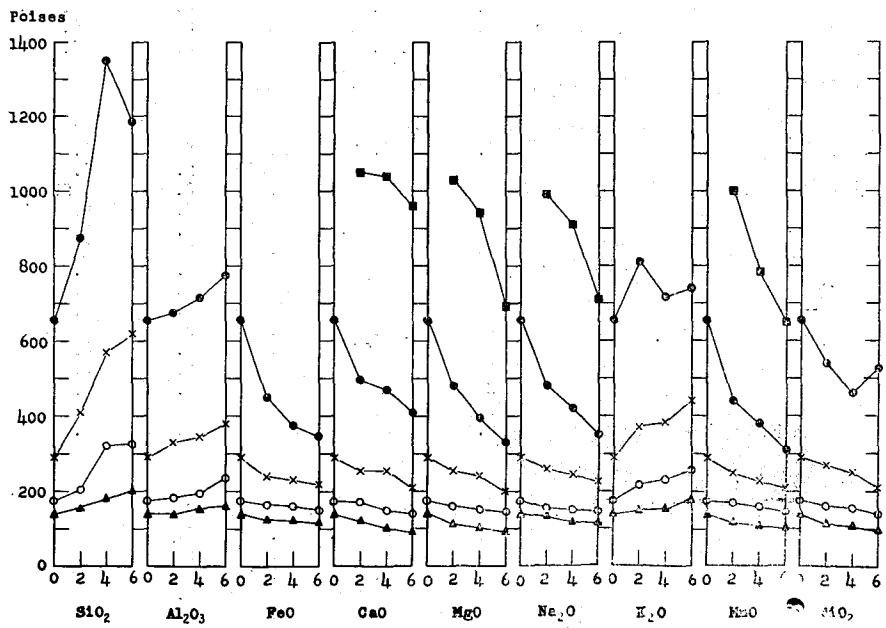

Fig. II-2. Effect of chemical composition on viscosity(after KANI and HOSOKAWA). ▲ 1400°C, ○ 1350°C, × 1300°C, ● 1250°C, ■ 1200°C.

KANI and HOSOKAWA (1) investigated the viscosities of 27 kinds of mixtures, each mixture having been prepared by adding 2, 4 or 6 parts of SiO_2, Al_2O_3, FeO, CaO, MgO, Na_2O, K_2O, MnO or TiO_2 respectively to 100 parts of basalt from Genbudo. At high temperatures, when SiO_2, Al_2O_3, or K_2O was mixed with the basalt, the viscosity increased as the amount of SiO_2, etc. was increased, and when other oxides were mixed the viscosity decreased except some results at low temperatures. The results obtained are shown in Fig. II–2. The change of chemical composition is shown in Table II–2. For

Table II–2. The chemical composition of Genbudo basalt melts to which are added nine different oxides. (after KANI and HOSOKAWA).

	Olivine basalt, Genbudo	Water free	Weight percentages of the chemical compositions of the Genbudo basalt melts to which are added nine different oxides in the ratios as stated.		
			100:2	100:4	100:6
SiO_2	49.29	49.75	50.74 (48.78)	51.68 (47.85)	52.59 (46.94)
Al_2O_3	18.49	18.66	20.25 (18.29)	21.79 (17.94)	23.26 (17.60)
Fe_2O_3	2.38	8.99 (as FeO)	10.77 (as FeO)	12.49 (as FeO)	14.14 (as FeO)
FeO	6.77		(8.81)	(8.64)	(8.48)
CaO	8.14	8.22	10.02 (8.06)	11.75 (7.90)	13.42 (7.75)
MgO	6.09	6.14	7.98 (6.02)	9.94 (5.90)	11.90 (5.79)
Na_2O	3.93	3.97	5.85 (3.89)	7.66 (3.82)	9.41 (3.75)
K_2O	1.79	1.81	3.74 (1.77)	5.59 (1.74)	7.37 (1.71)
MnO	0.22	0.22	2.18 (0.22)	4.06 (0.21)	5.87 (0.21)
TiO_2	2.22	2.24	4.16 (2.20)	6.00 (2.15)	7.77 (2.11)
H_2O	0.88	—	—	—	—
Total	100.20	100.00	100.00	100.00	100.00

example, in the case of addition of SiO_2=4 parts, which is denoted by Si_4, SiO_2=51.68% and other oxide contents correspond to the values in parenthesis, i.e., Al_2O_3=17.94, FeO=8.64, etc. For another example, in the case of addition of CaO=6 parts, which is denoted by Ca_6, CaO=13.42, SiO_2=46.94, Al_2O_3=17.60, etc.

From Fig. II–2 the ratio of increase or decrease of viscosity to the addition of oxides can be seen to have almost the same value in all oxides. Therefore, the value of $SiO_2+Al_2O_3+K_2O$ can be used as the measure of the increase of viscosity and the sum of other oxide contents as that of the decrease of viscosity. Thus, the ratio (other oxides)/$(SiO_2+Al_2O_3+K_2O)=\beta$ is a measure of the change of viscosity. The relation between logarithms of viscosity and β is shown in Fig. II–3.

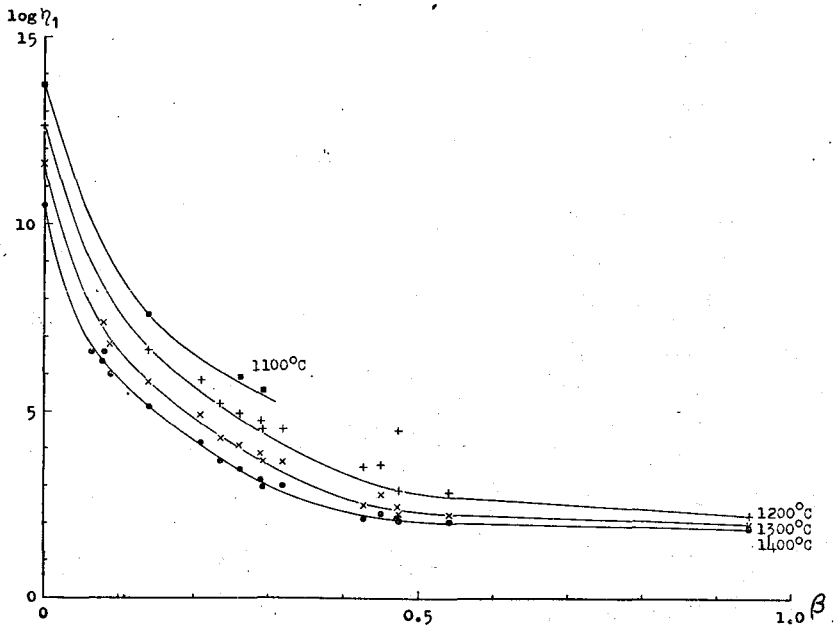

Fig. II–3. Viscosity vs. β-value.

On the other hand, it was stated in § 2 that the bridge density is related to viscosity. The quantitative relation between them is shown in Fig. II–4, where the logarithm of viscosity is represented as a function of the bridge density. The bridge density was calculated from Table I–2 (B) in Chapter I. Using Kani and Hosokawa's data, Inuzuka's data (9) and the present writer's data the respective viscosities of molten or glassy rocks are plotted and the smoothed curves are drawn by use only of values of the states which seem to be completely non-crystalline. This figure shows that the viscosity of molten rocks increases abruptly near $b/Si=0.8$, which corresponds to silica content= 55%. If the chemical composition of a molten rock is known, the value of

viscosity of the molten rock may be roughly estimated using Fig. II–3 or 4.

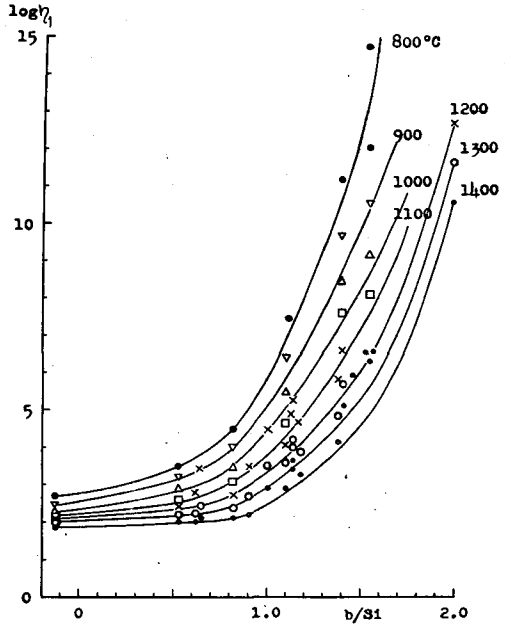

Fig. II-4. Viscosity vs. bridge density.

§ 4. Activation energy for viscous flow of molten rocks

The results of estimates of viscosity of glassy lava in Chapter I can be expressed by a function such that the logarithm of viscosity is proportional to the inverse of temperature. EYRING et al. (10) treated the viscosity of liquid from the viewpoint of the theory of absolute reaction rates. In general, the viscosity of a liquid, as a function of temperature, is represented by an equation of the form

$$ln\,\eta_1 = E_\eta/RT + B_1\,, \qquad \text{Eq. (II–10)}$$

where η_1 is the viscosity, E_η is the experimental activation energy for viscous flow and B_1 is represented as a function of the length of an element and the frequency of the vibration of an element (11). This formula of viscosity of molten glass will be applied to the viscosity of molten rock.

Calculation is made of values of E_η and B_1 by the use of above formula for Kani and Hosokawa's data and the present writer's data. The results which show that as SiO_2, b/Si or $P_2O_5+SiO_2+Al_2O_3+TiO_2$ decrease, E_η decrease

and B_1 increase, are shown in Figs. II–5–8.

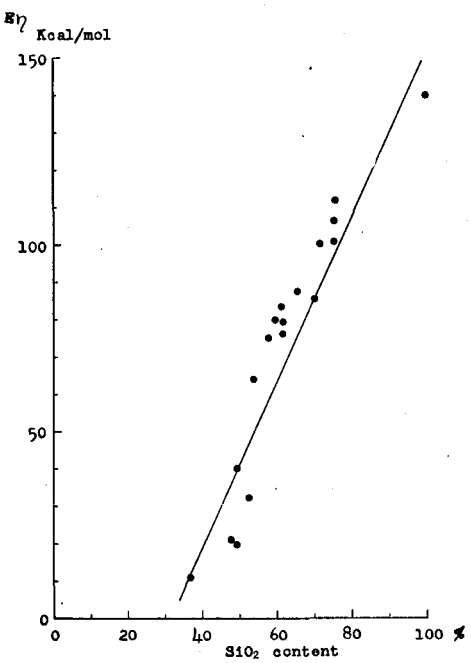

Fig. II-5. Activation energy for viscous flow vs. silica content.

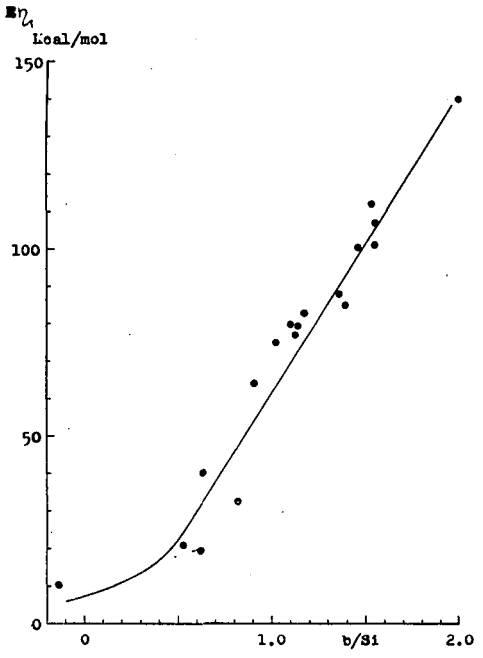

Fig. II-6. Activation energy for viscous flow vs. bridge density.

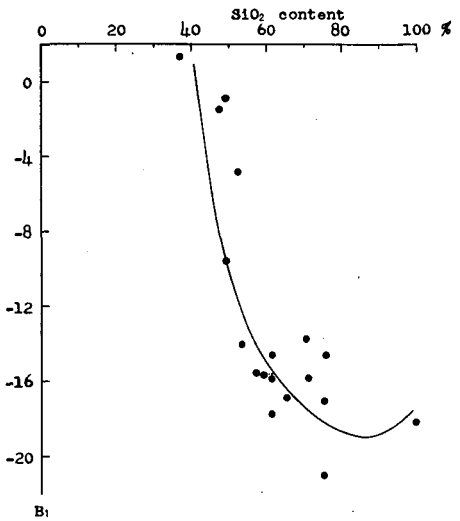

Fig. II-7. log pre-exponential factor vs. silica content.

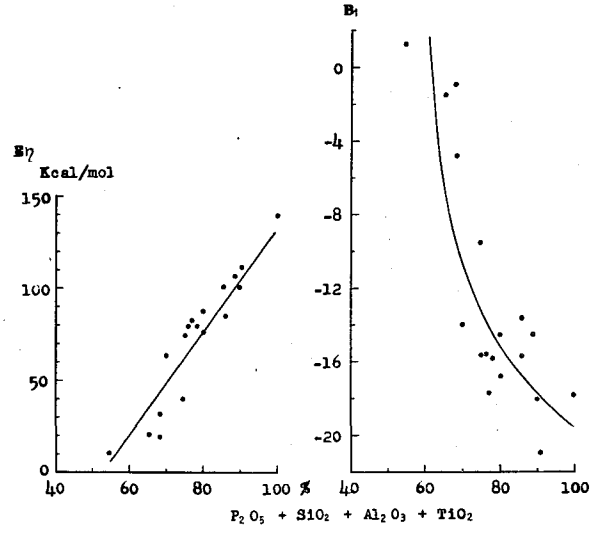

Fig. II-8. Activation energy for viscous flow and log pre-exponential factor vs. amount of oxides of ions which formed N.W.F.

A polycomponent glass is formed as long as the composition containes a high percentage of cations which are surrounded by oxygen in triangular or tetrahedral co-ordination. These polyhedra share corners, and at least some oxygen atoms are bound to two cations and do not share bonds with other cations (12). Thus, the ions in glass are classified into three groups,

Table II-3. Classification of the ion found in rocks.

M in MO_x	Valence	$2z/a^2$		
P	5	4.3	pure *N. W. F.*	
Si	4	3.14		
Ti	4	2.08	*N. W. F.* under normal conditions	
Al	3	1.69		
Fe	3	1.57	*N. W. F.* and *N. W. M.* coexist under equilibrium relation	*I*
Mg	2	0.95		
Fe	2	0.87		
Mn	2	0.83		
Ca	2	0.69	pure *N. W. M.*	
Na	1	0.35		
K	1	0.27		

viz., network-former (*N.W.F.*), intermediate (*I.*) and network-modifier (*N.W.M.*). For example, in a sodium silicate Si ions are *N.W.F.* and Na ions are *N.W.M.* (13). Table II–3 shows the classification of the ions found in rocks according to the electrostatic force (4) (14) (15), where z is the ion valence, a is the sum of the ionic radius of metallic ion and oxygen, and e is the electronic charge. In view of these points Figs. II–5 and 7 are the representation of E_η as a function of pure *N.W.F.* ions, whilst Fig. II–8 is that of the sum of pure *N.W.F.* ions and *N.W.F.* ions under normal condition.

At a relatively high silica content an activation energy for viscous flow (E_η) is greater than that for electrical conductivity (E_σ) caused by the migration of ions as will be treated in Chapter III. BACON et al. (16) concluded that the only unit taking part in viscous flow of silica up to the temperature of 2322°C was the silica molecule. In view of these facts the explanation of the results for E_η in Figs. II–5, 6 and 8 is that the addition of oxdies other than SiO_2 to molten rocks may break the strong covalent bonds of Si-O, therefore, E_η has large value in case of a slight addition, but as the additional oxide increases, the breaking of the Si-O bond increases, therefore, values of E_η become small. In the latter case the addition of oxdies, for example, Na_2O, causes the increase of E_η because of the Coulomb's force existent between Na^+ and O^{--} or SiO_4^{4-}, etc. but the effect of the break of Si-O bond is greater than it, so E_η only decreases with the addition of oxides. Similar explanation may be offered for constant B_1. Slight addition of oxides causes the breaking and weakening of Si-O bond and consequently it causes the decrease in the length of an element and the frequency of the vibration of an element. This is the reason that constant B_1 decreases as a result of small quantity of additional oxides, though this tendency for B_1 does not appear in these figures. As the additional oxides increase in quantity, B_1 increases because of the increase of the Coulomb's force between Na^+ etc. and O^{--} or SiO_4^{4-} etc., and consequent increase of the frequency of the vibration of an element.

§ 5. Relation between viscosity and ionic radius

It has been shown in the above discussion that the addition of oxides has effects on viscosity and activation energy for viscous flow. It is very interesting to know how various ions produce effects on those things. In Table II–2 one finds that compositions Al_2, Fe_2, Ca_2, etc., Al_4, Fe_4, Ca_4, etc. and Al_6, Fe_6, Ca_6, etc. represent the substitution of 1.96, 3.83 and 5.65% of silica in the rock of the composition Si_2, Si_4 and Si_6 by Al, Fe, Ca, etc. oxides respectively.

The effect on viscosity of substitution of silica in the Genbudo basalt by

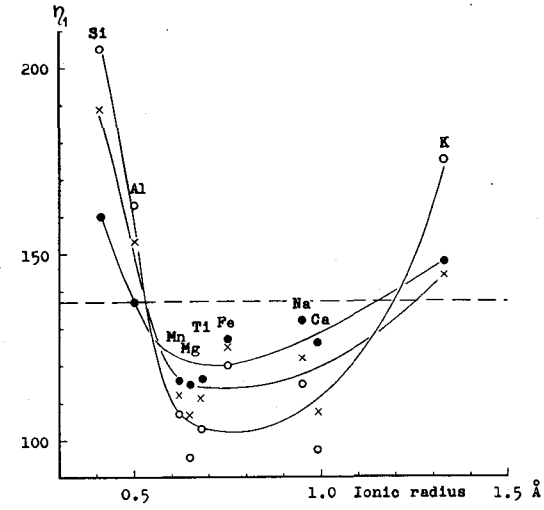

Fig. II-9. Effect on viscosity of substitutions of 1.96, 3.83 and 5.65% of silica in the Genbudo basalt melts by other oxides at 1400°C. Dotted line: value of original rock.
●: 1.96, ×: 3.83, ○: 5.65%.

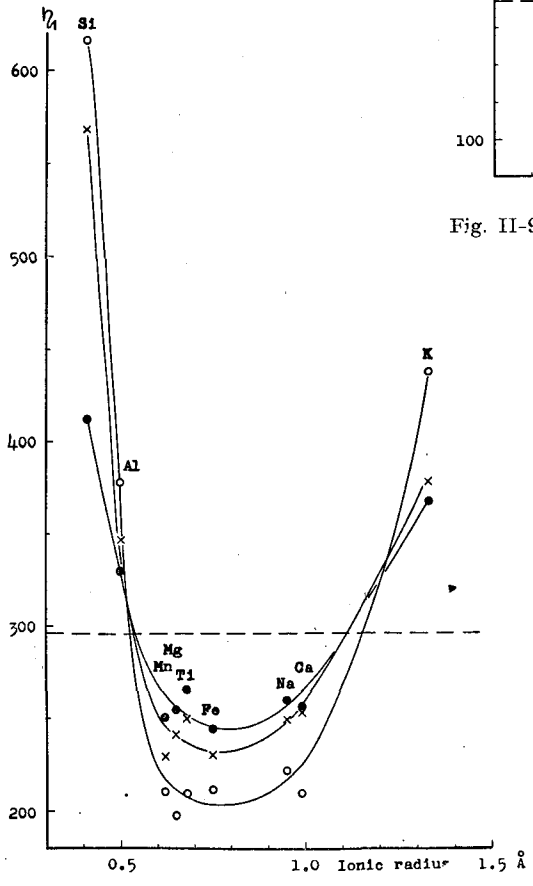

Fig. II-10. Effect on viscosity of substitutions of 1.96, 3.83 and 5.65% of silica in the Genbudo basalt melts by other oxides at 1300°C.

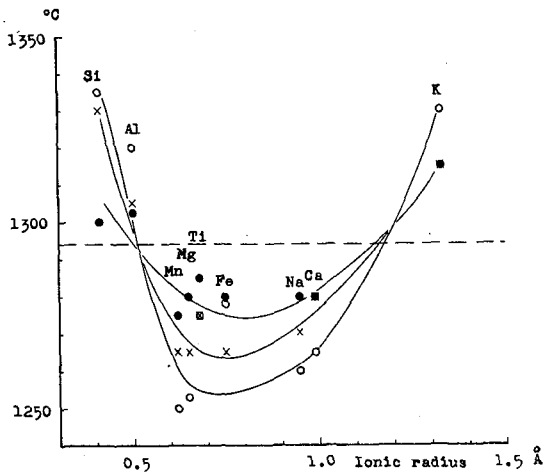

Fig. II-11. Effect on temperature, at which viscosity is $10^{2.5}$poises, of substitutions of 1.96, 3.83 and 5.65% of silica in the Genbudo basalt melts.

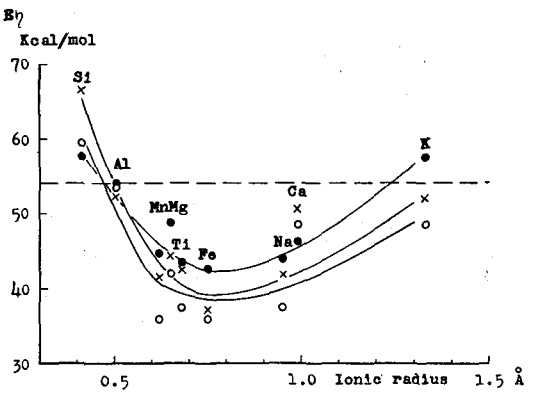

Fig. II-12. Effect on activation energy of substitution of 1.96, 3.83 and 5.65% of silica in the Genbudo basalt melts.

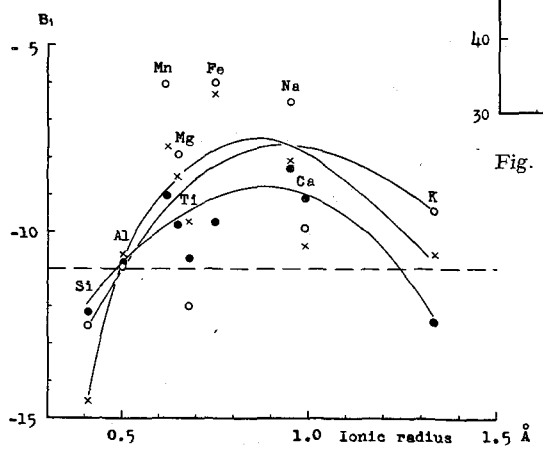

Fig. II-13 Effect on B_1 of substitution of 1.96, 3.83 and 5.65% of silica in the Genbudo basalt melts.

other oxides is plotted against different ionic radii in Fig. II–9 (at 1400°C) and Fig. II–10 (at 1300°C). The effect on the temperature level for a viscosity of $10^{2.5}$ poises is shown in Fig. II–11. Effects on activation energy and B_1 are shown in Figs. II–12 and 13. The values for the original Genbudo basalt are shown in these figures too.

These figures show that the effects of the substitution are not proportional to the ionic radius of the added oxides, but have minimum values, where B_1 has a maximum value near 0.8Å; the addition of Si, Al and K oxides to the original rock increased the various values except B_1 which was decreased by the addition, while other oxides inversely affected the various values. The explanation of these results is the same as that of the case discussed above in the preceding § 4.

§ 6. Viscosity of rocks containing water

In § 3 the relation between logarithm of viscosity and the bridge density (Fig. II–4) was determined experimentally. In case that an OH^- ion is substituted for an oxygen atom the bridge density is given by Eq. (II–5) in § 2.

Sabatier's data (6) on the influence of water content on the viscosity of a rétinite of Meissen are rewritten as the function of water content and water pressure in Figs. II–14 (a) and (b). An attempt will next be made to explain Sabatier's data by use of the concept of bridge density.

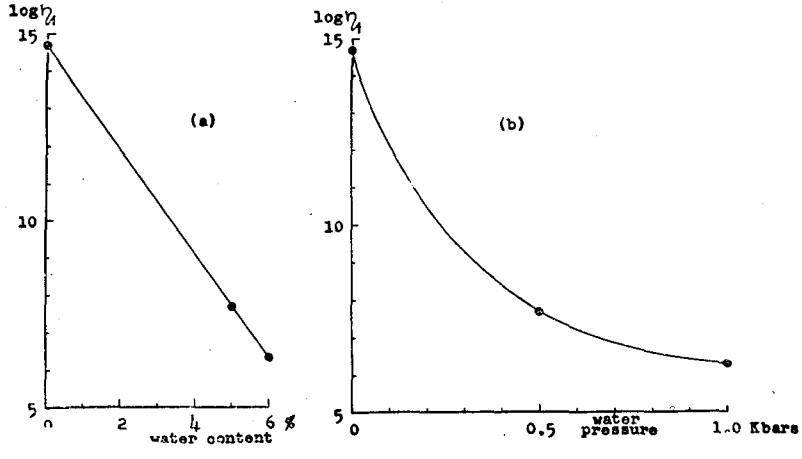

Fig. II-14. Effect of water content (a) and water pressure (b) on viscosity (rewritten on the basis of Sabatier's data).

At first, using Eq. (II–5) in § 2 and the chemical composition of rétinite as given in Table II–4 (17), the writer estimates the variation of the bridge density of the rock specimen containing water at high temperatures and pressures: $b/Si=1.54$ for the original rocks, $b/Si=1.08$ for the rock containing 5% water and $b/Si=0.99$ for the rock containing 6% water. The logarithms of viscosities which correspond to each case at 800°C are 14.6, 7.7 and 6.3 respectively. These values are plotted in Fig. II–15 which is the same as that exhibited in § 2. These plottings verify the possibility of estimating the viscosity in rocks containing water.

Table II–4. Chemical composition of rétinite.*.

SiO_2	70.4
Al_2O_3	13.3
Fe_2O_3	0.6
FeO	0.3
TiO_2	0.2
CaO	1.0
MgO	0.3
Na_2O	3.8
K_2O	3.1
H_2O	7.1
Total	100.1

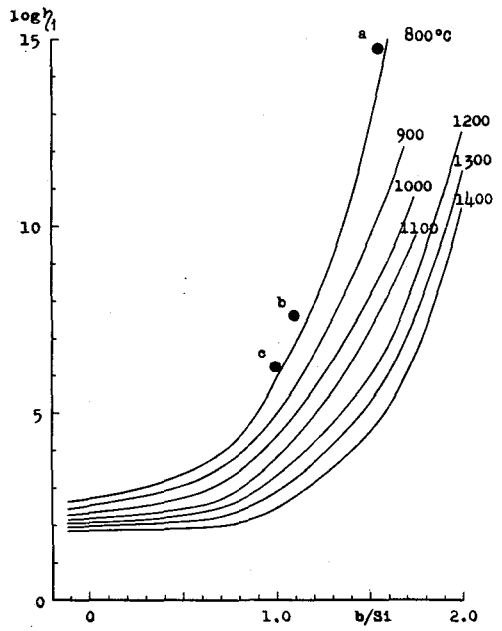

Fig. II-15. Viscosity vs. bridge density. Water content 0 (a), 5 (b), 6 %(c).

Since OH has quite a small atomic weight, even addition of a small weight percentage of water is very effective in decreasing viscosity; for rocks having a high bridge density the effect of water on viscosity is considerably great, while for rocks having low bridge density the effect is small because the large O/Si content breaks almost completely the Si-O-Si bridge, even if

* The chemical composition of rétinite was kindly supplied from Dr. G. SABATIER, Professor of University of Paris.

molten rock does not contain water. For example, the viscosities of the Showa-shinzan dome lava and Oshima 1950–lava (or 1951–lava) containing water were calculated; they are shown in Figs. II–16 and 17.

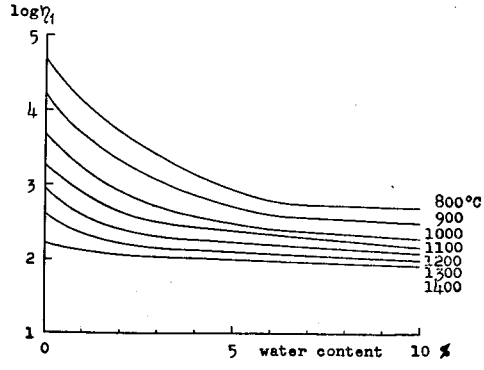

Fig. II-16. log viscosity vs. water content for the Oshima 1950-lava.

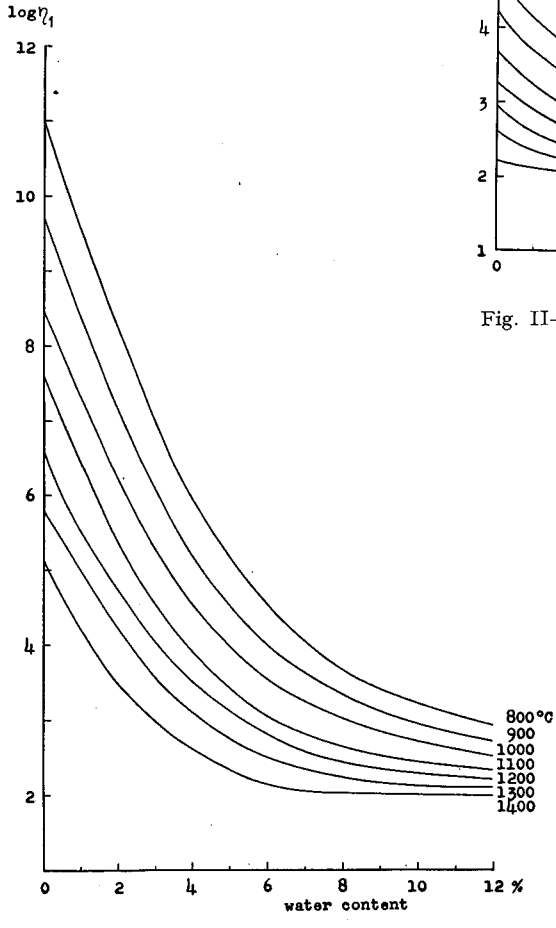

Fig. II-17. log viscosity vs. water content for the Showa-shinzan dome lava.

The observed maximum temperature and minimum viscosity of the fresh lava extruded in the 1951 Oshima eruption were ca. 1125°C and 6×10^3 poises respectively (18). Fig II–16 shows that the viscosity of the lava could not be reduced below 10^2 poises, even if the temperature of the lava were 1300°C and

the water content in the lava were 10%. On the other hand, the observed maximum temperature of the Showa-shinzan dome lava was ca. 1000°C (19). If that lava, having the average chemical composition of Japanese granite, had contained ca. 10% water, its viscosity could be reduced by water from ca. $10^{8.5}$ poises to ca. $10^{2.8}$ poises. Some problems concerning the viscosity of the Showa-shinzan dome lava at the time of extrusion will be discussed below in Chapter IV.

Now, let the effect of water on the viscosity of granite be estimated, as an example. The experimental studies concerning the origin of granite have been published (20). GORANSON (21) presented the following data on the solubility of water in the Stone Mountain granite glass: pressure effect at

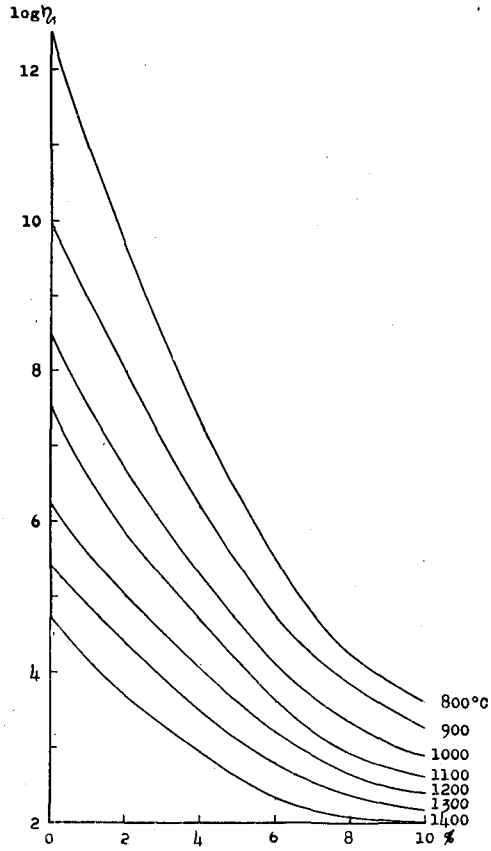

Fig. II-18. log viscosity vs. water content for the Stone Mountain granite glass.

900°C from 500 to 4000 bars; temperature effect at 980 bars from 600 to 1200°C. The variation of the bridge density of the Stone Mountain glass containing water is estimated by the writer, and logarithm of viscosity vs. water content diagram as shown in Fig. II–18 is derived from Fig. II–4. The former figure shows that a small water content exerts considerable effect on the viscosity of the granite. Thus, the relation between logarithm of viscosity and pressure at which the granite glass contains maximum water is obtained as shown in Fig. II–19. The viscosity is rapidly reduced until ca. 2 kbars and then it is slowly reduced. In this figure the depth scale in km was calculated from an assumed density of 2.70 g/cm³. Fig. II–20 shows the effect of temperature

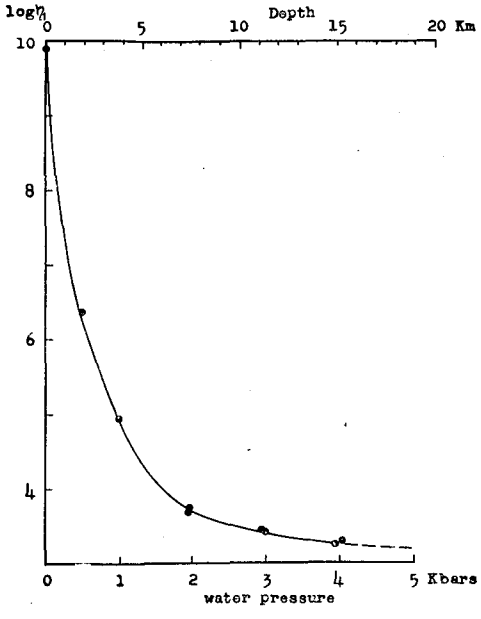

Fig. II-19 log viscosity vs. pressure for the Stone Mountain granite glass containing maximum water at 900°C.

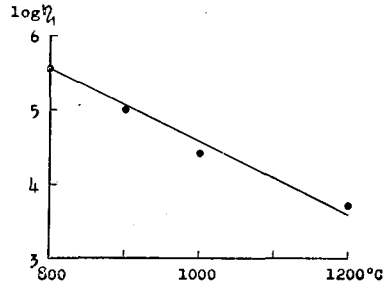

Fig. II-20. log viscosity vs. temperature for the Stone Mountain granite glass containing maximum water under the pressure of 980 bars.

under the pressure of 980 bars on viscosity, the logarithm of which decreases in direct proportion to temperature for the granite with maximum water content. The temperature of the granite glass is reduced, and consequently the viscosity of the glass must be decrease, if only the effect of water is considered. Fig. II–20, however, indicates that the effect of temperature on viscosity seems to be greater than that of water in the given range of both

factors.

Now, it should be noticed that the diagram of the relation between logarithms of viscosity and the bridge density, as shown in Fig. II–4 is not applicable to the case of a mineral having such chemical composition as albite ($NaAlSi_3O_8$) and orthoclase ($KAlSi_3O_8$). This is the reason that the viscosity of albite is considered to be equal to that of orthoclase, because they are equal in bridge density, i.e., $b/Si=4-8/3=4/3$; however, at 1400°C the logarithm of viscosity of the former (ca. 5.25) is smaller than that of the latter (ca. 7.01) (1). A qualitative explanation for the discrepancy in the viscosity is given by the results shown in Fig. II–10, i.e., the reduction effect of Na ion on the viscosity of Si_2, Si_4 or Si_6 rock is greater than that of K ion. Thus, a different diagram for each mineral must be used, but it cannot yet be made because there are few data concerning the viscosity of minerals in the present stage of experimental studies.

References

1) KANI, K. and HOSOKAWA, K. On the viscosities of silicate rock-forming minerals and igneous rocks, (in Japanese, with abstract in English), Res. Electrotech. Laboratory, No. 391 (1936), 1–105.
2) VOLAROVIČ, M.P. and KORČEMKIN, L. I. Der Zusammenhang zwischen der Viskosität geschmolzener Gesteine und dem Aziditätskoeffizienten nach F.J. Loewinson-Lessing, Compt. Rend. (Doklady) Acad. Sci. USSR, **17** (1937), 417–425.
3) MOREY G.W. The properties of glass, 2nd ed., Reinhold Pub. Corp. New York, (1954), 132–165.
4) DIETZEL, A. Strukturchemie des Glasses, Naturwissenschaften, **29** (1941), 537-547.
5) BUERGER, M.J. The structural nature of the mineralizer action of fluorine and hydroxyl, Amer. Min., **33** (1948), 744–747.
6) SABATIER, G. Influence de la teneur en eau sur la viscosité d'une rétinite, verre ayant la composition chimique d'un granite, Compt. Rend. Acad. Sci. (Paris), **242**, (1956), 1340–1342.
7) PAULING, L. The principles determining the structure of complex ionic crystals, J. Amer. Chem. Soc., **51** (1929), 1010–1026.
8) MIYAKE, Y. Geochemistry, (in Japanese), Asakura Book Co. Tokyo, (1954), Chapter 4.
9) INUZUKA, H. Measurement of viscosity on fused silica, (in Japanese), Mazda Kenkyu-Jiho, **14** (1939), 102–104.
10) GLASSTONE, S., LAIDLER, K. and EYRING, H. The theory of rate processes, McGraw-Hill Book Co., New York, (1941).
11) SHISHIDO, S. On the viscosity of glasses, (High viscosity (IV)), (in Japanese, with abstract in English), J. Electrochem. Soc. Japan, **18** (1950), 34–38.
12) KINGERY, W.D. Introduction to ceramics, John Wiley & Sons, Inc., New York, London, (1960), 147.
13) WARREN, B.E. Summary of work on atomic arrangement in glass, J. Amer.

Ceram. Soc., **24** (1941), 256–261.

14) DIETZEL, A. Die Kationenfeldstärken und ihre Beziehungen zu Entglasungsvorgängen, zur Verbindungsbildung und zu den Schmelzpunkten von Silicaten, Z. Elketrochem., **48** (1942), 9–23.

15) NARUSE, A. Glass Technology, (in Japanese), Kyoritsu Book Co. Tokyo, (1958), 207.

16) BACON, J.F., HASAPIS, A.A. and WHOLLEY, J.W. Viscosity and density of molten silica and high silica content glasses, Phys. Chem. Glass, **1** (1960), 90–98.

17) SABATIER, G. Recherches sur la déformation sous charge à haute temperature de queluqes roches éruptives, Bull. Soc. Franç. Miner. Crist. **82** (1959), 3–11.

18) MINAKAMI, T. On the temperature and viscosity of the fresh lava extruded in the 1951 Oo-sima eruption, Bull. Earthq. Res. Inst., **29** (1951), 90–98.

19) MINAKAMI, T., ISHIKAWA, T. and YAGI, K. The 1944 eruption of volcano Usu in Hokkaido, Japan: History and mechanism of formation of the new dome "Syowa-Sinzan", Bull. Volcan., Ser. 2, **11** (1951), 45–157.

20) TUTTLE, O.F. and BOWEN, N.L. Origin of granite in the light of experimental studies in the system $NaAlSi_3O_8$-$KAlSi_3O_8$-SiO_2-H_2O, Geol. Soc. Amer. Memoir 74 (1958),1–153.

21) GORANSON, R.W. The solubility of water in granite magmas, Amer. J. Sci., **22** (1931), 481–502.

Chapter III. Electrical conductivity

§ 1. Introduction

Study of the electrical conductivity of rocks and minerals over a wide temperature range is of great geophysical interest, and valuable conclusions concerning the internal constitution of the earth have been drawn from the variation of conductivity at lower temperature than melting point of minerals involved in rocks (1)–(4). However, little work has been done to estimate the electrical conductivity of molten rocks.

Interest in the similar temperature dependence of electrical conductivity and viscosity leads to an investigation of comparison between the two properties. NAGATA (5) investigated the properties of two molten rocks and suggested that the value of the temperature-coefficient of viscosity may be easily obtained by measuring electrical conductivity of rocks. VOLAROVICH and TOLSTOI (6) measured the electrical conductivity and viscosity of a lava of Mt. Vesuvius and showed a relation between them. In glasses some investigators have obtained empirically the relation between viscosity and conductivity (7)–(9). However, the relation between them over a wide range of silica content has never been made clear.

The purpose of this chapter is to describe a comparison between electrical conductivity and viscosity over a wide range of silica content and to discuss the related properties in some molten rocks.

§ 2. Method and specimens

The technique employed was essentially the same as that described by NAGATA (5). The measurement was carried out, using the frequencies of 50 and 1000 cycles per second to render the polarization effect as small as possible and to investigate the effect of the frequency difference which has been observed in glasses.

The diagram of the measuring circuit is shown in Fig. III–1. Alternating current from an oscillator was used as an electric power source and the balancing point of the bridge circuit was determined by an earphone.

The arrangement of cells is illustrated diagrammatically in Figs. III–2 (A) and (B). The electrodes, which were small Pt spheres of 1.7 mm diameter, were connected to the ends of Pt wires of 0.5 mm in diameter, inserted in porcelain tubes. The distance between two electrodes was 12.0 mm. The specimen used in this investigation was crushed and sieved to give a sample of $-170+325$ mesh. The cell is immersed in the specimen, contained in a

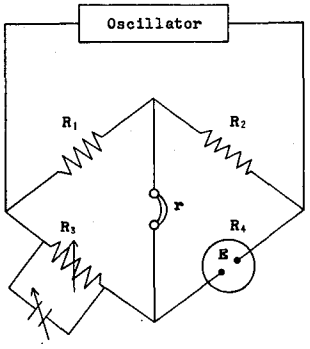

Fig. III-1. Circuit for measuring electrical conductivity. r: receiver, E: electrode, R: resistance.

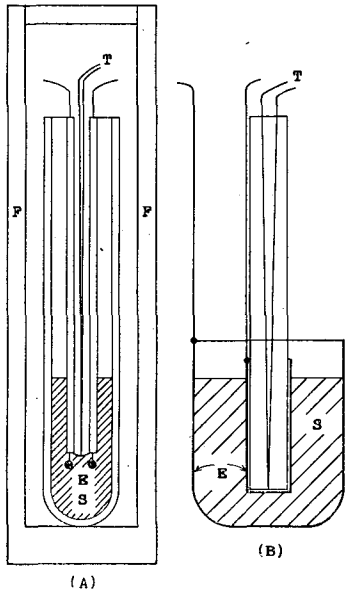

Fig. III-2. Furnace and conductivity cell. E: electrode, T: thermo-couple. S: specimen, F: furnace.

Tamman tube of 12.5 cm in length and 2.0 cm in diameter, to a depth sufficient to cover the electrodes together with a Pt-Pt Rh thermo-couple. The end of the cell is at least 1 cm above the base of the Tamman tube.

As the Tamman tube and the porcelain tube may be attacked chemically by molten rock, another arrangement of electrodes was constructed of a Pt crucible of 6.5 cm high and 4.2 cm in diameter and a cylindrical Pt electrode of 6.0 cm in length and 1.0 cm in diameter, connected to a porcelain tube. In this case the cell constant was determined for a number of different depths of liquid in the crucible at the room temperature. The results obtained with this arrangement accorded with those obtained in the former arrangement. The degree of attack seems to be relatively small within the temperature range in the present experiment. Therefore, the former arrangement was generally used because of its convenience in measurement.

The cell constant was determined at the room temperature, using aqueous KCl solution and is of the order of 2 cm^{-1}.

Thus, electrical conductivity σ is calculated from the bridge measurements,

$$R_4 = R_2 R_3/R_1 , \qquad \sigma = C/R_4 ,$$

where C is the cell constant.

Measurements of resistance could be made rapidly. The temperature of the melt was recorded during heating and cooling at a rate of 300°C/hour. This procedure was justified by agreement of measurements made during heating and cooling and with those obtained at a constant temperature. The absolute accuracy of the measurements was ±5% for the conductivity. The main source of error was the limitations in measuring high resistances.

For the comparison between viscosity and electrical conductivity over a wide range of silica content, specimens used in this experiment were selected from the rocks of which viscosity had already been measured. Their chemical composition is given in Chapter I, Table I–2.

§ 3. Results

The results of the measurements are shown graphically in Figs. III–3–11. From a consideration of these figures it appears that the main portion of the graph, obtained by plotting logarithms of conductivity (in ohm^{-1} cm^{-1}) against the inverse of the temperature, is a complex line for the first heating run and is approximately a straight line for the first cooling run which accorded with that for the second heating run within experimental error; further, as temperature is raised, the conductivity rapidly increases.

The results obtained with 50 cycles per second accorded with that with

Figs. III-3-11. Electrical conductivity vs. temperature for some volcanic rocks.
●: 1st heating run, ×: 1st cooling run, ○: 2nd heating run.

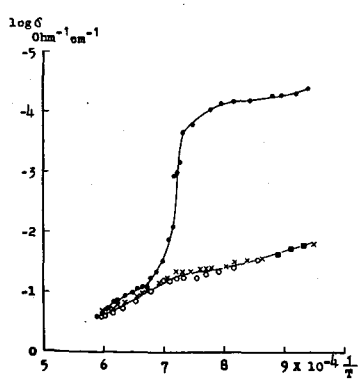

Fig. III-3. Nagahama nepheline basalt.

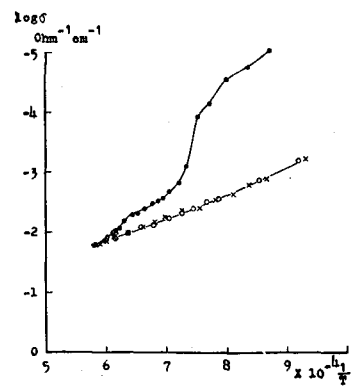

Fig. III-4. Genbudo basalt.

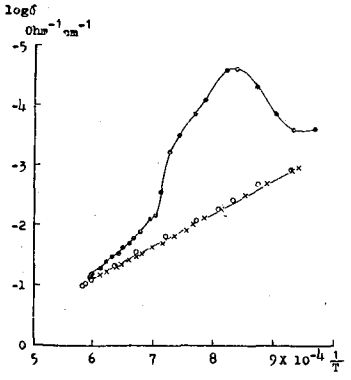

Fig. III-5. Oshima 1950-lava.

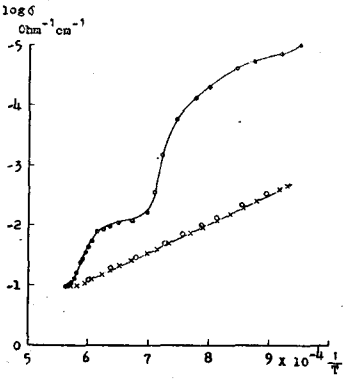

Fig. III-6. Asama Onioshidashi lava.

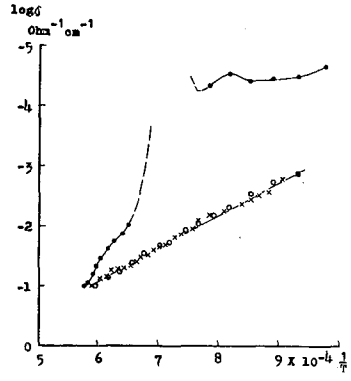

Fig. III-7. Tarumai dome lava.

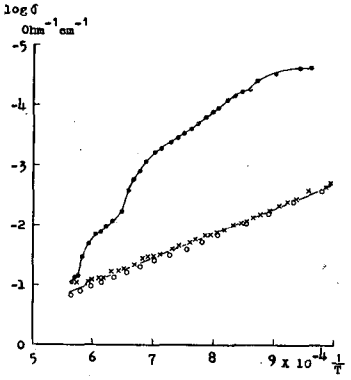

Fig. III-8. Komagadake pumice.

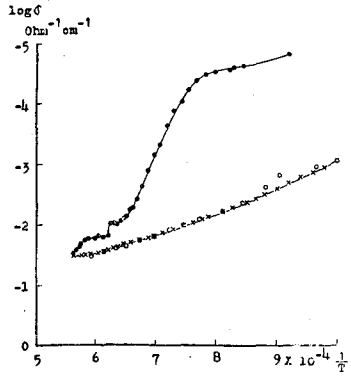

Fig. III-9. Showa-shinzan dome lava.

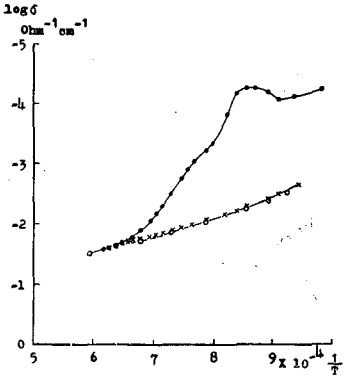

Fig. III-10. Shirataki obsidian.

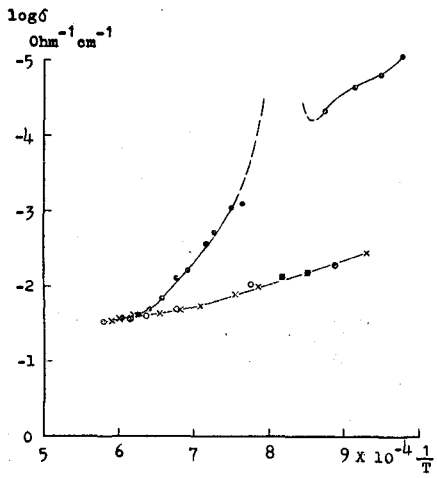

Fig. 11. *Niijima pumice.*

1000 cycles per second within the experimental error; also the change of the voltage of applied alternating current (2–8 volts) does not effect the results.

The structure of the specimen in the first heating run corresponds to that of a three-phase system, i.e., crystals +glasses+pores, at the room temperature. The conductivity of the specimen may be low at the room temperature, because it is controlled mainly by crystals+pores phase having low conductivity. As the temperature is raised, the change of crystalline phase into a liquid one causes the reduction of the porosity which increases the conductivity almost in the direct proportion for small values of porosity (10). The results of the first heating run, therefore, should be studied in view of the kinetics of crystal fusion.

The conductivity for the first cooling run or the second heating run is of an order of magnitude greater than that observed for the first heating run; over a considerable temperature range the conductivity can be expressed as

$$ln\,\sigma = -E_\sigma/RT + B_2\,, \qquad \text{Eq. (III–1)}$$

where E_σ is the experimental activation energy for conductivity and B_2 is represented as a function of the frequency of the vibration of ion (11).

The values of E_σ and B_2 as functions of silica content are shown in Fig. III–12. The value for 100% silica content is calculated from the data between 1000° and 1400°C for fused quartz, of which the impurity content is ca. 0.2% — the major impurities being Fe_2O_3 and B_2O_3, with traces of MgO and CaO (12).

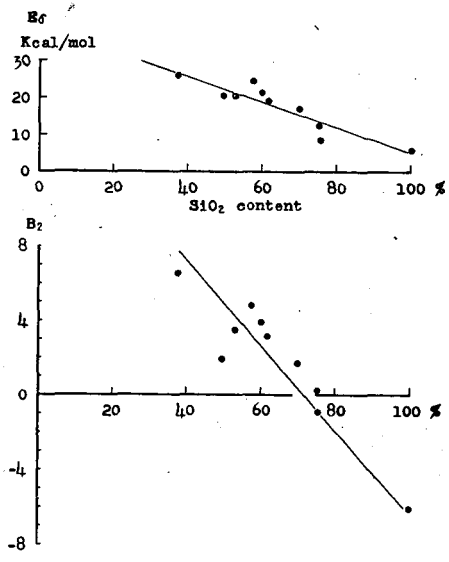

Fig. III-12. Activation energy for electrical conductivity and log pre-exponential factor vs. silica content.

§ 4. Discussion

(A) Electrical conductivity and viscosity.

The equation of conductivity to temperature is of the same form as that for the viscosity-temperature, relation described in Chapter II. Then, at first, let comparison be made between the activation energies for both processes. The comparison between them as a function of silica content is graphed in Fig. III–13, where it is seen that E_η is greater than E_σ and that with increasing silica content E_η increases, while E_σ decreases.

The explanation of the conclusion derivable from Fig. III–13 is that the conductivity is connected with the migration of ions which have a small mobility, and the viscosity is connected with a flow process involving mainly the strongest bonds in the structure, i.e., usually the Si-O bond (13). Some further considerations will be added to this explanation in the next discussion.

Combining the conductivity-temperature equation (Eq. (III–1) in Chapter III. §3.) with that of viscosity-temperature (Eq. (II–1) in Chapter II. §4.), one gets the following conductivity-viscosity equation,

$$ln\,\eta_1 = A\,ln\,(1/\sigma) + B\,,$$

where

$$A = E_\eta/E_\sigma \text{ and } B = B_1 + B_2\,E_\eta/E_\sigma\,.$$

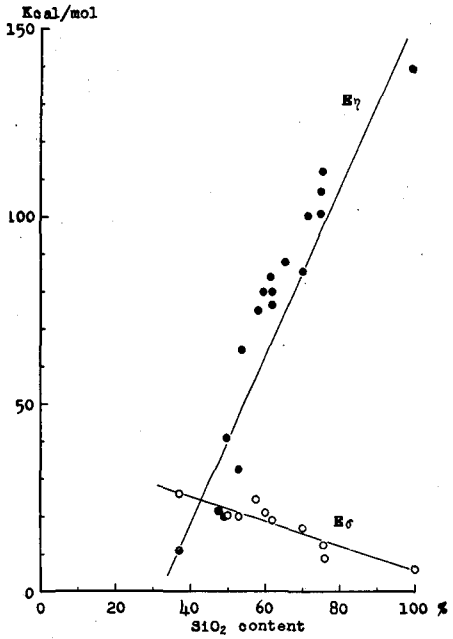

Fig. III-13. Comparison of the activation energies for viscous flow and electrical conductivity.

Fig. III–14 shows that constant A in this equation may be represented as a linear function of silica content, but B may not always be represented

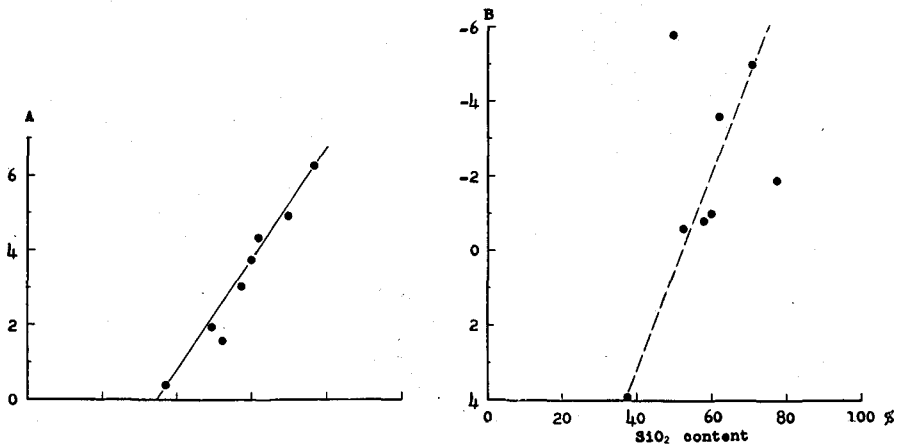

Fig III-14. A and B vs. silica content.

as a simple function of silica content; the latter is also true in the case of the sum of the number of Ca, Na and K ions too. Therefore, one can estimate the activation energy for viscosity of the molten rock, but can not estimate the absolute value of viscosity by measuring its electrical conductivity. Future investigation is expected to show that this relation can be generalized.

(B) Electrical conductivity and diffusion coefficient (14).

There is a relationship among diffusion coefficient, electrical conductivity, and the transfer number or fraction of the total electrical conductivity contributed by each charged particle (i):

$$D_i = B_i k T \ , \qquad \text{Eq. (III–2)}$$

$$\sigma_i = n_i z_i^2 e^2 B_i \ , \qquad \text{Eq. (III–3)}$$

$$D_i = t_i k \sigma T / n_i z_i^2 e^2 \ , \qquad \text{Eq. (III–4)}$$

where D_i is the self-diffusion coefficient of i, B_i its absolute mobility, σ_i the partial electrical conductivity, t_i the transfer number, n_i the number of ions per c.c., z_i the valence, and e the electronic charge. In this case the total conductivity is given by

$$\sigma = \sum_i \sigma_i \ . \qquad \text{Eq. (III–5)}$$

The fraction of the total conductivity contributed by each charge carrier is

$$t_i = \sigma_i / \sigma \ . \qquad \text{Eq. (III–6)}$$

The sum of the individual transfer numbers must obviously be unity,

$$\sum_i t_i = 1 \ . \qquad \text{Eq. (III–7)}$$

As noted in Chapter II, a liquid silicate structure consists of a network built up of SiO_4 tetrahedra which can form anything from a complete three-dimensional network as in silica, to chain or ring structures, fairly large but discrete ions, or isolated SiO_4 groups. Modifying ions such as alkalies and alkaline earths tend to take intermediate positions among silica tetrahedra, being present in holes in the liquid structure and having substantially higher mobility than the silicate groups. In this sense glass-forming ions are classified by electrostatic force as of the *N.W.F.*, *N.W.M.* and *I.* groups (Table II–3 in Chapter II) (15)–(17).

From the structure the mobility of the modifying alkali (Li, Na, K, etc.,)

can be estimated; alkaline earth ions (Ca, Sr, Mg, etc.,) which do not take part in the network can be expected to show the greatest mobility while that of the network forming ions to show the least.

In sodium silicate liquids and a number of other binary silicates, it has been shown that the electrical conductivity is caused by ions. In addition, the transfer number of cations has been shown to be unity and the conduction characteristics to be mainly determined by the alkali ion concentration and mobility. The qualitative explanation of these facts is simply that ions larger than Na^+ and K^+ have greater difficulty in moving through the gaps in the structure. It might expected that small doubly charged ions (such as Mg^{2+}) would also have a high mobility, but here the double charge gives the ion a more nearly intermediate role, and this apparently annuls its advantage in size. Though the Ca ion is a doubly charged ion, it is a pure network-modifier because of its large ionic radius. The contribution of Ca ions to conduction, therefore, is to be considered. This is ascertained from the fact that the

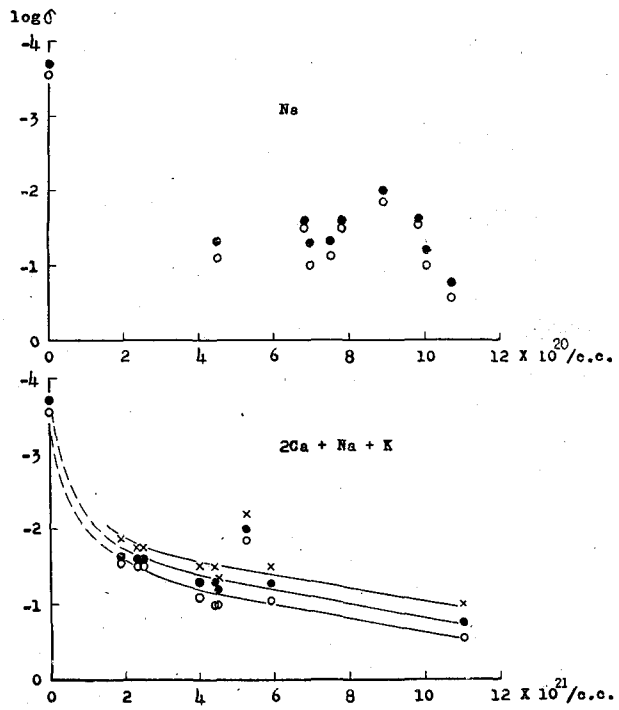

Fig. III-15. Electrical conductivity vs. number of ions per c.c.
×: 1200, ●: 1300, ○: 1400°C.

correlation between the conductivity and number of 2Ca (considering its valence)+Na+K per c.c. is better than that between the conductivity and number of only Na per c.c. as shown in Fig. III–15. The number of Ca, Na and K ions per c.c. (n_i) is from the chemical composition in water free (Table I–2),

$$n_i = \frac{(\text{wt. \% of } i \text{ oxide})}{(\text{molecular wt. of } i \text{ oxide})} \times \frac{(\text{atomic wt. of H})\ (\text{density of molten rock})}{(\text{absolute mass of H}) \times 100}$$

Values of the density of air quenched glasses were used as the density of molten rocks viz., Nagahama nepheline basalt: 2.92, Komagadake pumice: 2.30, Tarumai dome lava: 2.46, Shirataki obsidian: 2.32, Showa-shinzan dome lava: 2.32, Asama Onioshidashi lava: 3.94, Genbudo olivine basalt: 2.30, Oshima 1950–lava: 2.66 and Niijima liparite: 2.30.

Thus from the results of computations of electrical conductivity one can calculate the diffusion coefficients of Ca, Na and K ions in the molten Showa-shinzan dome lava, for example, if their coefficients are the same. From Eq. (III–4), putting $n_{Na}=15.8\times10^{20}$, $n_K=4.4\times10^{20}$ and $n_{Ca}=8.20\times10^{20}$

$$D = \frac{1 \times 1.38 \times 10^{-16} \times 9 \times 10^{11} T}{(32.8+15.8+4.4) \times 10^{20} \times (4.81\times10^{-10})^2} = 5.4 \times 10^{-7} T,$$

where 9×10^{11} is the factor to convert from the practical unit to e.s.u.

Fig. III–16 shows a graph of calculated coefficient which is close to the

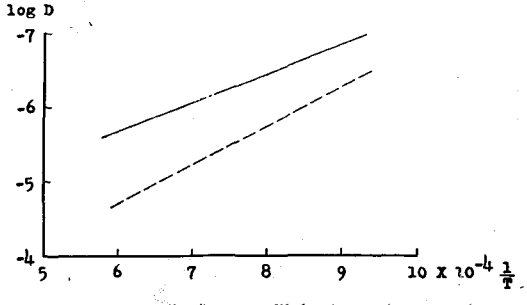

Fig. III-16. Diffusion coefficient vs. temperature.
Solid line: (Ca, Na, K) ion diffusion coefficient calculated from electrical conductivity,
Dotted line: diffusion of sodium ion in a sodium silicate glass (after JOHNSON et al.).

value of the Na ion in a sodium glass determined directly (18). Considering the fact that the coefficient of Ca is smaller than that of Na (19), the result obtained shows that Eq. (III–4), which is strictly applicable only to dilute solutions of electrolytes, may be applicable to the estimation of the order of diffusion coefficients of molten rocks too.

The activation energy for diffusion is ca. 20 kcal/mol and is close to that for electrical conductivity.

(C) Viscosity and diffusion coefficient.

There is a relation between diffusion coefficient (D) and viscosity (η_1), i.e., the Stokes-Einstein equation, $D=kT/6\pi r\eta_1$, where r is the radius of the flow unit. It has been frequently applied to organic liquids, and allowed of a calculation of viscosity, also, and vice versa (20), because the theory of absolute reaction rates (21) leads to the same equation which is free from such an assumption of the Stokes-Einstein's classical approach that the diffusion molecules should be large.

By use of the equation the radius of the diffusion particles is calculated for the molten Showa-shinzan dome lava, and r becomes equal to 3.1×10^{-14}cm $=3.1\times10^{-6}$Å by putting $D=5.2\times10^{-5}$cm^2/sec. and $\eta_1=3.2\times10^5$ poises at 1400°C. This result is entirely implausible, because the ordinary value of ionic radius is of the order of Å, and thus, one had better keep off the application of the Stokes-Einstein equation to molten rocks.

References

1) COSTER, H.P. The electrical conductivity of rocks at high temperature, M.N.R.A.S. Geophys. Suppl., **5** (1948), 193–199.
2) RIKITAKE, T. Electrical conductivity and temperature in the earth, Bull. Earthq. Res. Inst., **30** (1952), 13–24.
3) RUNCORN, S.K. and TOZER, D.C. The electrical conductivity of olivine at high temperatures and pressures. Ann. Geophys., **11** (1955), 98–102.
4) NORITOMI, K. The electrical conductivity of rock and the determination of the electrical conductivity of the earth's interior, J. Min. Coll. Akita Univ., Ser. A. **1** (1961), 27–59.
5) NAGATA, T. Some physical properties of the lava of volcanoes Asama and Mihara, I. Electric conductivity and its temperature-coefficient, Bull. Earthq. Res. Inst., **15** (1937), 663–673.
6) VOLAROVICH, M.P. & TOLSTOI, D.M. The simultaneous measurement of viscosity and electrical conductivity of some fused silicates at temperatures up to 1400°. J. Soc. Glass Tech., **20** (1936), 54–60.
7) MOREY, G.W. The properties of glass, 2nd ed., Reinhold Pub. Corp. New York, (1954), 465–501.
8) STANWORTH, J.E. Physical properties of glass, Oxford, (1949), 127–133.

9) EITEL, W. The physical chemistry of the silicates, Univ. Chicago Press, Chicago, Ilinois, (1954), 227.
10) KINGERY, W.D. Introduction to ceramics, John Wiley & Sons, Inc., New York, London, (1960), 681–684.
11) MATSUSHITA, Y. and MORI, K. A study on the properties and reactivity of molten slags, (in Japanese, with abstract in English), Rep. Inst. Ind. Sci. Univ. Tokyo, **3** (1953). 72–166.
12) COHEN, J. Electrical conductivity of fused quartz, J. Appl. Phys., **28** (1957), 795–800.
13) SHISHIDO, S. On the viscosity of glasses (High viscosity (IV)) (in Japanese, with abstract in English), J. Electrochem. Soc. Japan, **18** (1950), 34–38.
14) KINGERY, W.D. Op. cit. (10), 217–243 and 647–685.
15) DIETZEL, A. Strukturchemie des Glasses, Naturwissenschaften, **29** (1941), 537–547.
16) DIETZEL, A. Die Kationenfeldstärken und ihre Beziehungen zu Entglasungsvorgängen, zur Verbindungsbildung und zu den Schmelzpunkten von Silicaten, Z. Elektrochem., **48** (1942), 9–23.
17) NARUSE, A. Glass Technology, (in Japanese), Kyoritsu Book Co. Tokyo, (1958), 207.
18) JOHNSON, J.R., BRISTOW, R.H. and BLAU, H.H. Diffusion of ions in some glasses, J. Amer. Ceram. Soc., **34** (1951), 165-172.
19) TOWERS, H. and CHIPMAN, J. Cited by KINGERY, loc. cit. (10), 239.
20) JOST, W. Diffusion in solids, liquids, gasses, Academic Press Inc., Pub., New York, (1952), 462.
21) GLASSTONE, S., LAIDLER, K. and EYRING, H. The theory of rate processes, McGraw-Hill Book Co., New York, (1941).

Chapter IV. Formation of the Showa-shinzan dome

§ 1. Introduction

The results of experiments described in Chapter I showed that the crystals in the Showa-shinzan dome lava melt away at ca. 1350°C. The melting of the crystals may be caused mainly by a solid-solid reaction between plagioclase and quartz or cristobalite. The reaction between two crystals to form a new phase involves diffusion process. The diffusion process is related to the viscosity of melt produced in the boundary of each crystal. Then, it seems likely that the Showa-shinzan dome lava, whose viscosity is very high even at high temperatures as shown in Chapter I, Fig. I–29, may not reach a complete thermodynamical equilibrium within several hours of reheating process. In this chapter in order to discuss the problem concerning the restoration of the Showa-shinzan dome lava to the viscosity in natural cooling process, it is discussed whether there is a possibility that the crystals in the Showa-shinzan dome lava melt away at a temperature lower than that estimated in Chapter I. Using the conclusions arrived at, the writer will deduce a viscosity-temperature relation of the lava in the natural cooling process and also the cooling velocity of the lava.

§ 2. Crystallization temperature deduced from phase diagrams

Phase equilibrium diagrams (1) represent the relation between composition and temperature under a certain pressure, with reference to the melting and cyrstallizing process in mixtures containing various components. Using them, therefore, one can rough out the temperature at which the crystals began to crystallize in the molten Showa-shinzan dome lava. To utilize the results of present researches for some discussions, the writer determines the temperature of beginning of crystallization of plagioclase in some three-component systems.

At first, it is assumed that the dome lava consists of four components, viz., Q, Or, Ab and An, which account for 88.42% of all normative compositions as shown in Table IV–1 (2). For want of a phase equilibrium diagram of the above four components, use is made of the diagrams of three components chosen from among the four. Omitting the Q–Ab–An system which has no phase diagram, there are 3 systems, viz., the Q–Or–Ab, Q–Or–An and Or–Ab–An systems.

Recalculations of normative compositions consisting of the above three components are shown in Table IV–2.

Table IV–1. Mineralogical and normative compositions of the Showa-shinzan dome lava (after K. YAGI).

Mineralogical data		Mode of rock				Normative compositions	
Phenocrysts	Groundmass	Phenocrysts		Groundmass			
Plagioclase	Plagioclase	Andesine	17.6	Andesine	40.5	Q	34.86
n_1=1.555 A_{50}	n_1 not determined	Hypersthene	1.9	Quartz	13.5	Or	8.34
n_1=1.547 An_{39}	(010)∧X′=8°−14°	Magnetite	0.6	Cristobalite	12.1	Ab	28.82
2V(+)=82°−83°	An_{20-30}			Anorthoclase	1.6	An	16.40
Hypersthene	Quartz			Hypersthene	3.1	C	2.45
n_1=1.695 on(110)	Cristobalite			Magnetite	2.8	Di Wo	—
n_2=1.710 on(110)	c∧X=40°−45°			Apatite	0.1	Di En	—
2V(−)55°−59°	Anorthoclase			Glass	6.2	Di Fs	—
mean 56.5°	Hypersthene					Hy En	2.10
Pleochroism	Pleochroism					Hy Fs	2.90
X pale reddish brown	X′ pale brown					Mt	2.09
Y pale brown	Z′ pale green					Il	0.91
Z pale green	Apatite					Ap	0.67
Absorption	Magnetite						
X>Y>Z	Glass						
Composition							
En_{55} Fs_{45} (wt pct)							
Magnetite							

Table IV-2.

Q	39.4	48.4	58.5	43.6	
Or	9.5	11.6	14.0		15.5
Ab	32.6	40.0		36.0	53.9
An	18.6		27.5	20.4	30.6

These recalculated compositions are plotted on the triangular diagrams. From these diagrams one can estimate the temperature of beginning of crystallization as follows:

i) Q–Or–Ab system (1).

A liquid of Q–Or–Ab system begins to crystallize at about 1250°C with separation of tridymite. The liquid changes in composition as the temperature falls. Na, K feldspar segregates together with tridymite at about 1035°C. The above process is simplified thus:

T_l=1250 (Tr), 1035 (Na, K feldspar).

ii) Q–Or–An system

T_l=1380 (Tr), 1320 (An).

iii) Or–An–Ab system

T_l=1380 (Feldspar).

The results summarized above show that the temperature of beginning of crystallization of feldspar differs much in different systems. This difference is due to the fact that either An or Ab is respectively neglected, in the Q–Or–Ab system or Q–Or–An system, for example. The melting point of feldspar in each system is raised or lowered by the addition of An or Ab, i.e., the temperature 1035°C in Q–Or–Ab system or the temperature 1320°C in Q–Or–An system is raised or lowered by the addition of An or Ab respectively.

There are no minerals having SiO_2 composition as phenocrysts in the lava under consideration (Table IV–1). Therefore, among the results obtained above, system (iii) only seems to be suitable for application to the problem of the crystallization of the lava. For the addition of Q component to the system Or–An–Ab, the writer considers the substitution of Q for only Or, An or Ab in the system Or–An–Ab. Each system of Q–Or, Q–Ab is in an eutectic relation, for example, as seen in the diagram of Q–Or system, (1), thus, T_l= 1380 (Feldspar) in the result (iii) seems to be considerably reduced, though the accurate temperature can not be estimated in the present stage of the investigation.

In the next section the equilibrium relation of the Showa-shinzan dome lava will be discussed experimentally.

§ 3. Kinetics of crystal fusion

(A) Experimental

The material used for these experiments was the Showa-shinzan dome lava with the chemical composotion and the modes shown in Tables I–2 and IV–1.

The heating was performed in porcelain crucibles placed in the constant temperature zone (±5°C) of an "EREMA" tublar furnace, the temperature of which was kept constant by an electric controller. This controller can keep the temperature constant within ±10°C. Constant temperature runs were made at 1000, 1050, 1100, 1200, 1300 and 1400°C. In all cases the samples were heated in air. After each treatment, the sample was air quenched and subsequently ground in a porcelain mortar, until no scratchiness was felt while grinding and the material appeared to be smooth under the pestle. The particle size fraction –170 mesh was chosen.

The quantitative determination of the fusion was done by means of X-ray diffraction analysis, by the powder method, using a "Norelco" X-ray spectrometer, furnished with a 1°–0.006"–1° slit, and a nickel filter. Copper radiation was used in all cases.

The calibration curves of composition vs. X-ray peak intensity in scale reading (Fig. IV–1) were obtained by using mixtures of the Showa-shinzan

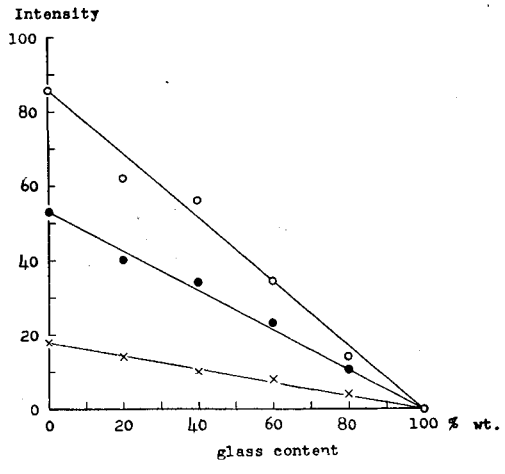

Fig. IV-1. X-ray calibration for mixtures of the Showa-shinzan dome lava and its artificial glass.
○: cristobalite, ●: plagioclase, ×: quartz.

dome lava and the glass from the same material in different proportions. The glass was prepared by heating the powder specimen prepared from the dome lava at 1550°C for 3 hours and subsequently the specimen was air quenched. This treatment gives a very well-built glass of the dome lava,

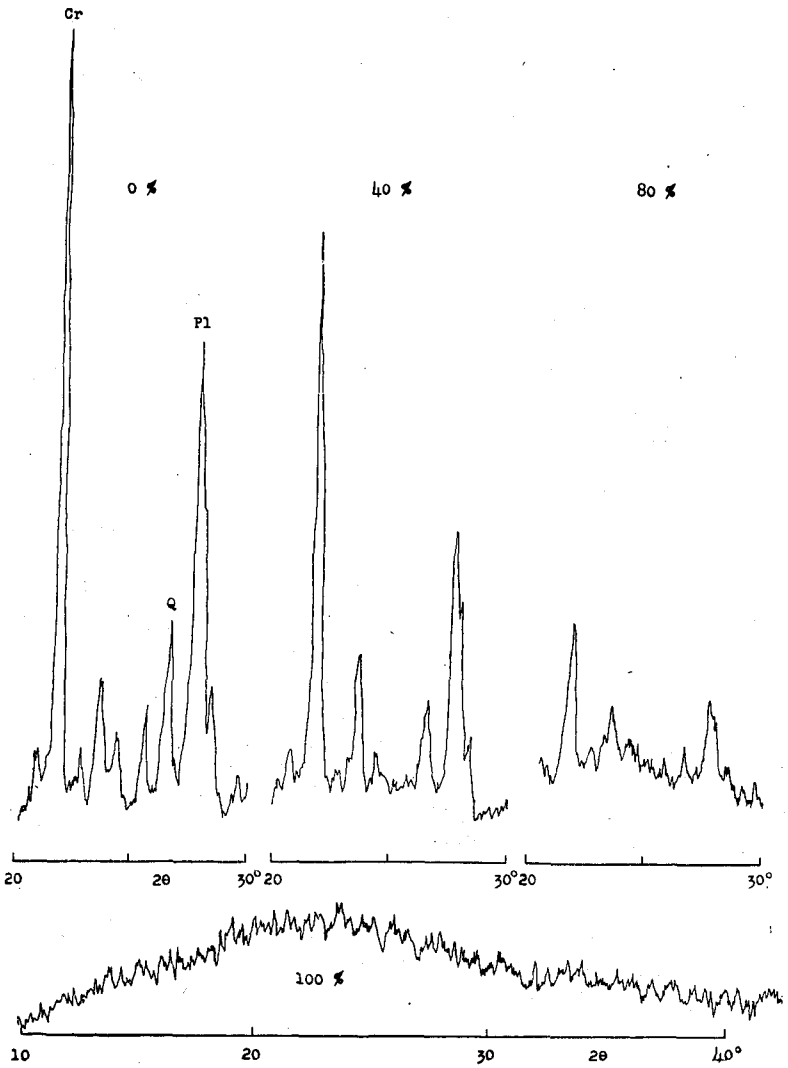

Fig. IV-2. X-ray diffraction patterns for mixtures of the Showa-shinzan dome lava and its artificial glass (0, 40, 80 and 100 wt. %).

which is proved under X-ray diffraction examination as illustrated in Fig. IV–2, together with the patterns of mixture of the glass and the original lava; therefore, it can be regarded as a good standard material.

The peak selected for each crystal was the strongest one, viz., $2\theta=27.7°$ for plagioclase, $2\theta=26.6°$ for quartz and $2\theta=22.0°$ for cristobalite. The peak of tridymite was not detected by means of the above treatment.

As plagioclases in the samples were of widely different chemical compositions and cristobalite and quartz were of widely different degrees of disorder, a direct correlation between X-ray peak intensity and percentage of glass content was not to be expected. The comparison with the standard would be absolutely valid only in a hypothetical case of each crystal consisting of a mixture of "perfect crystal" and the glass. In spite of the inability of this method to furnish a net yield of fusion, it was accepted as the best conventional way to follow the course of fusion. The apparent values of glass content of each mineral was drawn from the calibration curves graphed, if one assumes that the weight percentage $(C)_i$ of glass prepared from mineral i is proportional to that $[C]_i$ of mineral i in original rock, i.e.,

$$(C)_i = G\frac{[C]_i}{100}$$

where G is the total weight of glass prepared from all mineral in original rock. The accuracy of determination is within $\pm 5\%$.

(B) Rate of crystal fusion.

By using the techniques described, the variations of appearance of the patterns as results of heat treatments are illustrated in Fig. IV–3. Further, the fusion isothermal curves within a relatively short time are shown in Fig. IV–4 (a, b, c). In general, it is known that three very distinct steps may be considered in the course of fusion of crystals into liquids. The fact that the fusion does not become apparent from the beginning of each heating shows that the rather slow nucleation process of fusion is the rate-controlling factor in the first stages of the fusion. This nucleation period of fusion obviously is dependent on temperature.

The second step, which is very rapid, could be described as the growth of a fused state. Moreover in the isothermal curves a sharp break is observed after the second step of fusion has been accomplished. From there on an almost horizontal line follows, which means that a new process with a negligible rate of change is under way. From the practical point of view, the fusion

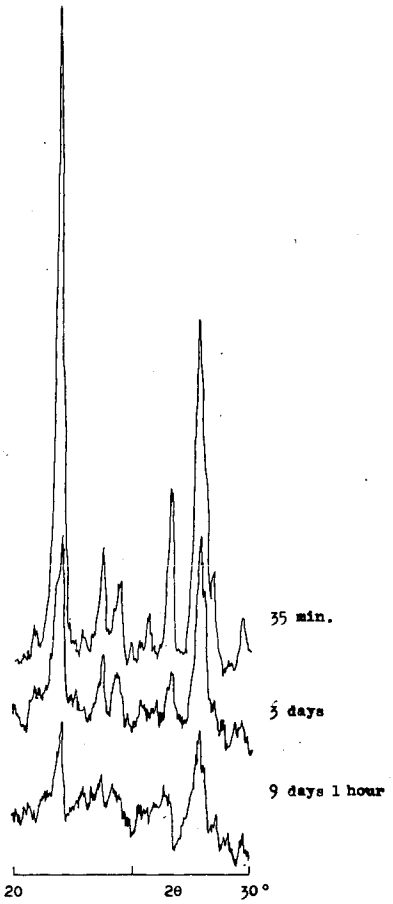

Fig. IV-3. Changes of X-ray diffraction patterns caused by heating the Showa-shinzan dome lava at 1100°C.

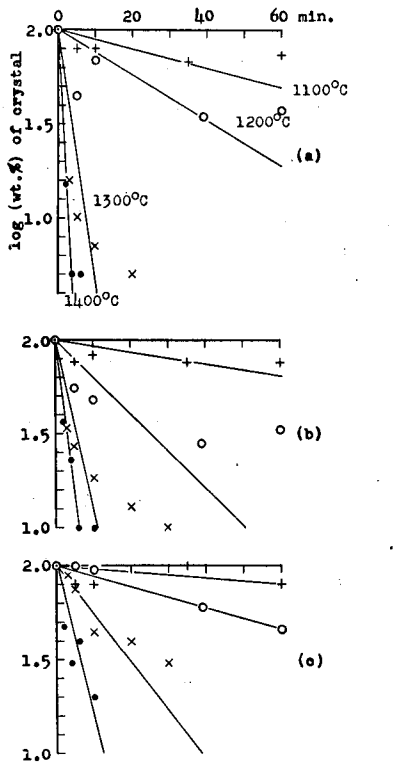

Fig. IV-4. Percentage of minerals remaining after heating the Showa-shinzan dome lava at various temperatures.
(a): plagioclase,
(b): cristobalite,
(c): quartz.

may be considered as completed by the attainment of a state of apparent equilibrium.

In the present investigation, the writer does not detect the nucleation period, but it may appear in an experiment with shorter treatment.

Although the data were few, the form of curves appeared to merit an attempt to interpretation on kinetical lines. At the second stage, i.e., the growing stage of fusion of the crystal, the necessary assumption is that the reaction consists of a first-order stage:

$$\textit{Crystal (plagioclase, cristoblite or quartz)} \xrightarrow[K_{crystal}]{} \textit{Liquid},$$

where $K_{crystal}$ is the rate constant for the reaction which transforms each crystal into liquid.

Then the concentration of each crystal ($C_{crystal}$) after time t is

$$C_{crystal} = a \exp(-K_{cry} \cdot t) .$$

Graphs of log $C_{cry.}$ vs. time for plagioclase, cristobalite or quartz are straight

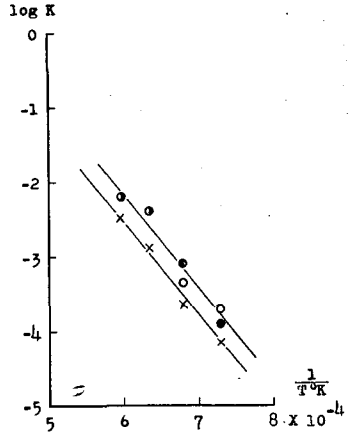

Fig. IV-5. Fig. IV-5. Rate constant for reaction of the Showa-shinzan dome lava.
○: plagioclase,
●: cristobalite,
×: quartz.

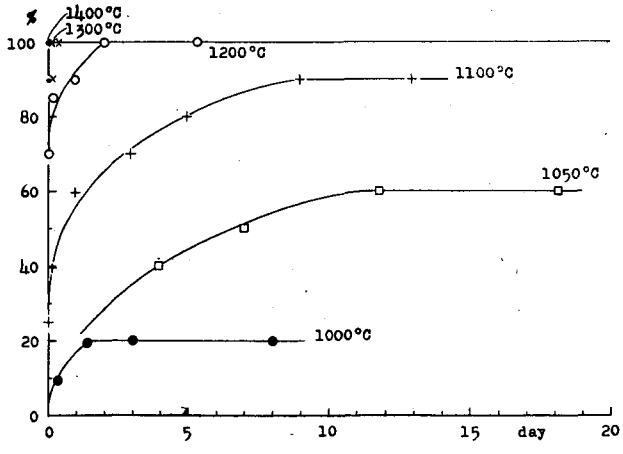

Fig. IV-6 Isothermal rate curves of transformation to liquid of plagioclase in the Showa-shinzan dome lava.

lines within narrow range of time. Fig. IV–5 shows a plot of log K vs. the inverse of the absolute temperature. From this plot a value of 46 kcal/mol for the activation energy of fusion has been calculated. The Arrhenius equation that holds for the fusion process is

$$ln\, K = A - B/T\ .$$

The fusion isothermal curves over a wide range of time of heat treatment are graphed in Figs. IV–6–8. These figures will be discussed in the next section.

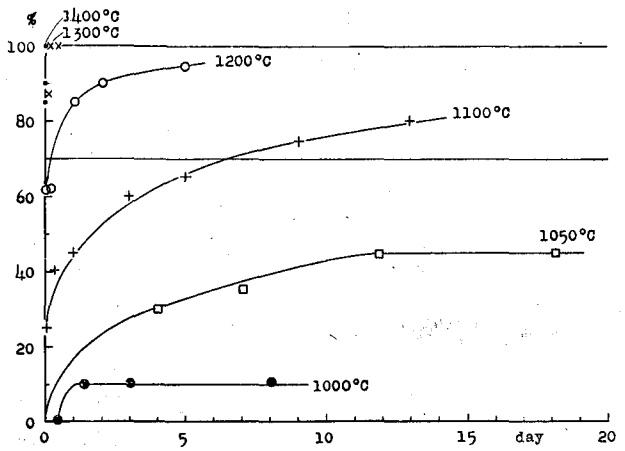

Fig. IV-7. Isothermal rate curves of transformation to liquid of cristobalite.

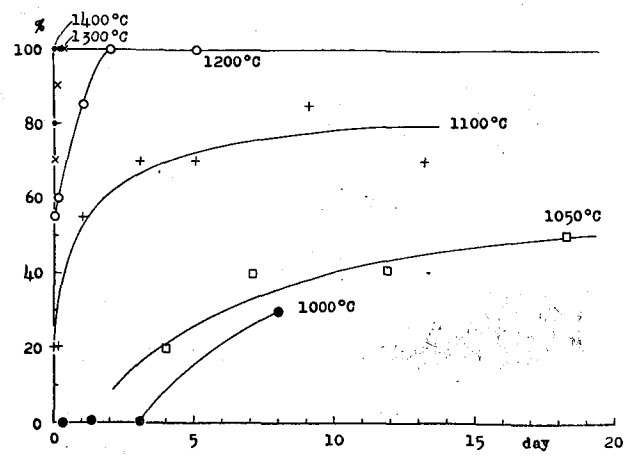

Fig. IV-8. Isothermal rate curves transformation to liquid of quartz.

§ 4. Discussion

(A) Viscosity-temperature relation of the dome lava in natural cooling process.

In order to investigate the viscosity-temperature relation of the dome lava in natural cooling process, let the process be separated into three stages, viz., (i) the stage of crystallization of phenocrysts, (ii) the stage of solidification of groundmass and (iii) the stage of the extrusion of the dome to the earth's surface.

(a) Estimation of temperature.

(i) Stage of crystallization of phenocrysts.

The mode of the Showa-shinzan dome lava as shown in Table IV–1 gives ca. 30/70, the volume ratio of plagioclase in phenocrysts to that in groundmass. If the density of plagioclase in phenocrysts is equal to that in groundmass, the weight ratio is also 30/70.

In reheating process of present experiment the plagioclase in groundmass should be fused at a temperature lower than the melting point of plagioclase in phenocrysts. The boundary line (glass content 70%) in Fig. IV–6, therefore, shows that even if all plagioclase in groundmass should melt, the amout of glass produced from the plagioclase would not cross this line. The 1100°C curve in Fig. IV–6 crosses the boundary line. This means that plagioclase in groundmass of the lava would melt away and plagioclase in phenocryst would begin to melt at 1100°C. The tendency of the 1100°C curve shows that all

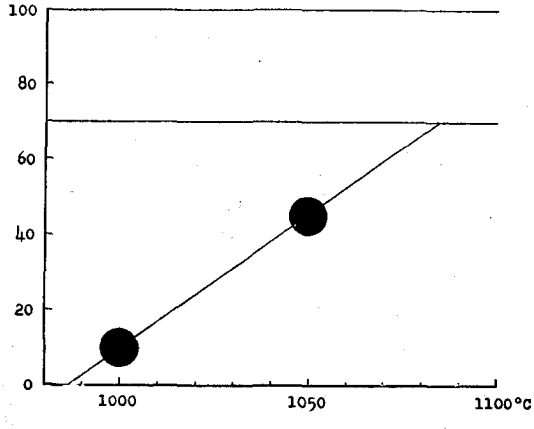

Fig. IV-9. Relation between amount of glass in equilibrium state and temperature.

plagioclase melt away by the heat treatment at 1100°C, i.e., the dome lava seems to be in a complete molten state at 1100°C. On the other hand, the 1050°C curve does not cross the boundary line and a heat treatment for more than 12 days seems to result in approach to the equilibrium stage, where the amount of glass produced from the plagioclase is ca. 45%. In the case of 1000°C curve, the equilibrium time is ca. 1 day and the amount of glass is ca. 10%. In Fig. IV–9 the amount of glass in the equilibrium state is plotted as a function of heating temperature. The extrapolated line of this relation crosses the boundary line (glass content 70%) at ca. 1085±10°C. This means that if the dome lava is heated to temperatures higher than ca. 1085°C, and lower than 1100°C, the plagioclase in phenocrysts in the lava may completely melt away. Thus, it is reasonable to conclude that the temperature of the lava in the crystallization stage of phenocrysts was ca. 1090°C.

(ii) Stage of solidification of groundmass.

From the discussion of the stage of crystallization of phenocrysts it is clear that the fusion isothermal curve approaching asymptotically the boundary line (glass content 70%) in Fig. IV–6 indicates the temperature at which the plagioclase in groundmass began to crystallize at the natural cooling stage. The temperature is estimated to be ca. 1085±10°C.

(iii) Stage of extrusion of the dome lava.

Judging from its colour, the temperature of the incandescent lava in July, 1945 soon after its appearance on the earth's surface was estimated to be at least nearly 1000°C (3). In September 1947 NAKAMURA (4) measured the temperature of new lava with the aid of a thermo-couple and obtained temperatures of 800–900°C of the exposed lava at numerous spots with 980°C as the maximum. The temperature inside the dome about 10 years after its formation was estimated to be ca. 1000°C from velocity measurements in the laboratory (5) in order to explain the P-velocity (ca. 4 km/sec.) of the inner part of the dome determined by the seismic surveys in the filed (6). Also the results shown in Fig. IV–9 give ca. 985±10°C at which the extrapolated line crosses the glass content 0% line, i.e., the plagioclase does not melt at a temperature lower than ca. 985±10°C.

The matters as mentioned above allow one to conclude that the temperature of the dome lava in the extruding stage was ca. 1000°C.

(b) Estimation of viscosity.

(i) Stage of crystallization of phenocrysts.

From the viscosity-temperature curve for the glass artificially prepared

from the dome lava, the viscosity at 1090°C is estimated to be $10^{7.7}$ poises.

(ii) Stage of solidification of groundmass.

First, the chemical composition of the melt free from phenocrysts was estimated. It was calculated from Table I–2 (B), from the modes of Table IV–1 and moreover by use of the standard density of minerals; the result is shown in Table IV–3 together with β and b/Si values. The β or b/Si values

Table IV-3.

		water-free	phenocryst-free
SiO_2	69.74	70.12	75.27
Al_2O_3	15.59	15.67	13.57
Fe_2O_3	1.52	1.53	0.86
FeO	2.59	2.60	2.00
MgO	0.85	0.85	0.32
CaO	3.63	3.65	2.44
K_2O	3.43	3.45	2.84
Na_2O	1.36	1.37	1.78
H_2O_+	0.67		
H_2O_-	0.23		
TiO_2	0.45	0.45	0.59
P_2O_5	0.22	0.22	0.28
MnO	0.08	0.08	0.10
Total	100.36	99.99	100.05
β	0.15	0.15	0.10
b/Si	1.40	1.40	1.66

as illustrated in Fig. II–3 or 4 give the viscosity-temperature curve for the phenocryst-free melt, and then the viscosity at ca. 1085°C is estimated to be ca. $10^{8.7}$ poises. The phenocrysts occupy ca. 20% in volume (Table IV–1), so under the assumption that the phenocrysts are spheres they must mechanically increase by ca. $10^{0.5}$ poises the viscosity of the mixture of crystal and liquid from the theoretical relation between relative viscosity (viscosity of suspension to that of fluid) and volume concentration of suspensions of uniform spheres which is in good agreement with existing data over a wide range of concentration (7). Thus in conclusion, the viscosity of the dome lava at the solidifying stage is estimated to be ca. $10^{9.2}$ poises.

(iii) Stage of extrusion of the dome lava.

Considering the results shown in Fig. IV–6 it seems allowable to conclude

that the dome lava at ca. 1000°C was in an equilibrium stage. Then the viscosity-temperature relation obtained by the reheating experiment for the original lava described in Chapter I may be available for the present estimation at temperatures below 1000°C.

The viscosity of the molten parts of the dome lava in this stage is estimated as follows:

The chemical composition of the molten parts may be almost Ab_{100} because the plagioclase in groundmass is An_{20-30} in its chemical composition (1), thus the viscosity of the melt is estimated to be $10^{9.3}$ poises at 1000°C which is based on the extrapolation of Kani and Hosokawa's data (8). Therefore, the viscosity of fused silica at 1000°C may be that of the molten parts.

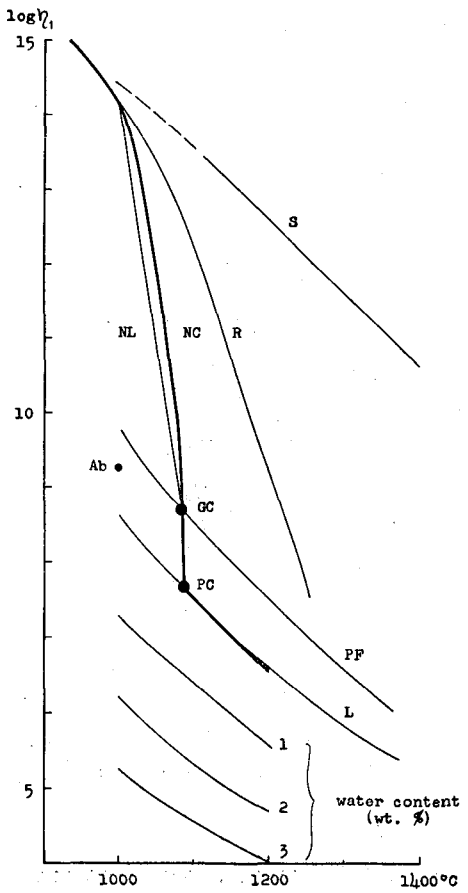

Fig. IV-10. Viscosity vs. temperature of the Showa-shinzan dome lava. S:silica glass,
R: reheating exp.,
NC: natural cooling process of the dome lava containing crystals,
NL: maximum value of natural cooling process of liquid,
PF: phenocrysts free,
L: liquid state,
GC: groundmass crystals crystallize,
CP: phenocryst crystals crystallize,
Ab: albite melts.

The viscosity of fused silica has been measured by many investigators (9) (10) (11). As the actual molten parts may constitute a mixture of both liquids, i.e., Ab and silica, so it may be concluded that the viscosity of the molten parts was $10^{9.3}$ to $10^{14.5}$ poises and that the upper limit was $10^{14.5}$ poises.

All the estimations stated above are plotted in Fig. IV–10. Thus the broad line in this figure may correspond to the viscosity-temperature relation of the Showa-shinzan dome lava in natural cooling process, if the lava does not contain water. The effect of water on viscosity in the case of the Showa-shinzan dome lava was discussed in Chapter II. The considerable reduction of viscosity of the lava containing a little water is illustrated in Fig. IV–10 too. In this case the viscosity-temperature relation cannot be accurately deduced, because it seems to be impossible to know the amount of water contained in the lava at and before the time of extrusion. In the strict sense, therefore, it must be concluded that the heavy line in Fig. IV–10 shows the upper limit of viscosity in the viscosity-temperature relation.

(B) Cooling rate of the dome lava.

Next, the writer will estimate roughly the cooling rate of the dome lava during the extrusion, and consequently the time when the lava began suddenly to cool underground. As the sudden decrease of the temperature of the lava must correspond to the solidification of groundmass, so attention should be paid to the crystallization of plagioclase occupying 40.5% of mode (Table IV–1).

Many investigators (12) (13) (14) (15) have shown either experimentally or theoretically various equations relating the rate of crystal growth to temperature, viscosity and the liquidus temperature. Here, in the present investigation, as the estimation of the order of the time rate of cooling is made, so any of those equations will do. Here use is made of Preston's equation (16) which shows excellent fit to the observed data of growth rate of devitrite in soda-lime glass (17),

$$\dot{G} = k\,(T_l - T)/\eta_T\,, \qquad \text{Eq. (IV–1)}$$

where $\dot{G}$ is the time rate of crystal growth, T the temperature, T_l the liquidus temperature, η_T the viscosity of the liquid at T°C and k a constant. LITTLETON (18) showed the maximum crystal growth rate $\dot{G}_{\max.}$ in the same glass is proportional to fluidity (F) as follows:

$$\dot{G}_{\max.} = C\,F = C/\eta_{T\max.}\,, \qquad \text{Eq. (IV–2)}$$

where C is a constant and $\eta_{T\max.}$ is the viscosity at the temperature of

maximum growth rate ($T_{\max.}$). The viscosity is expressed by the following equation as stated in Chapter I and II.

$$\eta_T = A \exp(B/T) , \qquad \text{Eq. (IV–3)}$$

where A and B are constants.

From Eqs. (IV–1, 2), one gets

$$k = C/(T_l - T_{\max.}) ,$$

where $$T_{\max.} = (-B + \sqrt{B^2 + 4BT_l})/2 .$$

Thus if the viscosity of melt, the liquidus temperature of the marked crystal and constant C are known, the growth rate of the crystal can be estimated. The constant C in the molten rock was determined in the following way: LEONTIEVA (15) measured the growth rate of plagioclase, pyroxene, olivine and magnetite in basalt and the viscosity of the same basalt. Though there are a few data, the relations of Eq. (IV–2) are illustrated in Fig. IV–

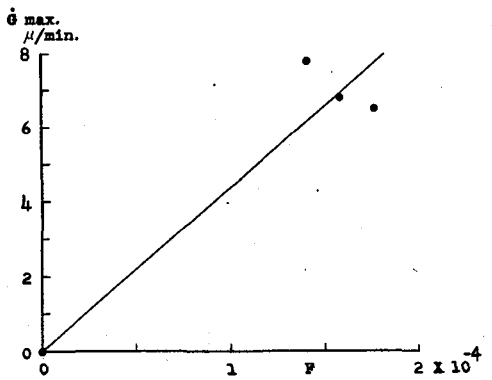

Fig. IV-11. $\dot{G}_{\max.}$ vs. fluidity for plagioclase.

11 on the basis of her data. Thus Eq. (IV–2) in the molten rock is as follows:

$$\dot{G}_{\max.} = 2.4 \times 10^{10}/\eta_{T\max.} \ (\mu/year) \qquad \text{Eq. (IV–4)}$$

The liquidus temperature of groundmass plagioclase (T_l) is 1085°C as estimated above in (A) (a) (ii) of this section. The process is taken as the viscosity-temperature relation for the molten Showa-shinzan dome lava, i.e., the process going on between phenocrysts and groundmass melt free from crystal, i.e., NL-curve in Fig. IV–10.

The cooling rate is determined as follows:

The rate is assumed to be constant, i.e.,

$$dT/dt = U \ . \qquad \text{Eq. (IV-5)}$$

In Eq. (IV-1), $\dot{G} = dG/dt$, so $dG = \dfrac{k\,(T_l - T)\,dt}{\eta_T}$.

From Eq. (IV-5), one gets $dG = k\,(T_l - T)\,dT/U\eta_T$. The length of crystal (L) which grew during cooling process from T_l ($t=0$) to $T(t=t)$ is given as

$$L = \int_0^t \dot{G}\,dt = \int dG = \int_{T_l}^{T} \frac{k\,(T_l - T)}{U\,\eta_T}\,dT \ . \qquad \text{Eq. (IV-6)}$$

U is constant, so

$$U = dT/dt = \frac{\displaystyle\int_{T_l}^{T} \frac{k\,(T_l - T)}{\eta_T}\,dT}{L} \qquad \text{Eq. (IV-7)}$$

From Fig. IV-12 and the maximum size of plagioclase in the groundmass, ca.

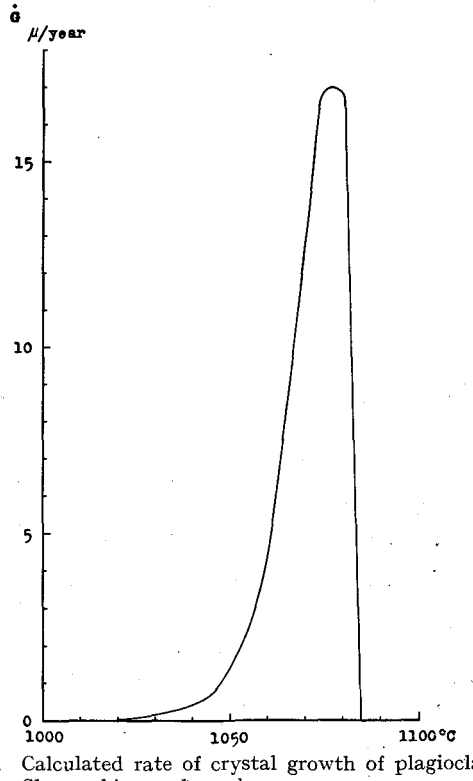

Fig. IV-12. Calculated rate of crystal growth of plagioclase in the Showa-shinzan dome lava.

50μ (19), it follows that

$$U = ca.\ 6°C/year$$

for the process of NL-curve in Fig. IV-10.

Then the time which was necessary to cool from $T_l = 1085$ to 1000°C is

$$(T_l - T)/U = ca.\ 15\ years.$$

As the calculation above performed is estimation of the order, so it may be concluded that the sudden solidification of the dome lava was antecedent to the appearance of the dome in the order of a few decades at most. Well known eruptions of Usu volcano, being six times since 1663, are listed in following Table IV-4 (3).

Table IV-4. Eruptions of volcano Usu.

1). August 16, 1663.
2). January 23, 1768.
3). March 9,····July, 1822.
4). April 13,····May, 1855.
5). July 19,····October, 1910.
6). 1943····1945.

From the Table, then, it may be suggested that the sudden solidification of the dome lava may be connected with the activity of the 1910 eruption.

It has been assumed that the dome lava which had been in molten state was put in a natural cooling process connected with the formation of the dome, but from the viewpoint of petrology, viz., the fact that the chemical composition of the lava is similar to that of granite, the lava which was already in a solid state might have begun to move at the time of extrusion (6). Therefore, the present conclusion obtained according to the kinetics of the fusion of the lava should be investigated from new point of view in future.

References

1) LEVIN, E.M., MCMURDIE, H.F. and HALL, F.P. ed. Phase diagrams for ceramists, Amer. Ceram. Soc., Inc. (1956), "All diagarms used by the present writer are cited from this book".
2) YAGI, K. *Recent activity of Usu volcano, Japan, with special reference to the* formation of Syowa Sinzan, Trans. Amer. Geophys. Union, **34** (1953), 449–456.
3) MINAKAMI, T., ISHIKAWA, T. and YAGI, K. The 1944 eruption of volcano Usu in Hokkaido, Japan. History and mechanism of formation of the new dome "Syowa-Sinzan", Bull. Volc. Sér, 2, **11** (1951), 45–157.
4) NAKAMURA, S.T. Read at Geophys. Inst. Tohoku Univ., Sendai, Japan, (1947).
5) SHIMOZURU, D. Elasticity of rocks and some related geophysical problems, Japanese J. Geophys., **2** (1960), 1–85.

6) NEMOTO, T., HAYAKAWA, M., TAKAHASHI, K. and OANA, S. Report on the geological, geophysical and geochemical studies of Usu volcano (Showa-Shinzan), (in Japanese, with abstract in English), Geol. Surv. Japan, Report No. 170 (1957), 1–149.
7) HAPPEL, J. Viscosity of suspensions of uniform spheres, J. Appl. Phys. **28** (1957), 1288–1292.
8) KANI, K. and HOSOKAWA, K. On the viscosities of silicate rock-forming minerals and igneous rocks, (in Japanese, with abstract in English), Res. Electrotech. Laboratory, No. 391 (1936), 1–105.
9) INUZUKA, H. Measurement of viscosity on fused silica, (in Japanese), Mazda Kenkyu-Jiho, **14** (1939), 102–104.
10) VOLAROVICH, M.P. and LEONTIEVA, A.A. Determination of the viscosity of quartz glass within the softening range, J. Soc. Glass Tech., **20** (1936), 139–143.
11) BACON, J.F., HASAPIS, A.A. and WHOLLEY, W. Viscosity and density of molten silica and high silica content glasses, Phys. Chem. Glass **1** (1960), 90–98.
12) FRENKEL, J. Kinetic theory of liquids, Clarendon Press, Oxford, (1956).
13) RICHARDS, W.T. Formation and crystallization of vitreous media, J. Chem. Phys., **4** (1936), 449–457.
14) BROWN, S.D. Temperature dependence of growth processes in glass devitrification, J. Amer. Ceram. Soc., **43** (1960), 116–117.
15) LEONTIEVA, A.A. Vliyanie atmosfery na vyazkost' jelezosoderjaschikh silikatnykh rasplavof i na lineinuyu skorost' kristallizatstii tverdykh fas iz nikh, (in Russian), Tr. Inst. Geol. Nayk. Akad, Nayk, SSSR. Byp. 137, Petr. Ser., No. 40 (1951), 19–31.
16) PRESTON, E. The crystallization relationships of a soda-magnesia-silica glass as used for drawn sheet and the process of devitrification, J. Soc. Glass Tech., **24** (1940), 139–158.
17) SWIFT, H.R. Some experiments on crystal growth and solution in glasses, J. Amer. Ceram. Soc., **30** (1947), 170–174.
18) LITTLETON, J.T. A review of recent progress in the study of the thermal treatment of glass. J. Soc. Glass Tech., **15** (1931), 262–306.
19) YAGI, K. Petrological studies on Syowa-Sinzan, Usu volcano, Hokkaidó, Japan, (in Japanese), Gan-Ko, (J. Japanese Assoc. Min. Petro. Eco. Geol), **33** (1949), 3–17.

Acknowledgements. During the course of this work, many people have given the writer, not only critism, but also suggestions and encouragement. The writer takes this opportunity of thanking them all for their kindenss. His cordial thanks are, especially, offered to the late Professor Shuzo SAKUMA, without whose early guidance this investigation would have been impossible. Thanks are also due to Professor Takeo MATUZAWA and Dr. Izumi YOKOYAMA for critical reading of the manuscript, their valuable critisms from the physical and the geophysical points of view and much encouragement throughout the course of this study. The writer further cordially thanks Professors

Toshio ISHIKAWA, Kenzo YAGI and Dr. Yoshio KATSUI for their valuable suggestions from the petrological and geological points of view. The writer is also indebted to Miss Michiko CHIBA for her assistance in carrying out the experiments and her drawing of all figures in this paper.

A part of the expenses of this study was defrayed from the Research Funds for Science of the Ministry of Education and the Government of Hokkaido.

This work is based on thesis, submitted in partial fulfillment of D. Sc. requirements at the Hokkaido University, 1962.